PERIODICA POLYTECHNICA

Electrical engineering

ELECTRICAL ENGINEERING — ELEKTROTECHNIK

VOL. 1 * NO. 1 * 1957

POLYTECHNICAL UNIVERSITY
TECHNISCHE UNIVERSITÄT
BUDAPEST

PERIODICA POLYTECHNICA

Contributions to international technical sciences published by the Polytechnical University, Budapest (Hungary)

Originalbeiträge zur internationalen technischen Wissenschaft, veröffentlicht von der Technischen Universität, Budapest (Ungarn)

PERIODICA POLYTECHNICA

includes the following series

Engineering
Electrical Engineering
including Applied Physics
Chemical Engineering

enthält folgende Serien

Maschinen- und Bauwesen
Elektrotechnik und angewandte Physik
Chemisches Ingenieurwesen

The issues of each series appear at quarterly intervals

Einzelnummern der genannten Serien erscheinen vierteljährlich

The rate of subscription to a series is $ 4,00 a year. For subscription or exchange copies please write to

Jahresabonnement pro Serie: $ 4,00. Bestellungen und Anträge für Tauschverbindungen sind zu richten an:

PERIODICA POLYTECHNICA

BUDAPEST 62, POSTAFIÓK 440

PREFACE

In the academic year 1956/57 technical sciences will have been taught in Hungary for 175 years. The Institutum Geometricum inaugurated in 1781 was only an institute of the Péter Pázmány University. The other predecessor of our University, the independent Hungarian Polytechnical School was founded one hundred years ago, in 1856. The Budapest Polytechnical University, created by the amalgamation of these institutes, started its 85th university year in 1956.

On the occasion of this treble anniversary the University had intended to organize a large-scale international Congress of scientists. It was on this occasion again that the University Council decided to publish scientific quarterlies.

The full implementation of these decisions was, however, prevented by unforeseen events. The Congress had to be postponed to a later date, and thus the other decision concerning the publications acquired added importance.

During the months that elapsed between the decision of the University Council and the publication of the first issue of our quarterly the Hungarian nation has seen many a grave and tragical day. Thus by the publication of the quarterlies we wish not only to celebrate the 175th anniversary of the existence of our University but also to express our desire to take again an active part in the scientific progress of the world.

Budapest, January 1957.

Dr. László Gillemot
Corresp. member
of the Hungarian Academy of Sciences
Rector Magnificus
of the Polytechnical University

VORWORT

Vor 175 Jahren erfuhr in Ungarn der höhere technische Unterricht eine namhafte Entwicklung. Das im Jahre 1781 eröffnete Institutum Geometricum war nur eins der Institute der von Petrus Pázmány begründeten Univeristät. Im Jahre 1856, also vor genau 100 Jahren, wurde ein zweiter Vorfahr unserer Hochschule gegründet — das selbständige Ungarische Polytechnikum. Aus dem Zusammenschluß der beiden Institutionen entstand die heutige Budapester Technische Universität, die in diesem Jahre zum 85en Male ihre Tore den Studenten öffnet.

Anläßlich des dreifachen, im Hinblick auf den höheren technischen Unterricht namhaften Jubiläums beabsichtigte die Universität, einen internationalen Kongreß zu veranstalten. Gleichfalls in Erinnerung an den Jahrestag beschloß der Senat der Universität, die wissenschaftlichen Mitteilungen der Universität in einer eigenen vierteljährlich erscheinenden Zeitschrift herauszugeben.

Diese Beschlüsse konnten wegen der inzwischen eingetretenen Ereignisse nicht vollständig durchgeführt werden ; so sind wir leider gezwungen, den Kongreß auf einen späteren, vorläufig noch nicht festgesetzten Zeitpunkt zu verschieben. Um so größere Bedeutung gewann also der Beschluß des Universitätssenats über die Gründung der jetzt erscheinenden Zeitschrift.

Zwischen diesem Beschluß und dem Erscheinen unserer Zeitschrift hat die ungarische Nation eine schwere und tragische Erschütterung erlitten. Unsere jetzt angehende Periodica hat deshalb nicht nur das Ziel, das 175jährige Bestehen der Universität zu feiern, sondern will gleichzeitig ein neuer Beweis dafür sein, daß die ungarischen Gelehrten unentwegt bestrebt sind, zum Fortschritt der Wissenschaft der Welt tatkräftig beizutragen.

Budapest, Januar 1957.

Dr. László Gillemot
Korresp. Mitglied der Ungarischen Akademie der Wissenschaften, Rektor der Technischen Universität zu Budapest

A NEW INSTRUMENT FOR TESTING STEREOSCOPIC VISION

By

N. BÁRÁNY

Institute for Instrumental Design and Precision Mechanics of the Polytechnical University, Budapest

(Received December 24, 1956)

The phenomenon of *stereoscopic* vision is known to be the result of two independent and laterally more or less displaced images, each of them being projected on the retina of one eye. The two images are blended by the optical centre of the brain, in a so far inexplored manner, bringing about the effect of space perception.

In case of *monocular* vision space perception cannot be formed on a purely geometrical basis. Nevertheless, the relative spatial positions of the objects are fairly well distinguished by the observer. The underlying reason cannot be satisfactorily explained by the laws of geometrical optics, and it is supposed that intricate psychological processes are preponderant, among which a series of empirical factors gathered in the course of time seem to play the chief part.

To begin with the simplest case, *i. e.*, with objects of identical sizes placed at various distances, the images formed on the retina by the adaptive crystalline lens will be the larger, the closer the observed objects are positioned. If their general order of magnitude is known, the object distance may be inferred upon by a comparison of the retinal images varying in shape and size, a measure far from satisfying the exigencies of tacheometry as set by geometrical optics. Consequently, except in the case of close objects, this is scarcely more than an approximate estimation.

Let us trace two straight lines to connect the extreme points of the retina with the posterior principle point of the crystalline lens (Fig. 1). The subtended angle α, i. e. the visual angle, will vary with the object distance for identical object sizes, or with the object size for a constant distance. The visual angle unambiguously determines the field of sight for the actually viewed object, not to be identified with the far more comprehensive term of the eye's general field of vision. Experience, acquired through the continual variation of the visual angle, has taught us to perceive the relative spatial position of the objects, even when viewing with one eye only, although this faculty of estimation rather than of discernment rapidly decreases with growing distances and, finally, when distance becomes very great, falls off entirely. In locating the

relative positions of objects at longer distances, that is, in perceiving the respective impression, the decisive part is played by optical, physiological and psychological processes, although the faculty of estimation may be substantially led astray incorrect judgement of the object size.

On the other hand, monocular estimation of distance may considerably be supported with the effect varying in the individual case, by such factors as one object being screened to some extent by a nearer one, recognition of the details of familiar objects, intensity and direction of artificial or natural illumination, spectral composition of the luminous source, coloured and overlapping or colourless arrangement in plane of the observed objects, absolute and relative speed of the object in relation to the observer, vapour and dust

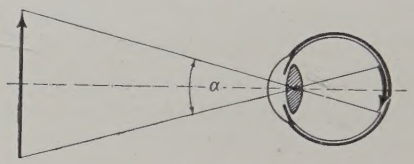

Fig. 1

percentage of the atmosphere and, finally, coloured and colourless contrast effect.

An investigation into the nature of influences exerted jointly and severally by the factors outlined above discloses a remarkably wide range of how experiences are collected. Not to be neglected is, among others, the problem, which of these factors will gain the upper hand in the course of time. May it be remembered in this context, what blunders, or even grave errors people belonging to different categories — rural and urban people, lowlanders and highlanders, etc. — are liable to commit. Town inhabitants generally measure distances in terms of time, whereas the measuring unit applied by country folk is highly varied. Furthermore, estimation of distance may be improved upon or distorted, as the case may be, due to the influence of familiar or, on the contrary, unfamiliar surroundings.

The apparent increase or decrease of the object size as caused by the changing visual angle brings us to the notion of *perspective*. The theory of perspective, together with its geometrical correlations, was first established and developed, from the artistic point of view, by the great masters of Italian renaissance. Incidentally, the constant changes in impressions of perspective also contribute to distance estimation in monocular viewing.

Let us sum the foregoings by saying that monocular space perception and distance estimation were formed out, in addition to the laws of geometrical optics, by physiological and psychological processes. However, taking into account and adding hereto the effect of surroundings and the temporal succession of phenomena, space perception is possible within rather narrow limits

only, subject to further variation for the individual viewer. The collection of experiences, as a function of time, can also be but one-sided and dissimilar. It is the simultaneous cooperation of all other senses coupled with monocular viewing, giving rise to impressions based on numerous and changing phenomena, that guide us in estimating distance. Such estimation is of a relative value only. A number of physiological procedures still unknown as to origin and issue, such as after-images, optical hallucinations, inducations, etc. play an important part therein. As soon as any one factor is eliminated from the series of experiences obtained by routine, one finds that space observation issuing from estimation undergoes a considerable change.

In the case of binocular (stereoscopic) vision an independent and dissimilar image of the viewed object is formed on the retina of each eye. According to classical theories, however, space perception only arises when image pairs fall upon identical nerve endings. If that is not so, the result should be, instead of space perception, a confusion of double images unsuitable for being blended into one stereoscopic image by the visual centre. This approach to the problem, however, must be reconsidered in our days. The rods and cones of the nerve endings are supposed to be of a more or less hexagonal section, and unite into a thin layer of honeycomb pattern. Recent researches, however, suggest that their cross-section is not hexagonal ; thus, the role played by the disc of least confusion representing the image point is differently interpreted in the theory of resolving power. Investigations into the theoretical deduction of resolving power start from the supposition relying upon anatomic tests that human eye is able to separate (resolve) images received from two indentically bright point objects as long as the distance between the two point images on the retina is equal to the radius of the disc of least confusion. In terms of angular measurement, the angle subtended by the radius amounts to an average 20 seconds of arc. Nevertheless, even the most careful and precise tests were unable to produce a value approximating this figure, as the average results obtained fluctuated around 90 seconds of arc. By reading a vernier and bringing into coincidence straight lines of varying length, much better results have been arrived at, but this problem is not identical with the task of resolving two luminous points.

Rayleigh's version for the criterion of the resolving power was that the retinal images of two luminous points may be separated as long as their relative distance is equal to at least the radius of the disc of least confusion. Another explanation held that the eye is able to resolve two point objects, if the two cones stimulated by the images are separated by an unstimulated one. Researches carried out by Davson, Hartridge, Ogle, Schober, Tonner et al. suggest that, similarly to monocular vision, resolving power largely relies upon optical, physiological and psychological factors, in addition to geometrical-optical correlations. As the enumeration of said factors is beyond the scope of this paper,

the reader is referred to literature for more details, particularly as regards the anatomy of the retina.

Recent researches have lead to the conclusion that, owing to psychological reasons, resolving power is a function of the size and shape of the point object-to be resolved. A maximum of resolution may be attained by viewing bidimens sional diagrams, but the critical factor for resolving two luminous points is definitely the contrast effect in relation to the surroundings. Added hereto must be the variation of illumination prevailing in the area of the retinal image and last not least, the image-forming power of the human eye.

Resolving power plays a significant part in stereoscopic vision, owing to the already mentioned importance of the parallactic difference of image pairs. It is supposed that there exists a maximum and a minimum value already or still permitting stereoscopic vision.

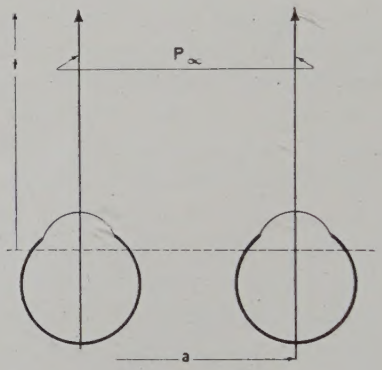

Fig. 2

The retina elements of the two eyes are correlated. When viewing objects at infinity, the visual axes are parallel while upon viewing close objects, they are convergent (Fig. 2). The magnitude of convergence is determined by the object distance t and by the viewer's visual distance a as a base. Convergence, or its variation may suggest the idea of space estimation. This, however, holds true only for near-by objects, while our sensory organs are not suited for determining the magnitude of convergence for medium and long distances. Thus, convergence as well as accomodation offer but limited possibilities for the development of space perception. A point of primary importance is the lateral displacement value of the two point image pairs, called *parallactic difference* (Fig. 3). Distance estimation is termed *real* (absolute) when it concerns the distance T between the viewer and point P, and is called *relative* when it means the distance t between points P and (P). In both cases the relative displacement of the point image pairs is characteristic of the parallactic difference.

When viewing a point object P at infinity, the visual axes are parallel, and their distance from each other is equal to the visual distance a of the

observer as a base. There is no lateral displacement between retinal images P_1 and P_3, consequently, no vision of depth can arise. Images from point objects P positioned at a distance T are formed at P_2 and at P_4. The left-hand image is displaced by $P_1P_2 = x_1$, and the right-hand one by $P_3P_4 = x_2$. The difference, $(x_1 - x_2)$ is called parallactic difference, irrespective of whether the

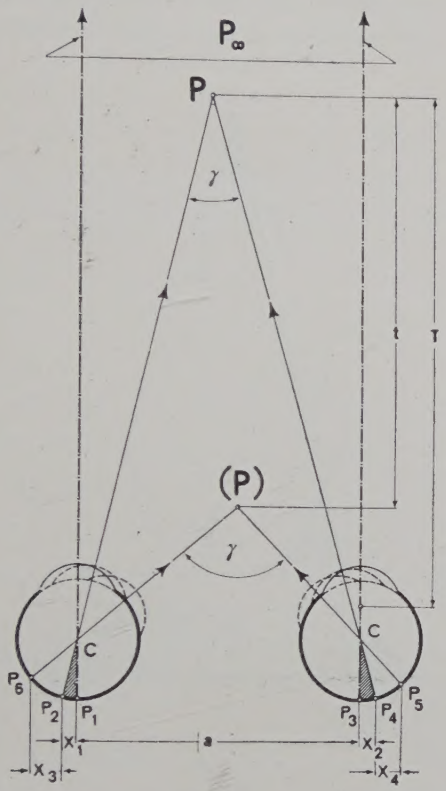

Fig. 3

sign is negative or positive. On this basis an estimate may be formed of the *real* distance T from point P for a visual distance a. Images P_5 and P_6 of the still closer point (P) arise at distances x_3 and x_4 from the above point images P and (P), respectively. Parallactic difference $(x_3 - x_4)$ permits estimating the relative distance t between point images P and (P). Distance T is called *depth perception* whereas distance t represents *space depth*.

Whether the observer's estimation is concerned with real distance from a far-away or from a near-by object, or with the relative distance between these two, the points will spring into relief against infinity — that is, they will be viewed stereoscopically — only if the value of the parallactic difference is not less than the resolving power of the eye. According to earlier anatomical

data and other investigations into the nature of the retina, the generally accepted value of the human eye's resolving power is 1 minute of arc. However, values of 30, 20, 10 or even 2 seconds of arc have been encountered, as Pulfrich found in his tests accomplished by means of stereoscopic range-finders with travelling signals. Upon first thought, one might attribute this to a finer structure of the retina. The wave theory derivation with respect to the disc of least confusion, however, disclosed that a finer structure of the retina would not

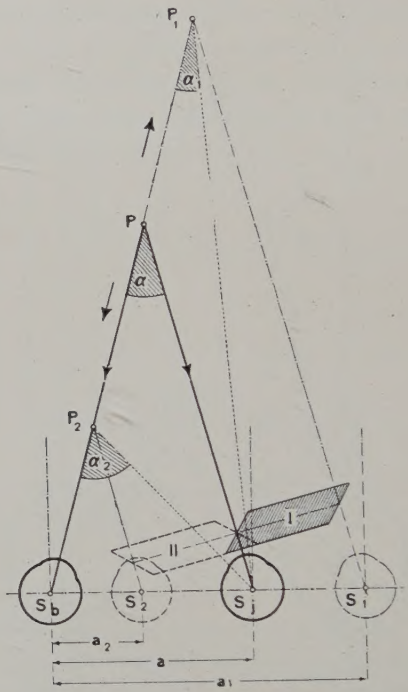

Fig. 4

render vision more acute. Just like in the event of results obtained by reading a vernier, or bringing into coincidence straight lines, such superior resolving power can only be ascribed to the shape of the retina elements, and physiological as well as psychological factors.

Fig. 3 leads to the conclusion that depth perception for binocular vision increases in direct proportion to the visual distance and to the depth difference of the two point objects to be compared, while decreasing in square proportion to the real distance of the points. Consequently, the value of parallactic difference may not fall below a certain minimum required for recording a sensation of space. As one but seldom encounters single points in space, in the majority of cases sensation of depth is a relative estimation rather than depth perception.

The varying sensation of depth concomitant to an intentional extension or cutting down, respectively, of the visual distance may be illustrated by the following experiment (Fig. 4) :

Let us place before the right eye a rhombic prism in position No. I. In this manner the unaided left eye will view directly, while viewing by the right eye will be intercepted by the prism. Thus, the original visual distance a of the right eye will be increased to a_1. at the same time reducing the angle of con-

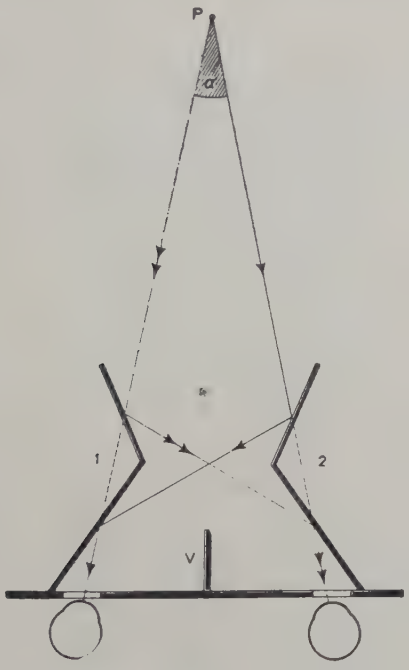

Fig. 5

vergence to —1. The mind then records a sensation of the objects being widely spaced in depth, hence they will appear considerably smaller. By turning the prism into position No. II, the base is reduced to a_2, whereas the convergence angle is increased to α_2. The objects thus contracted in depth appear much larger.

In position No. I. of the prism the object P is seen as if viewed from eye position S, that is, as if the point object had travelled to P_1. The convergence angle being lessened to —1, the objects appear smaller. If, on the other hand, bringing the prism into position No. II., the objects viewed at an increased visual angle —2 appear to be larger, that is, as if observed from eye position S_2.

In both cases the prism placed before the eye will considerable impede not only movement in space but also orientation, as a consequence of the limited

field of vision due to the apparent contraction and extension, respectively of depth. If the prism is suitably shaped, visual distance may not only be reduced to zero but may have a negative value, in which case the rays incident from the left will be received by the right eye and vice versa. Thus, space perception will be reversed, giving rise to a pseudoscopic impression, that is, nearer objects will appear more distant and far away objects closer. This phenomenon may be created by means of a system of mirrors, schematically represented in Fig. 5. The view unfolding itself to the observer presents a fascinating world.

The two mirror arrangements 1 and 2, each consisting of two parts and subtending a certain angle, are separated by a wall *V*, in order to avoid the appearance of confusing images. Mirror 1 leads to the right eye the ray incident from the left and marked by a double-pointed arrow, while mirror 2 leads to the left eye the arrow-marked ray incident from the right. The mirror arrangement thus reverses object *P*. The angle of convergence of point object *P* projected to the eye by the two mirror arrangements equals that of the unaided eye.

The minimum value of the parallactic difference representing the acuity of depth vision is 5 to 10 seconds of arc, a value subject to a great number of factors ; which, in turn, account for the surprising results obtained through experiments, resulting in much smaller, that is, more advantageous, values than expected, seemingly at variance with the laws of geometrical optics.

In describing binocular vision it is understood that the two eyes are entirely similar as to their anatomic structure, image forming power, optic data, physiological, and, in the figurative sense, mechanical action. In reality, however, such ideal eyes are very rarely encountered. In most cases the observer does not even realize major or minor aberrations. According to the current definition, the right eye forms an image of the right side of the object, and the left eye of the left side. At the slightest lateral turning, however, the first image is received by the eye first perceiving the object. Hence, in the case of continuous observation, the images are not simultaneously formed on the two retinae. Leaving aside exceptional cases, image formation on the two retinae is thus deferred in relation to each other, a phenomenon called "the race of visual fields". Simultaneous image formation is, incidentally, precluded by the fact that, in the event of a change of direction, the turning of the eyeball is not continuous but intermittent, as a result of the specific structure of the eyes' motorial muscles. The turning motion of the eyeball is not perfectly synchronized. Of the two images, the stronger prevails over the other one, attempting to check the weaker one's effect. Several investigators consider this continuous change one of the chief conditions to stereoscopic vision. *Panum* holds that stereoscopic vision may arise even if the conjugate image pairs do not fall on identical nerve endings. Let us now leave aside the section and arrangement of rods and cones, the distortion of the disc of least confusion due to

aberrations in image formation, as well as the chromatic aberration caused by oblique pencils of ray, — a stereoscopic image will be formed even if image formation no longer follows the principle of conjugate point pairs. Assuming that image points do not fall on identical nerve endings, it suffices that they should be overlapping in the vicinity of the nerve endings.

In theory, even the most accomplished optical instrument is unable to form a point-like image of a pointlight lamp : the image will be a system of mensurable surfaces comprising a nucleus and several surrounding rings. Irrespective of the image-forming device, the diameter of the disc is a function of wave-length and it is caused by the interference resulting in connection

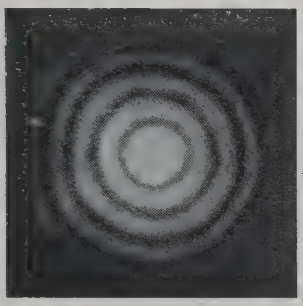

Fig. 6

with diffraction. Such a disc may be produced by means of an extremely fine bore or slit, in line with the principles of wave theory. This so-called disc of least confusion suffers a certain distortion due to the more or less considerable aberrations in image formation of the instrument in question. On the other hand, the extent said distortion offers a basis for determining the accuracy of the optical instrument. It must be remembered that the human eye is far less perfect as regards image formation than might be inferred from the conventional anatomical sections and diagrams. The shape and distortion of the disc of least confusion arising on the retina are subject to various factors, thus it differs substantially from photographic representations. The disc of least confusion shown in Fig. 6 has been produced by a very fine bore. The infinitesimal divergencies at the edge and wall of the bore were sufficient for distorting the rings of the disc.

Several investigators have drawn the conclusion from the "race of visual fields" that the law of conjugate points is far less important than the competition of fields occurring in connection with image pairs. However, no satisfactory explanation has been given so far for the real nature of physiological and psychological procedures taking place in the centre of vision. Among others, this insufficiency accounts for the awkward sensation felt when viewing a stereoscopic cinema performance. Obviously, the image projected only

approximates and imitates normal space perception, but cannot replace reality until light has been thrown upon every aspect of the psychological factors participating in stereoscopic vision.

Whatever be the viewpoint from which the theories and opinions with respect to stereoscopic vision are being criticized, it is of primary importance to be able to determine the numerical value of the stereoscopic vision power of both observers and testers in certain selected and special professions, also for the sake of comparison.

Besides the Pulfrich balance, and the methods and apparatus of Mach and Dvorak, Chantraine and Luft, Hering, Garten, Monyé, etc. stereoscopic vision is mostly tested by means of the stereoscope. In such tests the observer has to determine the stereoscopic effect produced by a picture of geometric — bidimensional — lines and diagrams differently spaced in depth. In other words, he has to ascertain how the individual lines, signals and signal groups are spaced in depth in relation to each other and to the whole of the picture. Obviously, this is an estimation of depth. The relative depth of the signals can be determined numerically. Stereoscopic vision of the observer is considered best if he is able to pick out with certainty the line, signal or diagram positioned at the minimum depth. Depth determination is, of course, not continuous but intermittent, progressing from signal to signal. The tests are to be conducted under strict observation of the rules, carefully precluding any disturbing factors. The correctness of orally stated depth data should be checked by using a table. The primary conditions for successful stereoscopic tests are proper illumination as regards intensity and direction, transparent positives rich in contrast or dull positives, and, last not least, a certain ability on the part of the tested person, a condition which may cause difficulties particularly in the case of group tests. The optimum results may be attained by using transilluminable positives rich in details, as the confusing spots presenting themselves in connection with bright positive photos may be found very inconvenient. On the other hand, the stereoscop has the advantage of low cost, small weight, ease of handling and of transport.

It is commonly assumed that stereoscopic vision power may be improved and developed by viewing pictures widely spaced in depth. This assumption has proved to be wrong, whereas it is true that, by continual practice, stereoscopic vision may be kept on the same level. The effect of mere repetition is the clue to the phenomenon of improved stereo-vision.

Good results may be achieved by taking advantage of the stereoscopic "travelling signal", an element upon which are based military stereo-rangefinders, with a base line of varying length, stereocomparators, and stereoplanigraphs or -autographs, tracing maps from aero stereophotographs. One convenient embodiment of the stereoscop is provided with a stereomicrometer (Fig. 7) mounted on the object table. The centres fastened to the ends of fla$_t$

tongues vertically shiftable over the test board laid on the object table may be laterally displaced, jointly or separately, by means of a spindle bearing an indiced drum, visible on the right side of the Figure. When the centres point toward any one conjugate point of the picture, the observer will see the two centres as one united centre floating in the same depth as the observed point.

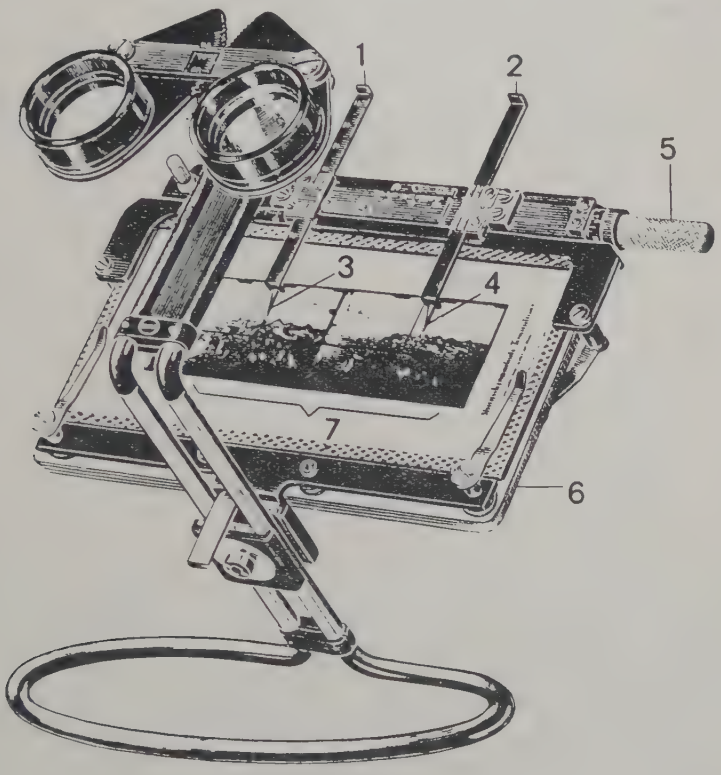

Fig. 7

Measuring is effected by shifting the right-hand centre transversely to the left-hand centre by means of the micrometer spindle. Thereupon, the centre appears to be displaced *in depth*, closer or farther away from the observer. By using conveniently selected stereo-photographs the centres can be brought into coincidence with the object points. The real or the relative distance of the point may then be computed from the exposure data of the photograph, coupled with the readings of the drum. In the absence of a micrometre only an estimate can be formed as to the distance and spatial position of the objects.

Conversations with the oculists Dr. Emil Galla and Dr. György Aczél gave the author the impetus for constructing a new instrument for the deter-

mination of stereoscopic vision power. It is to be understood that the numerical values obtained are not concerned with measuring the parallactic difference as such, but with obtaining figures and diagrams for the observer's stereoscopic vision power.

An important consideration in the design of the instrument according to the invention was to secure conditions under which — in the absence of disturbing factors acting upon the subconscious of the observer — he might concentrate all his attention upon the signal, whatever be the nature, colour and intensity of illumination.

Measuring, or rather determination is arrived at by bringing into depth coincidence an object and the corresponding image. This latter is produced

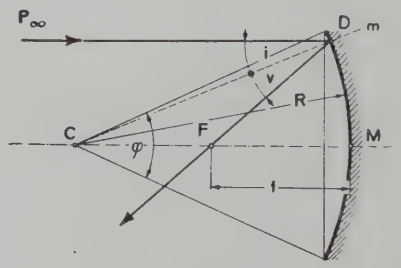

Fig. 8

by means of a concave spherical mirror. The apparatus according to the invention also causes the image to be displaced simultaneously with the object but this is done in depth and not transversely, as is the case with the stereo-micrometer. It has been found that at a certain degree of displacement of the centres confusing double images are liable to occur in connection with the stereo-micrometer. The present instrument permits a much higher degree of displacement in the direction of viewing without producing confusing double images. It is true that the familiar phenomenon of double images may occur, as a result of accomodation of object and image to varying distances. The new instrument obviates various inconveniences inherent in the stereo-micrometer. Thus, no vertical adjustment of the centres is required, and no troublesome measures are to be taken to avoid intercrossing of the centres. The new apparatus has the further advantage over the stereo-micrometer that the image perceived is more natural. Finally, the apparatus is constructed so that the observer is not disturbed by accessories, and both centre and image are viewed in depth free of all confusion.

Before describing the instrument in more details, let us recapitulate briefly the basic characteristics of spherical mirrors.

If the spherical mirror is concave, the pencils of rays parallel to the optical axis are focused after reflection in focus F (Fig. 8) situated at a focal length

f from the apex M of the mirror, the focus representing the image formed by the mirror of an object at infinitiy.

It will be noted that the mirror employed is front-coated, with a reflecting surface consisting of an aluminium deposite.

Describing now in more detail the action of the instrument, we find that it works in the following manner, represented in Fig. 9 :

A ray, emitted by point P lying on the optical axis, is reflected at B, the reflected ray intersecting the axis at P_1. This latter represents the image of point P, the angle of incidence being i, and the angle of reflection being v. The above proposition holds true only for a mirror of a small angular aperture, in which case one may write $PB = PM = t$, also $P_1B = P_1M = k$, k standing

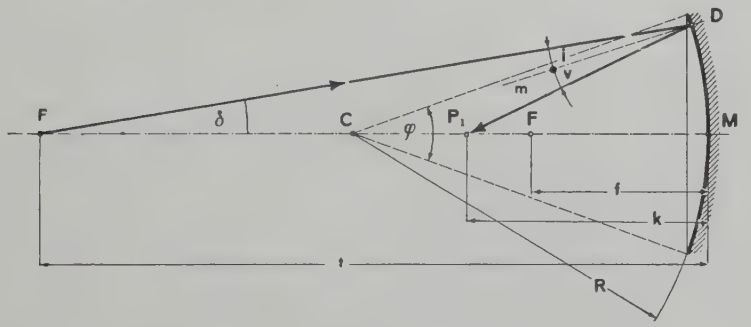

Fig. 9

for the image and t for the object distance. For a spherical mirror of infinitesimal aperture one may write, neglecting the derivation,

$$\frac{1}{k} + \frac{1}{t} = \frac{1}{f}$$

The image distance is a function of the object distance and of the radius of the mirror, but it is independent from the angle δ subtended by the radius starting from point object P, and by the optical axis. If P is at infinity, then $t = \infty$, also $l : t = 0$, that is, the parallel rays will unite in Focus F at a distance of $k = f = R : 2$. Hence, the focus of a spherical mirror of small angular aperture lies at the half of the radius of curvature. Is must be pointed out that in spherical mirrors of large angular aperture the aberrations in image formation render impossible an even approximate intersection of reflected rays in one point.

Returning now to our instrument, in the case last set forth, the image distance equals the focal length, or ($k = f$), and $f = R : 2$. Let point object P be placed

in the centre C of the radius of curvature R, we will find the object distance to equal the radius that is

$$t = R = 2f$$

and

$$k = 2f.$$

If the object is being displaced, the image distance as well as the image size are changed. If the object lies in the centre of the radius of curvature

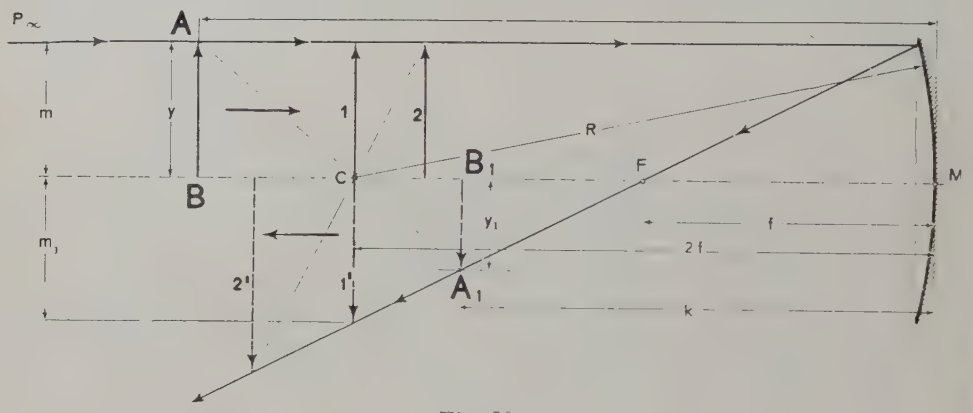

Fig. 10

it actually lies at twice the focal length from the mirror. The image distance from the mirror equals the object distance (Fig. 10). The closer the object is approached to the mirror, the speedier will the image remove therefrom, a phenomenon accompanied by a continuous increase in the image size. If the object is at the centre C of the radius, it equals the image ($m = m_1$). If the object coincides with the focus, then the rays are reflected parallelly, and the image is thus viewed at infinity.

The real image is always inverse, and is to the size of the object as the image distance is to the object distance. Let the object size be $AB = y$, and the image size be $AB = y_1$, then the magnification will be $N = y_1 : y = k : t$.

A further approximation of the object to the mirror within the range of focal length will cause the rays to be reflected divergently. In this case the image appears to be behind the mirror and is rectified. The analysis of this virtual image, however, falls beyond the scope of the present paper.

Figs. 11 and 12 illustrate the use of a spherical mirror in connection with the new instrument. Tests may be carried out either with the unaided eye, or with the aid of a telescope 8. In both cases, centre 4 fixed onto the upper end of the vertically shiftable metal pipe 3 mounted on carriage 6 may be displaced by means of a wheel 7. Centre 4 is illuminated by a low-tension bulb

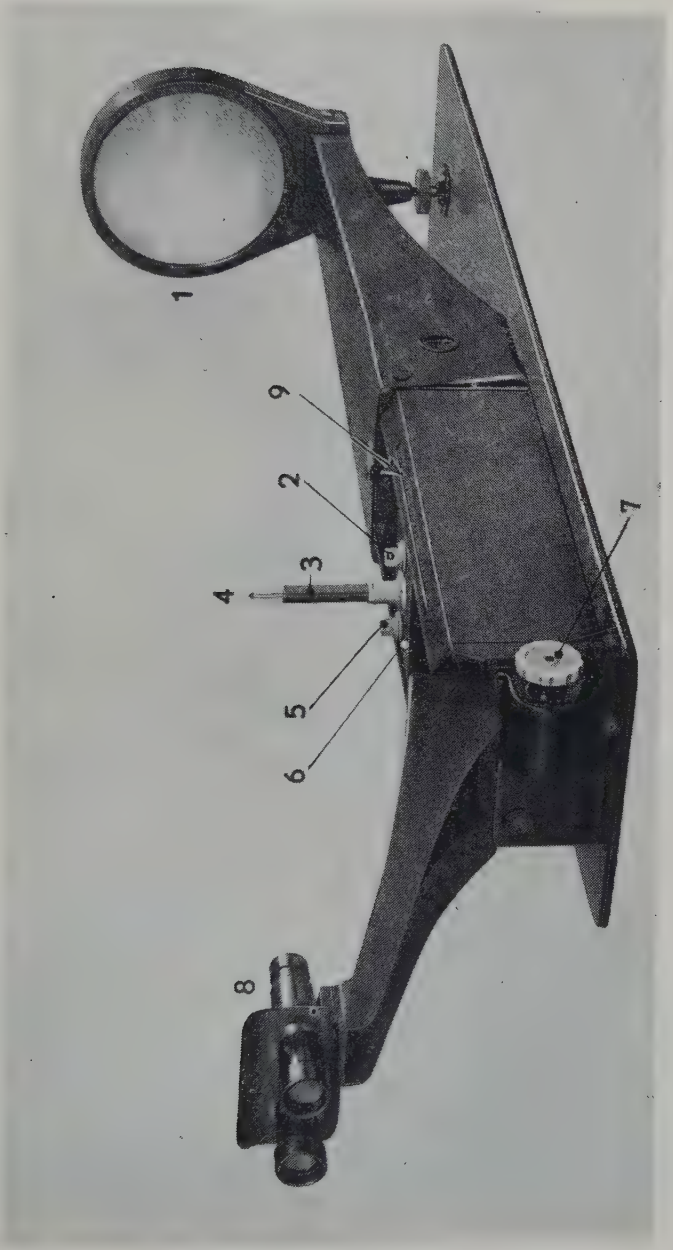

Fig. 11

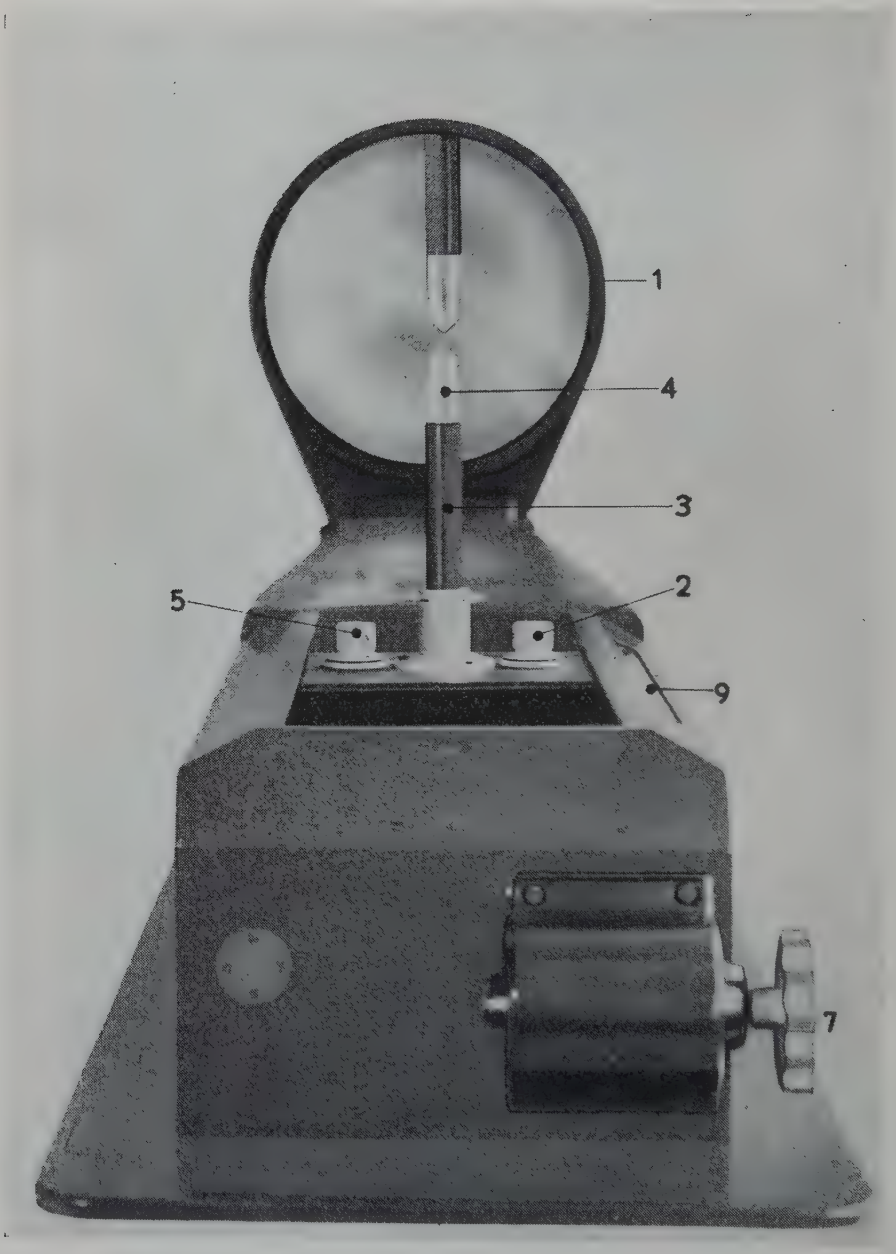

Fig. 12

fixed at the lower end of the pipe. A button 2 is provided for regulating the intensity of illumination by means of an iris diaphragm placed into the pencil of rays. The dial wedged upon the button may have linear, squared or logarithmic indices.

Coming now to the particulars of the apparatus in action, it will be noticed that under normal circumstances the centre will appear white (colourless) but may be turned red, yellow, green or blue, by means of the colour filter adjustable through button 5. If the room is dark, nothing but the illuminated centre and its image will be viewed. The spherical mirror will create an inverse floating image of the centre. If the centre is shifted nearer to or away from, respectively, the mirror, the image will travel in inverse sense. The observer's task is to bring centre and image into depth coincidence. If coincidence is established, centre and image will be of equal size, the centre being distanced at twice the focal length from the mirror. The latter position is called the basic or zero position of the carriage.

Starting now from the basic position, forward or backward adjustment may be read through window 9 from a scale engraved into the non-represented track of the carriage. There being no probability of major errors in adjustment, there are provided 150 1-mm-indices to the right and left of the zero point.

It will be noticed that the size of the travelling image will change with the shifting of the centre. Hence, the question may arise whether it will not be possible for the observer to conclude from the variation of image size upon coincidence, particularly after repeated tests. If the focal length of the mirror is very small, the size of the travelling image will considerably change on the slightest displacement of the object. To obviate this disadvantage, a mirror of great focal length would be necessary which, however, would require considerable displacement of the object in order to achieve a perceivable displacement of the image. It has been found possible to compute, from the variation of the retinal image, the maximum focal length and the corresponding change in image size where this latter does not attain the threshold of perception. Instead of such calculations, however, it has been deemed preferable to determine the focal length and the radius of curvature for the mirror by means of experiments.

Let us consider an example. It is supposed that the observer will not perceive the change in image size as long as the difference in size between the base line on the one hand and the images arising in the two extreme positions — before and behind the centre — on the other does not exceed the one minute of arc resolving power of the eye. Let us now find the focal length of the mirror which will satisfy the said requirement (Fig. 13).

Let the distance of observation between the observer and the centre P in basic position be $S = 5000$ mm, let the centre have a diameter of $d = 20$ mm, and the focal length of the mirror be $f = 800$ mm. When centre P will

stop at twice the focal length ($2f$) before the mirror, object and image will coincide and their sizes will become equal ($t = k$). If this is the case, both centre and image will be in the centre C of the radius of curvature R of the mirror, that is, $t = k = 1{,}600$ mm.

The observer sights both the centre and its equal-sized image at an angle of $\alpha = 13{,}745$ minutes of arc.

1. Shifting the centre by 150 mm, that is, from the basic position P to P_1, the object distance will be $t_1 = 1{,}750$ mm. Image K_1 is at a $k_1 = 1{,}473.68$ mm distance from the mirror, and the observer will perceive the image, magnified to $N = 0{,}842$, at a distance $S_1 = 5{,}126.32$ mm. The image will have a

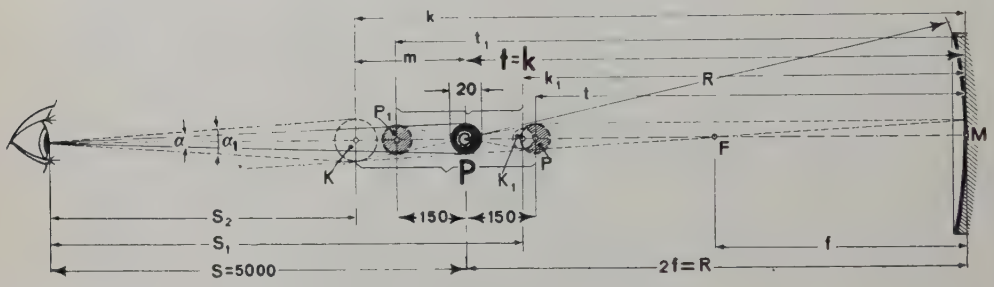

Fig. 13

diameter of 16,842 mm which appears at an angle of $\alpha_1 = 11{,}292$ minutes of arc.

The difference in visual angle between the base line on the one hand, and of the image of the centre in the above-mentioned extreme (exterior) position is $\triangle\alpha = 2{,}453$ minutes of arc, a sensation liable to be perceived, at least theoretically.

2. Let us now displace centre P to position P, that is, behind the basic position. The object distance will then be $t = 1{,}450$ mm and the image distance $k = 1{,}784.61$ mm. The image will be magnified by $N = 1{,}23$ with a diameter of 24,61 mm, and will be viewed by the observer at a distance $S_2 = 4{,}815.39$ mm at an angle $\alpha_1 = 17{,}567$ minutes of arc. The difference in size between the images perceived in the basic position and in the second extreme (posterior) position will be $\triangle\alpha = 3{,}821$ seconds of arc, a sensation falling within the range of perception. In the second case, that is, if the centre is approached to the mirror, the image size will vary at greater speed than in the first case. Hence, it will be more difficult for the observer to perceive the difference in image size than in the first case.

Temporarily accepting the above results, let us find the focal length at which the perception of the variation of image size may be excluded. According to the correlations valid for the spherical mirror and indicated in Fig. 11,

that is, $t = 2f - 150$, $N = k : t$. $m = k - 2f$ one can write

$$S_2 = \frac{4850f - 750{,}000}{f - 150}$$

The mirror of unknown focal length f must come up to the requirement that the visual angle of the observer for the image of the centre be 1 minute of arc in the second — and less advantageous — case. It is therefore necessary that

$$\operatorname{tg} \frac{\alpha}{2} = \frac{10f}{4850f - 750{,}000} = 0{,}002\,291.$$

Of this, the focal length to be determined is

$$f = 1{,}546.092 \text{ mm},$$

and the radius of curvature

$$R = 3{,}092.184 \text{ mm}.$$

It is possible but has been found inconvenient to construct a mirror relying upon these results. The new apparatus was designed with a focal length of $f = 800$ mm, a distance at which the differences of size were no longer perceived by the observer. There may be various reasons for this phenomenon. First, the possibility of perception is reduced by the fact that the displacement of images, that is, the change of the image size is continuous. Surely an intermittent change of image size would not fail to strike the eye. Moreover, the mirror conveys an image of the short illuminated centre only, thus, if the test room is dark, the centre itself appears to be floating in the air. Finally, convergence variation and accomodation also exert a certain influence upon viewing, by distracting the observer's attention from perceiving the sensation caused by the varying image sizes.

The distance for bringing into coincidence object and image with the unaided eye is stipulated by international agreements to be 5 m. This, however requires much space, particularly if there is provided more than one test apparatus. In order to eliminate this inconvenience it has been suggested by the physician Dr. Sándor Lukács to add to the instrument a Galilean telescope (of negative magnification) creating the impression of viewing both centre and image from an actual distance of 5 m. At the present moment, experiments are being conducted to ascertain whether telescoping viewing may be employed without impairing the results. A series of tests will have to be accomplished before a definite answer can be given to the problem.

It was found impossible, owing to the inaccessibility of the adjusting wheel 7, to conduct the test with the unaided eye from a 5 m distance. Hence, the apparatus was designed so as to enable the observer to set the carriage

in motion by means of an electric synchronizing device from any distance, including, of course, that of 5 m.

The following will describe the function of the synchronizing device.

The observer at *S* (Fig. 14) adjusts carriage 9 by means of a wheel 1 bedded in the upper part of column 3 at a 5 m-distance from the apparatus 5. Connection between the two parts of the apparatus is effected by an electric axis, that is, a relay servo system. The servo transmitter 2 is fixed on wheel 1, and the servo receiver is built into apparatus 5. By rotating the servo part 6 the transmission element 10 (and endless rope or chain) wedged on the axis and flung over wheel 11 pushes carriage 9 together with the centre 8 in the direction indicated by the arrows. Images 8′ and 8″ of centre 8, formed by means of the mirror 7 are viewed as the function of the centre's position. The servo transmitter 2 and receiver are connected by a five-stranded cable 4. The stationary part of the servo elements (Fig. 15), that is, of transmitter *A* to be rotated by the observer and of the receiver *B* built into the apparatus is induced by a 110 V mains a. c. Upon turning the adjusting wheel, current is induced in the rotor of transmitter *A*, causing the rotor of receiver *B* to rotate in the same direction and at identical angle. The system is out of gear if the symmetrically wound rotors are in coincidence between the poles of the induced stationary part, so that the connecting cable is free of current. Apart from a very slight slip, there is no lost motion in the function of the machines, that is, they are practically in synchronism.

The apparatus as represented in the last two figures is but a first embodiment intended for laboratory purposes. Any optical and mechanical changes that might seem advantageous will be determined and put into practice after experiments will have been terminated.

It will be noticed that the readings in connection with the centre's position, and their recording require a certain amount of time, to be felt particularly in the case of group tests. Moreover, the tables obtained after repeated tests are not sufficiently distinct. It is, therefore, intended that the next embodiment will comprise a printing device attached to the instrument for recording the repeated positions of the carriage on squared plotting paper. The curve to be obtained by connecting these points will represent the error curve and may be deposited as case history for future reference. This will facilitate the comparison of several observers' stereoscopic vision power.

The image forming power of the simple spherical mirror designed for the purpose of the instrument is far from being perfect. Yet the aberrations in image formation will not confuse the observer as both object and image are positioned in the vicinity of the optical axis. Another reason why said aberrations will not act confusingly is the small size of object and of image.

The apparatus was constructed by the Central Optical and Precision Mechanical Research Laboratory. I should like to express my gratitude therefore

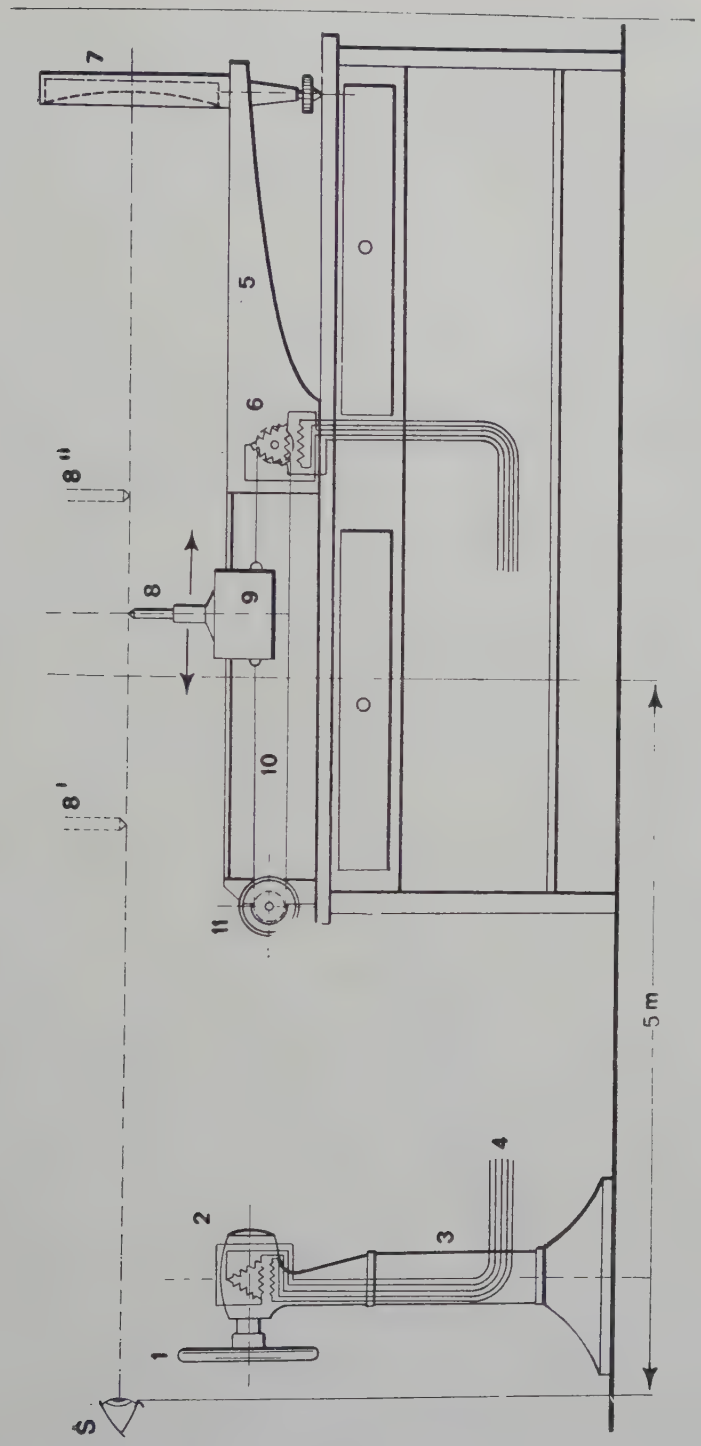

Fig. 14

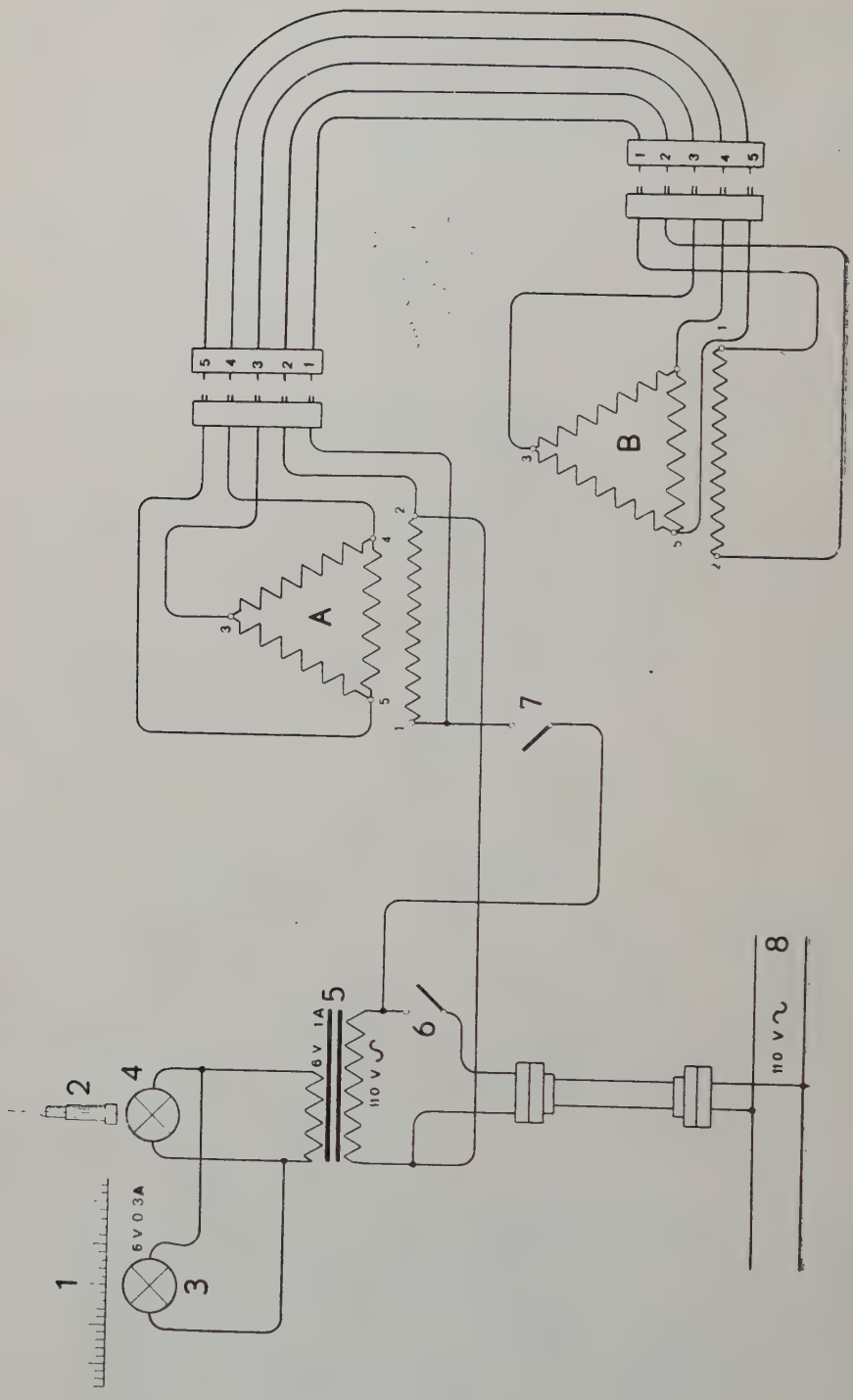

Fig. 15

to the Director of the Institute, the physicist Dr. Ferenc Szalkay whose aid rendered it possible to have the apparatus constructed. I should also like to take this opportunity to express my gratitude to the oculists Dr. Emil Galla and Dr. György Aczél for their untiring work in assisting me with information and helpful suggestions with regard to the technicalities in carrying out and putting into practice the basic idea.

Summary

There are several kinds of instruments for the assessment and determination of stereoscopic vision. In this article author describes a new instrument which can be used independently of the conditions of illumination, taking into account the optical and psychological phenomena connected with stereoscopic vision. The tests are carried out by means of radiation having different wave-lengths and whose strength of illumination can be regulated. The determination of the vision power, which hitherto took place in an intermittent manner, becomes continuous by the use of this instrument and the numerical values are capable of being laid down by means of diagrams. The stereoscopic signal is represented by a movable signal illuminated from the inside by radiation of varying wavelength and by its image produced by a spherical mirror. For the theoretical determination of the focus of spherical mirrors author deals with the general optical-geometrical relations of spherical mirrors. The signal is displaced by hand or by electric command from any distance. Using the instrument in question, it is possible to carry out — in addition to the determina tionof stereoscopic vision power — other tests, too, which latter, however, are not being dealt with in this paper and will be reserved for another publication.

Professor Dr. N. Bárány, Budapest XI., Gombocz Z. u. 17, Hungary

STROMVERDRÄNGUNG VON IN KREISFÖRMIGEN NUTEN GEBETTETEN MASSIVEN LEITERN

Von

R. TUSCHÁK

Lehrstuhl für Betriebswesen elektrischer Maschinen der Technischen Universität, Budapest

(Eingegangen am 1. Januar 1957)

Im Aufsatz angewandte Bezeichnungen

Allgemeine Bemerkung:
Wenn kein besonderer Hinweis, sind sämtliche Größen im MKS Maßsystem zu verstehen.
Einzelne Bezeichnungen:

a_1, a_2	Abkürzung [Gleichungen (A. 3.2), (A. 3.6) und (A. 3.7)]
A_n	Abkürzung [Gleichung (A. 2.1)]
b	Breite der Nutenöffnung
b_1, b_2	Abkürzung [Gleichungen (A. 3.3), (A. 3.8) und (A. 3.9)]
D	Rundstab-Durchmesser
$\mathbf{e}_z$	komplexer Momentanwert der Axialkomponente der elektrischen Feldstärke
$\mathbf{E}_z\ (r, \varphi)$	Komplexamplitude von $\mathbf{e}_z$ in Funktion von r und φ
f	Frequenz
$\mathbf{G}_r$	Komplexamplitude der Radialkomponente des POYNTINGschen Vektors
$\mathbf{h}_r$, $\mathbf{h}_\varphi$	komplexer Momentanwert der Radial- und Tangential-Komponente der magnetischen Feldstärke
$\mathbf{H}_r\ (r, \varphi)$ $\mathbf{H}_\varphi\ (r, \varphi)$	Komplexamplituden von $\mathbf{h}_r$ bzw. $\mathbf{h}_\varphi$
$\hat{\mathbf{H}}\ (r, \varphi)$	Konjugierte von $\mathbf{H}\ (r, \varphi)$
$\mathbf{i}$	komplexer Momentanwert des Stromes
$\mathbf{I}$, $\hat{\mathbf{I}}$	Komplexamplitude von $\mathbf{i}$ bzw. deren Konjugierte
$J_n\ (w)$	BESSELsche Funktion n-ten Grades mit Argument w
$J_n'\ (w)$	Ableitung von $J_n\ (w)$ nach w
k_r, k_{kr}	Widerstandserhöhungsfaktoren [Gleichungen (13a) und (23a)]
κ_x, k_{kx}	Reaktanzabnahmefaktoren [Gleichungen (18) und (26)]
l	Axiallänge des Leiters
$N_n\ (w)$	Neumannfunktion n-ten Grades mit Argument w
R_b	Widerstand des Rundstabes mit Berücksichtigung der Stromverdrängung
R_0	Gleichstromwiderstand des Rundstabes
R_k	zusätzlicher Widerstand des unteren Käfigs auf Wirkung der im oberen Käfig entstehenden Wirbelstromverluste
r_0	Radius des Rundstabes
v	$\frac{w_0}{2}$
w	Abkürzung [Gleichung (8a)]
w_0	Wert von w an der Stelle $r = r_0$
X_b	Teil der Reaktanz des Rundstabes, der von den mit dem Leiter verketteten Nutenstreukraftlinien herrührt
X_k	Teil der Reaktanz des unteren Käfigs, der von den mit den Stäben des oberen Käfigs verketteten Kraftlinien herrührt
$\mathbf{Z}_b$, $\mathbf{Z}_k$	Impedanzen mit derselben Deutung wie X_b und X_k
$\mathbf{Z}_{12}$	gegenseitige Impedanz zwischen den Stäben des unteren und oberen Käfigs
$\mathbf{Z}_{12}'$	Teil von $\mathbf{Z}_{12}$, der von den mit dem oberen Rundstab verketteten Kraftlinien herrührt
$\mathbf{Z}_{22}$	Eigenimpedanz des unteren Käfigs
$\mathbf{Z}_{22}'$	dasselbe wie $\mathbf{Z}_k$
α	b/D
δ	Abkürzung [Gleichung (15a)]
λ	Streuleitfähigkeit
$\lambda_= : \lambda_\sim$	Gleichstrom- bzw. Wechselstrom-Streuleitfähigkeit
λ_k	dem Reaktanzteil X_k entsprechende Streuleitfähigkeit
μ_0	Permeabilität der Luft
ω	Kreisfrequenz des Wechselstromes
σ	spezifische Leitfähigkeit
ϱ	spezifischer Widerstand in Ohm/m/mm²

I. Einleitung

Die Dämpferwicklung von Ein- und Dreiphasen-Synchronmaschinen sowie die Läuferwicklung von Doppelkäfigläufer-Asynchronmaschinen besteht in vielen Fällen aus Rundstäben. Die sich in den Stäben abspielenden Wirbelstromerscheinungen können einige wichtige Kennwerte der Maschinen (z. B. in selbstanlaufenden Synchronmaschinen das Anlaßmoment, in Einphasen-Synchronmaschinen die Größe des gegenlaufenden Feldes usw.) in starkem Maße beeinflussen, weshalb es erwünscht ist, beim Entwurf der Maschine die infolge der Stromverdrängung der Stäbe entstehende Widerstandserhöhung bzw. Reaktanzabnahme zu kennen.

Die Stromverdrängungserscheinungen in rechteck- und trapezförmigen oder aus diesen zusammenstellbaren verwickelteren, z. B. L-förmigen Nuten sind in der Literatur ausführlich erörtert. Für diese Fälle stehen zur Berechnung der Leiterimpedanzen entsprechende Beziehungen und in den meisten Fällen auch Tabellen zur Verfügung [5, 7, 8, 9]. Für die in kreisförmige Nuten gebetteten Stäbe sind unseres Wissens in der Literatur keine ähnlichen genauen Berechnungen zu finden. Es sind zwar einige, durch sehr starke Vereinfachung des physikalischen Bildes abgeleitete oder auf empirischem Wege erhaltene Ergebnisse bekannt, deren Anwendungsgebiet und Annäherungsgüte jedoch nur dann befriedigend bestimmt werden könnten, wenn sie mit ins physikalische Bild besser passenden, genaueren Ergebnissen verglichen werden könnten.

Im nachfolgenden wird ein Verfahren beschrieben, das mit dem physikalischen Bild in sehr guter Übereinstimmung steht und mit welchem die infolge Stromverdrängung eintretende Widerstandserhöhung und Reaktanzabnahme der in kreisförmige Nuten gebetteten Stäbe bestimmt werden kann.

II. Grundgleichungen

Nehmen wir an, daß in einem Stab vom Durchmesser D laut Abb. 1*a* in Axialrichtung ein zeitlich sinusförmiger Wechselstrom von maximalem Wert $\mathbf{I}$ fließt. Der Stab füllt die Nut vollkommen aus, entweder gibt es keine Isolierung oder sie ist vernachlässigbar dünn. Nutenöffnung b ist im Verhältnis zum Stabdurchmesser nicht übermäßig groß. Die Permeabilität des Eisens wird — wie bei solchen Rechnungen allgemein üblich — für unendlich groß betrachtet, d. h. die auf das Eisen entfallende magnetische Spannung wird im Vergleich zur auf die Nutenöffnung entfallenden magnetischen Spannung vernachlässigt. Es wird angenommen, daß das axiale Maß des Stabes im Vergleich zum Durchmesser äußerst groß, also die Wirbelstrom- bzw. Magnetfeld-Verteilung in Axialrichtung homogen ist.

Unter obigen Bedingungen hat die elektrische Feldstärke am Stab nur axiale ($\mathbf{e}_z$), die magnetische Feldstärke radiale ($\mathbf{h}_r$) und tangentiale ($\mathbf{h}_\varphi$) Komponenten.

Die Verteilung der elektrischen und magnetischen Feldstärke im Innern des Stabes und in der Nutenöffnung wird durch solche Funktionen ausgedrückt,

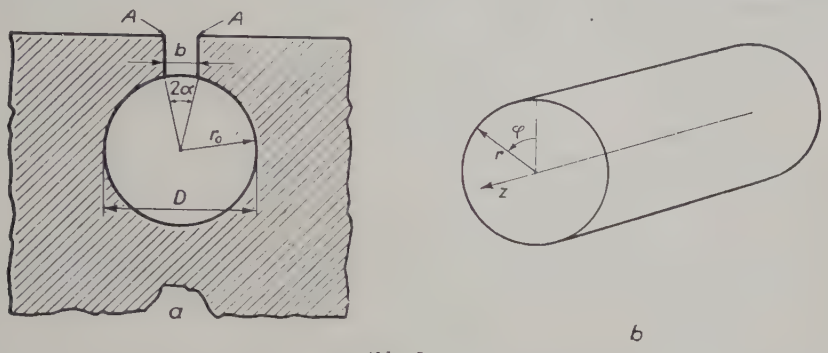

Abb. 1

die in den einzelnen Feldteilen sowohl die MAXWELLschen Gleichungen befriedigen als auch den auf die Grenzflächen bezüglichen Brechungsgesetzen Genüge

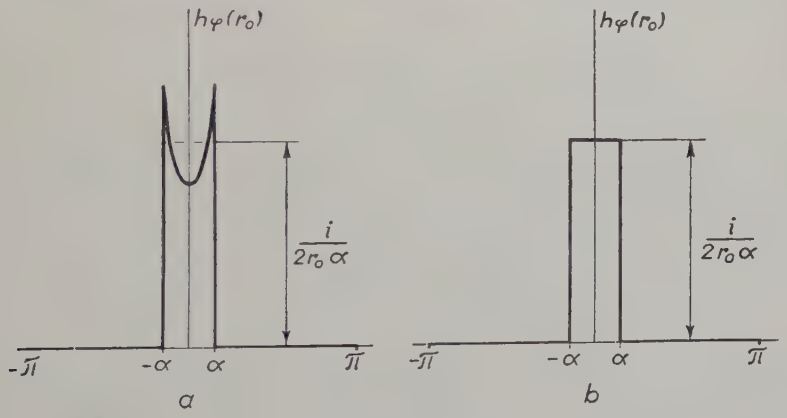

Abb. 2

leisten. Eine genaue Bestimmung solcher Lösung stößt auf große mathematische Schwierigkeiten. Zwecks Vermeidung dieser Hindernisse wird auch eine annähernde, aber mit dem physikalischen Bild gut übereinstimmende vereinfachende Annahme gemacht.

In der Nutenöffnung verteilt sich die Tangentialkomponente der Feldstärke am Radius $r = r_0$ in der Wirklichkeit qualitativ laut Abb. 2*a*. Die Punkte α bzw. $-\alpha$ entsprechen den Punkten *A* in Abb. 1*a*. Innerhalb der Strecke zwi-

schen den beiden Punkten ändert sich der Wert der Feldstärke nicht stark, in den Punkten α und $-\alpha$ sowie in ihrer unmittelbarer Umgebung kann er — vor allem von den Krümmungsverhältnissen der Punkte A abhängig — von den im Innern der Strecke erscheinenden Werten in größerem Maße abweichen.

Im folgenden wird die Ungleichmäßigkeit der Feldstärken-Verteilung außer acht gelassen und mit der durchschnittlichen tangentialen Feldstärke der gestrichelten Linie in Abb. 2*a* entsprechend gerechnet. Somit ist laut Abb. 2*a* auf der Strecke $-\pi < \varphi < -\alpha$ und $\alpha < \varphi < \pi$

$$\mathbf{h}_\varphi (r_0) = 0 ,$$

und auf der Strecke $-\alpha < \varphi < \alpha$

$$\mathbf{h}_\varphi (r_0) = \frac{\mathbf{i}}{b} = \frac{\mathbf{i}}{2 r_0 \alpha} , \tag{1}$$

wo

$$\mathbf{i} = \mathbf{I} e^{j\omega t} \tag{2}$$

der komplexe Momentanwert des Stromes ist.

Die in Abb. 2*b* dargestellte Feldstärkenverteilung kann als ein Abschnitt der periodischen Funktion nach 2π aufgefaßt werden, somit mit der FOURIERschen Reihe erzeugt werden. Nach Bestimmung der Koeffizienten der FOURIERschen Reihe erhalten wir:

$$\mathbf{h}_\varphi (r_0) = \frac{\mathbf{i}}{2 r_0 \pi} + \sum_{n=1}^{\infty} \frac{\mathbf{i}}{r_0 \pi} \frac{\sin n \alpha}{n \alpha} \cos n \varphi . \tag{3}$$

Die Aufgabe ist nun, im Innern des Stabes eine, die MAXWELLschen Gleichungen befriedigende Lösung zu finden, die am Radius $r = r_0$ auch der obigen Gleichung Genüge leistet.

Die auf den Stab bezüglichen MAXWELLschen Gleichungen sind:

$$\operatorname{rot} \mathbf{h} = \sigma \mathbf{e} \tag{4a}$$

$$\operatorname{rot} \mathbf{e} = -\mu \frac{\partial \mathbf{h}}{\partial t} . \tag{4b}$$

Nehmen wir an, daß die Lösung folgende Form hat:

$$\mathbf{h}_r = \mathbf{H}_r (r, \varphi) e^{j\omega t} \tag{5a}$$

$$\mathbf{h}_\varphi = \mathbf{H}_\varphi (r, \varphi) e^{j\omega t} \tag{5b}$$

$$\mathbf{e}_z = \mathbf{E}_z (r, \varphi) e^{j\omega t} . \tag{5c}$$

Werden diese Werte in die Gleichungen (4) eingesetzt und die Komponenten der Rotation nach Abb. 1*b* im Zylinderkoordinatensystem aufgeschrieben, so gelangen wir zum folgenden Differentialgleichungssystem :

$$\frac{\partial^2 \mathbf{E}_z(r,\varphi)}{\partial r^2} + \frac{1}{r}\frac{\partial \mathbf{E}_z(r,\varphi)}{\partial r} + \frac{1}{r^2}\frac{\partial^2 \mathbf{E}_z(r,\varphi)}{\partial \varphi^2} - j\omega\mu_0\sigma\mathbf{E}_z = 0 \qquad (6a)$$

$$\mathbf{H}_r(r,\varphi) = -\frac{1}{j\omega\mu_0 r}\frac{\partial \mathbf{E}_z(r,\varphi)}{\partial \varphi} \qquad (6b)$$

$$\mathbf{H}_\varphi(r,\varphi) = \frac{1}{j\omega\mu_0}\frac{\partial \mathbf{E}_z(r,\varphi)}{\partial r}. \qquad (6c)$$

Die Lösung des Gleichungssystems mit Berücksichtigung der Gleichung (3) (s. Anhang 1) ergibt :

$$\mathbf{E}_z(r,\varphi) = \mathbf{I}\left[\frac{j\omega\mu_0}{2\pi w_0}\cdot\frac{\mathrm{J}_0(w)}{\mathrm{J}_0'(w_0)} + \frac{j\omega\mu_0}{w_0\pi}\sum_{n=1}^{\infty}\frac{\mathrm{J}_n(w)}{\mathrm{J}_n'(w_0)}\cdot\frac{\sin n\alpha}{n\alpha}\cos n\varphi\right] \qquad (7a)$$

$$\mathbf{H}_r(r,\varphi) = \frac{\mathbf{I}}{\pi}\left[\frac{1}{w_0 r}\sum_{n=1}^{\infty}\frac{\mathrm{J}_n(w)}{\mathrm{J}_n'(w_0)}\cdot\frac{\sin n\alpha}{\alpha}\sin n\varphi\right] \qquad (7b)$$

$$\mathbf{H}_\varphi(r,\varphi) = \frac{\mathbf{I}}{\pi}\left[\frac{1}{2r_0}\frac{\mathrm{J}_0'(w)}{\mathrm{J}_0'(w_0)} + \frac{1}{r_0}\sum_{n=1}^{\infty}\frac{\mathrm{J}_n'(w)}{\mathrm{J}_n'(w_0)}\frac{\sin n\alpha}{n\alpha}\cos n\varphi\right], \qquad (7c)$$

wo

$$w = \sqrt{-j\omega\mu_0\sigma}\, r \qquad (8a)$$

$$w_0 = \sqrt{-j\omega\mu_0\sigma}\, r_0 \qquad (8b)$$

$\mathrm{J}_n(w)$ — BESSELsche Funktion n-ten Grades mit Argument w,
$\mathrm{J}_n'(w)$ — Ableitung von $\mathrm{J}_n(w)$ nach w ist.

Die Komplexleistung des Leiters kann einerseits mit dem Flächenintegral des komplexen Vektors der Energieströmung (POYNTINGscher Vektor), andrerseits mit der Innenimpedanz $\mathbf{Z}_\mathrm{b}$ und dem Strom $\mathbf{I}$ des Stabes ausgedrückt werden. Aus dem Vergleich der beiden verschiedenartig gewonnenen Ergebnisse kann die Innenimpedanz $\mathbf{Z}_\mathrm{b}$ bestimmt werden.

Die Radialkomponente des komplexen POYNTINGschen Vektors am Radius $r = r_0$ ist

$$\mathbf{G}_r(r_0) = \mathbf{E}_z(r_0,\varphi)\,\hat{\mathbf{H}}_\varphi(r_0,\varphi), \qquad (9)$$

wo $\hat{\mathbf{H}}$ die Konjugierte des Vektors $\hat{\mathbf{H}}$ ist.

Die komplexe Leistung ist

$$\mathbf{S} = \int_F \mathbf{G}_r \, dF = \int_F \mathbf{E}_z (r_0, \varphi) \, \hat{\mathbf{H}}_\varphi (r_0, \varphi) \, dF = \mathbf{I} \hat{\mathbf{I}} \mathbf{Z}_b = I^2 (R_b + jX_b) , \tag{10}$$

wo

$$\mathbf{Z}_b = R_b + jX_b . \tag{11}$$

Nach Ermittlung des Integrals der Gleichung (10) mit Hilfe der Gleichung (7) (die Einzelheiten der Berechnung sind im Anhang 2 zu finden) erhalten wir für Z_b folgenden Ausdruck:

$$\mathbf{Z}_b = R_0 \left\{ \frac{|w_0|^2}{2} \frac{j J_0 (w_0)}{w_0 J_0' (w_0)} + |w_0|^2 \sum_{n=1}^{\infty} \frac{j J_n (w_0)}{w_0 J_n' (w_0)} \left(\frac{\sin n\alpha}{n\alpha} \right)^2 \right\}, \tag{12}$$

wo R_0 der Gleichstromwiderstand des Stabes ist:

$$R_0 = \frac{l}{\sigma r_0^2 \pi} .$$

Nach Absonderung der realen und imaginären Teile erhalten wir

$$R_b = R_0 \left\{ \mathrm{Re} \left[\frac{|w_0|^2}{2} \cdot \frac{j J_0 (w_0)}{w_0 J_0' (w_0)} + |w_0|^2 \sum_{n=1}^{\infty} \frac{j J_n (w_0)}{w_0 J_n' (w_0)} \left(\frac{\sin n\alpha}{n\alpha} \right)^2 \right] \right\} =$$

$$= R_0 (1 + k_r) \tag{13a}$$

$$\lambda = \frac{X_b}{\omega \mu_0 l} = \frac{1}{\pi} \mathrm{Im} \left\{ \frac{j J_0 (w_0)}{2 w_0 J_0' (w_0)} + \sum_{n=1}^{\infty} \frac{j J_n (w_0)}{w_0 J_n' (w_0)} \left(\frac{\sin n\alpha}{n\alpha} \right)^2 \right\}. \tag{13b}$$

Zur Ermittlung von R_b und λ ist die Kenntnis des Wertes der Besselschen Funktionen mit Argument $\sqrt{-j}$ notwendig. Diese Funktionen sind nur für die Werte $n = 0, 1, 2$ tabelliert [12]. In den Berechnungen mit den Gleichungen (13) sind bei den praktisch vorkommenden Leiterabmessungen mindestens 6—8 Glieder in Betracht zu ziehen, wenn wir annehmbare Genauigkeit zu erreichen wünschen. Glücklicherweise können die Besselschen Funktionen im Falle der praktischen Werte von w_0 mit den ersten Gliedern ihrer Potenzreihe gut angenähert werden, so daß mit den Potenzreihen die Gleichungen (13) verhältnismäßig einfach berechnet werden können.

III. Wechselstromwiderstand des in kreisförmige Nuten gebetteten Stabes

Nach Gleichung (13*a*) ist

$$R_b = R_0(1 + k_r). \tag{13a}$$

Mit den vorerwähnten Potenzreihen wurden die Werte des Faktors k_r bestimmt. Die ausführlichen Berechnungen sind im Anhang 3 zu finden. Die Endergebnisse sind in Tab. I und im Diagramm der Abb. 3 enthalten.

Die in der Tabelle und im Diagramm benützten Bezeichnungen sind:

$$\delta = \sqrt{2}\,|w_0| = \sqrt{\frac{\omega\mu_0\sigma}{2}}\,D; \tag{14}$$

δ ist eigentlich das Verhältnis zwischen Eindringtiefe und Durchmesser. Wird der Durchmesser, wie in der Praxis üblich, in mm gemessen und anstatt mit der Leitfähigkeit mit dem in Ohm/m/mm² ausgedrückten spezifischen Widerstand ϱ gerechnet, so wird:

$$\delta = \frac{2\pi}{10}\sqrt{\frac{10^{-5}f}{\varrho}}\,D^{[\mathrm{mm}]}. \tag{15a}$$

Tabelle I

Werte des Faktors k_r

δ	$\alpha = 0{,}05$	$\alpha = 0{,}1$	$\alpha = 0{,}2$	$\alpha = 0{,}3$	$\alpha = 0{,}4$	$\lvert w_0\rvert$
0,282	0,00	0,00	0,00	0,00	0,00	0,2
0,424	0,00	0,00	0,00	0,00	0,00	0,3
0,565	0,01	0,01	0,01	0,01	0,01	0,4
0,705	0,02	0,02	0,02	0,02	0,02	0,5
0,850	0,04	0,04	0,04	0,04	0,04	0,6
0,990	0,08	0,08	0,07	0,07	0,07	0,7
1,130	0,13	0,13	0,12	0,12	0,11	0,8
1,270	0,20	0,20	0,19	0,19	0,18	0,9
1,420	0,30	0,30	0,29	0,28	0,27	1,0
1,555	0,43	0,43	0,42	0,40	0,38	1,1
1,700	0,59	0,59	0,57	0,55	0,52	1,2
1,840	0,78	0,77	0,75	0,72	0,68	1,3
1,980	1,00	0,99	0,96	0,92	0,87	1,4
2,120	1,24	1,23	1,20	1,14	1,08	1,5
2,260	1,51	1,50	1,45	1,38	1,31	1,6

Für Kupferleiter ergibt sich bei $f = 50$ Hz, $\varrho = 0{,}021$ Ohm/m/mm^2

$$\delta = \frac{D^{[\mathrm{mm}]}}{10{,}3}. \tag{15b}$$

Die Breite der Nutenöffnung ist durch Winkel α gekennzeichnet. Auf Grund der Abb. 1 ist

$$\alpha = \frac{b}{D}. \tag{15c}$$

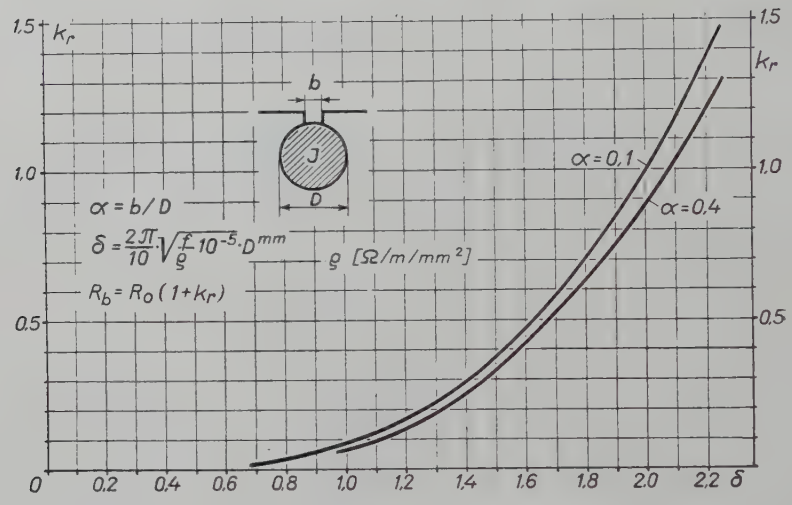

Abb. 3

Nachdem der Widerstandserhöhungsfaktor nur in geringem Maße von α abhängt, wurden im Diagramm im Interesse der Übersichtlichkeit nur die den Werten $\alpha = 0{,}1$ und $\alpha = 0{,}4$ entsprechenden Kurven gezeichnet. In Tab. I sind auch für andere α-Werte Angaben enthalten.

Auf Grund der Kurven kann festgestellt werden, daß der Widerstandserhöhungsfaktor etwa so groß ist wie der eines Quadratprofilleiters, dessen Seite dem Kreisdurchmesser gleicht.

Beispiel

Dämpferwicklungsstab aus Kreisprofilkupfer von 15 mm Durchmesser. Nutenöffnung $b = 3$ mm. Es werde die Widerstandserhöhung für $f = 50$ Hz und $f = 100$ Hz bestimmt.

$$\alpha = \frac{b}{D} = 0{,}2$$

Für $f = 50$ Hz:

$$\delta = \frac{15}{10{,}3} = 1{,}45.$$

Aus dem Diagramm bzw. aus der Tabelle erhalten wir durch Interpolation

$$k_r = 0{,}33.$$

Für $f = 100$ Hz:

$$\delta = \frac{2{,}15}{10{,}3} = 2{,}06 \qquad k_r = 1{,}08\,.$$

IV. Streuleitfähigkeit des in kreisförmigen Nuten gebetteten massiven Leiters

Auf Grund der Gleichung (13*b*) wird vor allem die sogenannte Gleichstrom-Streuleitfähigkeit ($\omega \to 0$) bestimmt. Nachdem in der Gleichung der Grenzübergang $w_0 \to 0$ gemacht wurde (s. Anhang 4), erhalten wir:

$$\lambda_= = \frac{1}{\pi}\left[\frac{1}{8} + \sum_{n=1}^{\infty} \frac{1}{n}\left(\frac{\sin n\alpha}{n\alpha}\right)^2\right]. \tag{16}$$

Dieses Resultat könnte auch unmittelbar aus der Differentialgleichung der Feldverteilung gewonnen werden, falls angenommen würde, daß die Stromverteilung im Querschnitt gleichmäßig erfolgt.

Die Summe der unendlichen Reihe in Gleichung (16) ergibt sich für die untersuchten α-Werte folgendermaßen:

$$\sum_{n=1}^{\infty} \frac{1}{n}\left(\frac{\sin n\alpha}{n\alpha}\right)^2 \cong \frac{3}{2} - \ln 2\alpha = 0{,}807 - \ln \alpha\,. \tag{17}$$

Durch Berechnung mit Hilfe dieser Gleichung der Gleichstrom-Streuleitfähigkeit für verschiedene α-Werte erhalten wir die Kurve der Abb. 4. Die berechneten Werte sind in Spalte $\delta = 0$ der Tab. II*a* enthalten.

Diese Werte der Gleichstrom-Streuleitfähigkeit sind in der Literatur bereits bekannt. Rhea [1, 3] hat schon im Jahre 1927 die Differentialgleichung der Feldverteilung für kreisförmige Nuten mittels Fourierscher Randbedingung und unter Voraussetzung einer gleichmäßigen Stromverteilung gelöst. Später hat Rothert [2] ähnliche Rechnungen durchgeführt und ein Kraftlinienbild gezeichnet, das er auf Grund des analytischen Ausdruckes für das Vektorpotential erhielt. Daraus hat er für einige Fälle die Streuleitfähigkeit bestimmt. Auf die hier beschriebene Weise können aber die Rechnungen bedeutend einfacher und schneller gemacht werden. Übrigens sind in Abb. 4 die von Rothert berechneten Werte mit Kreisen bezeichnet. Wie ersichtlich, fallen diese — den ersten Punkt ausgenommen — auf die von uns festgestellte Kurve. Rothert hat auch Messungen durchgeführt, deren Ergebnisse mit den Rechnungen praktisch gut übereinstimmten.

Jedenfalls ist aus den Kurven ersichtlich, daß die Streuleitfähigkeit beträchtlich vom Verhältnis der Nutenöffnung und des Durchmessers abhängt.

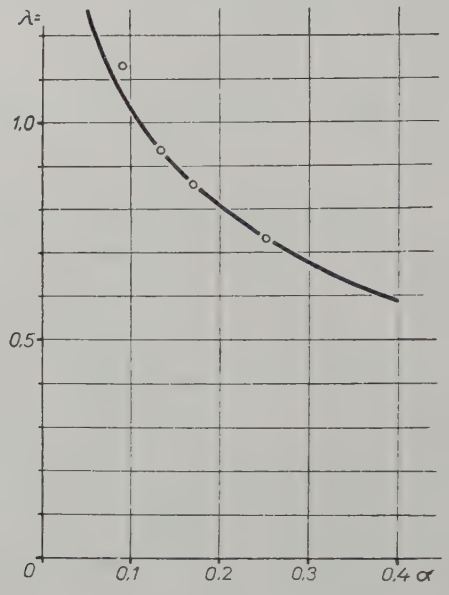

Abb. 4

Die in der Literatur oft vorkommende Feststellung, wonach die Gleichstromleitfähigkeit der Kreisprofilnute 0,66 ist, trifft nur unter bestimmten Bedingungen zu und kann in ungünstigem Falle beträchtliche Fehler verursachen.

Aus Gleichung (13*b*) kann auch die mit Berücksichtigung der Wirbelstromwirkungen berechnete Streuleitfähigkeit bestimmt werden. Die Ergebnisse der im Anhang 4 angegebenen Berechnungen sind in Tab. II*a* und II*b* sowie

Tabelle IIa

Werte der Streuleitfähigkeiten $\lambda_=$ und $\lambda_\sim$

δ	$\alpha = 0{,}05$	$\alpha = 0{,}1$	$\alpha = 0{,}2$	$\alpha = 0{,}3$	$\alpha = 0{,}4$	$\lvert w_0 \rvert$
0	1,250	1,028	0,810	0,680	0,589	0
1,415	1,237	1,005	0,785	0,657	0,567	1,0
1,700	1,210	0,985	0,766	0,637	0,548	1,2
1,98	1,177	0,954	0,739	0,609	0,520	1,4
2,26	1,143	0,921	0,695	0,576	0,488	1,6

Tabelle IIb

Werte des Faktors $k_X = \frac{\lambda_\sim}{\lambda_=}$

δ	$\alpha = 0{,}05$	$\alpha = 0{,}1$	$\alpha = 0{,}2$	$\alpha = 0{,}3$	$\alpha = 0{,}4$	$\lvert w_0 \rvert$
1,415	0,982	0,978	0,970	0,967	0,964	1,0
1,700	0,968	0,958	0,946	0,939	0,932	1,2
1,980	0,942	0,927	0,912	0,896	0,883	1,4
2,260	0,914	0,895	0,864	0,847	0,829	1,6

in Abb. 5 enthalten. In der Abbildung und in den Tabellen bedeutet k_x den Reaktanzabnahmefaktor:

$$k_X = \frac{\lambda_\sim}{\lambda_=}. \tag{18}$$

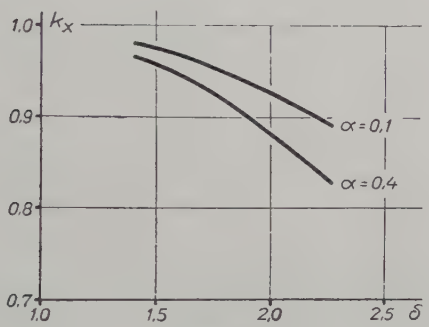

Abb. 5

Nachdem k_x bei den kleineren Werten von δ in der Nähe der Einheit liegt, wurden hier im Vergleich zum Widerstandserhöhungsfaktor wesentlich weniger Punkte berechnet.

V. Gegenseitige Impedanz in Doppelkäfig-Anordnung

Auf Grund des Vorhergehenden ist es möglich, auch verwickeltere Fälle zu untersuchen.

Abb. 6 zeigt eine Doppelkäfiganordnung. Der obere Käfig besteht aus Rundstäben, der Leiterquerschnitt des unteren Käfigs kann beliebig sein. Die obere und untere Nutenöffnung der Kreisprofilnute ist b. Die im oberen

und unteren Käfig fließenden Ströme sind:

$$\mathbf{i}_1 = \mathbf{I}_1 e^{j\omega t} \tag{19a}$$

$$\mathbf{i}_2 = \mathbf{I}_2 e^{j\omega t} . \tag{19b}$$

Bevor wir uns mit der Frage im allgemeinen beschäftigen, wollen wir untersuchen, welche Wirkung die Wirbelströme des oberen Käfigs auf die Impe-

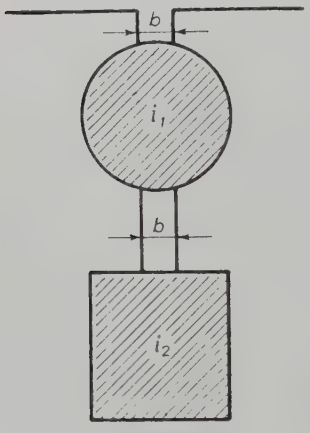

Abb. 6

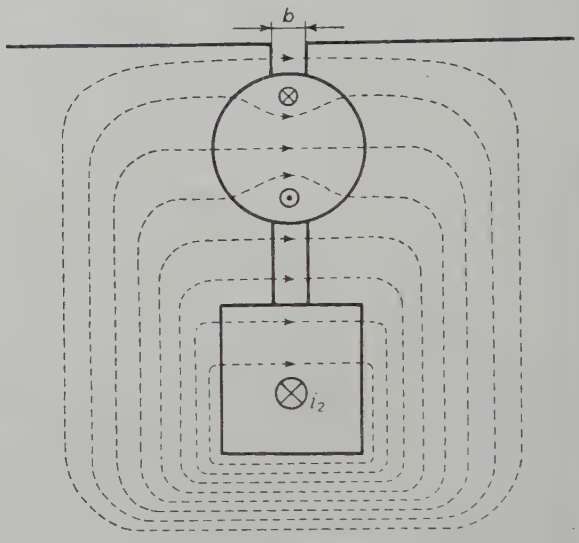

Abb. 7

danz des unteren Käfigs im Falle $\mathbf{i}_1 = 0$ ausüben. Dieser Fall kommt nämlich bei den sogenannten Blindstabläufern vor, wo die oberen Stäbe nicht mit Ringen zum Käfig vereint sind und in diesen nur die Nutstreukraftlinien der unteren Stäbe Wirbelströme induzieren, die sich innerhalb des Stabes schließen.

Die Verteilung der Streukraftlinien und der Wirbelströme des oberen Stabes ist in Abb. 7 schematisch dargestellt.

Die Impedanz des unteren Leiters ist, entsprechend den Kraftlinien, aus mehreren Teilen zusammengesetzt, die über die einzelnen Abschnitte durchgehen. Im weiteren wollen wir uns nur mit der Berechnung jenes Teiles beschäftigen, der den Streukraftlinien über den oberen Leiter von Durchmesser D entspricht, da die übrigen Teile der Impedanz von der Form des oberen Käfigs unabhängig sind und auf übliche Weise berechnet werden können. Wird der erwähnte Teil der Impedanz des unteren Leiters mit Z_k bezeichnet, ergibt sich die dementsprechende komplexe Leistung zu:

$$\mathbf{S} = \mathbf{I}_2 \hat{\mathbf{I}}_2 \mathbf{Z}_k = \mathbf{I}_2 \hat{\mathbf{I}}_2 (R_k + jX_k) . \tag{20}$$

Diese komplexe Leistung kann, ähnlich zum im Abschnitt II angewendeten Verfahren, auch mit Hilfe des auf die Oberfläche des Rundstabes berechneten POYNTINGschen Vektors bestimmt werden. Die Änderung der tangentialen Feldstärke am Stabumfang bei den angedeuteten Bedingungen ist — gleichmäßige Feldstärkenverteilung bei der Nutenöffnung vorausgesetzt — in Abb. 8 dargestellt.

Die der Abb. 8 entsprechende FOURIERsche Reihe ist :

$$\mathbf{h}_{\varphi}(r_0) = \frac{2\mathbf{I}_2}{r_0 \pi} \sum_{\nu=1}^{\infty} \frac{\sin(2\nu-1)\alpha}{(2\nu-1)\alpha} \cos(2\nu-1)\varphi\, e^{j\omega t}. \tag{21}$$

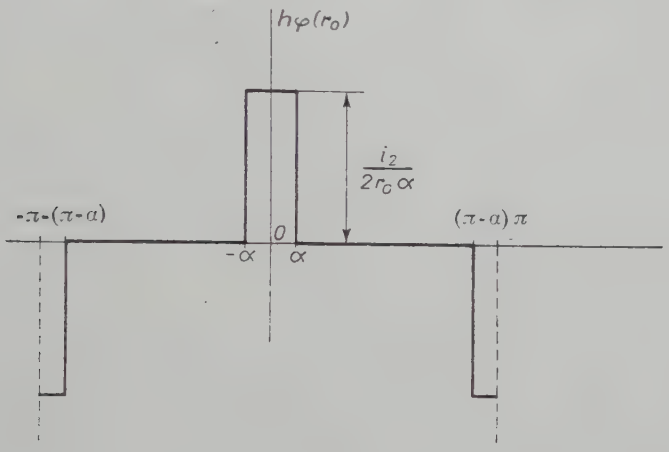

Abb. 8

Die die Randbedingung (21) befriedigende Lösung des Differentialgleichungssystems (6) weicht lediglich insofern von den Gleichungen (7) ab, daß $2\mathbf{i}_2$ an Stelle von $\mathbf{i}$ einsuzetzen ist und bei der Summierung nur die Glieder von ungerader Ordnungszahl zu berücksichtigen sind ($n = 2\nu - 1$). Somit wird :

$$\mathbf{E}_z(r, \varphi) = \frac{2j\omega\mu_0}{\pi w_0} \mathbf{I}_2 \sum_{\nu=1}^{\infty} \frac{J_{(2\nu-1)}(w)}{J'_{(2\nu-1)}(w_0)} \cdot \frac{\sin(2\nu-1)\alpha}{(2\nu-1)\alpha} \cos(2\nu-1)\varphi\,. \tag{22}$$

Werden der Vektor der Energieströmung und die komplexe Leistung auf die im Anhang 5 angegebene Weise berechnet und mit Gleichung (20) verglichen, so ergeben sich für die realen und imaginären Teile von $\mathbf{Z}_k$ nachstehende Ausdrücke :

$$R_k = 4R_{01}|w_0|^2 \cdot \mathrm{Re}\left\{\sum_{\nu=1}^{\infty} \frac{j\,\mathrm{J}_{(2\nu-1)}(w_0)}{w_0\,\mathrm{J}'_{(2\nu-1)}(w_0)} \left[\frac{\sin(2\nu-1)\,\alpha}{(2\nu-1)\,\alpha}\right]^2\right\} = R_{01}\,k_{kr} \qquad (23a)$$

$$\lambda_k = \frac{X_k}{\omega\mu_0 l} = \frac{4}{\pi}\,\mathrm{Im}\left\{\sum_{\nu=1}^{\infty} \frac{j\,\mathrm{J}_{(2\nu-1)}(w_0)}{w_0\,\mathrm{J}'_{(2\nu-1)}(w_0)} \left[\frac{\sin(2\nu-1)\,\alpha}{(2\nu-1)\,\alpha}\right]^2\right\}. \qquad (23b)$$

Die Werte von k_{kr} sind in Tab. III und im Diagramm der Abb. 9 in Funktion von δ und α angegeben. Wie ersichtlich, sind bei gleichen Abmessungen die zusätzlichen Verluste wesentlich größer, als wenn Strom $\mathbf{i}_2$ durch einen Rundstab fließen würde.

Die Streuleitfähigkeit beträgt bei der Frequenz $f = 0$:

$$\lambda_{k=} = \frac{4}{\pi} \sum_{\nu=1}^{\infty} \frac{1}{2\nu-1} \left[\frac{\sin(2\nu-1)\,\alpha}{(2\nu-1)\,\alpha}\right]^2 . \qquad (24)$$

Im Falle der untersuchten Abmessungen ergibt sich die Summe der unendlichen Reihe zu:

$$\sum_{\nu=1}^{\infty} \frac{1}{2\nu-1} \left[\frac{\sin(2\nu-1)\,\alpha}{(2\nu-1)\,\alpha}\right]^2 \cong \frac{3}{4} - \frac{\ln\alpha}{2} . \qquad (25)$$

Tabelle III

Werte des Faktors k_{kl}

δ	$\alpha = 0{,}05$	$\alpha = 0{,}1$	$\alpha = 0{,}2$	$\alpha = 0{,}3$	$\alpha = 0{,}4$	$\lvert w_0\rvert$
0,282	0,00	0,00	0,00	0,00	0,00	0,2
0,424	0,01	0,01	0,01	0,01	0,01	0,3
0,565	0,03	0,03	0,03	0,02	0,02	0,4
0,705	0,07	0,07	0,07	0,06	0,06	0,5
0,850	0,14	0,14	0,14	0,13	0,13	0,6
0,990	0,25	0,25	0,24	0,24	0,23	0,7
1,130	0,42	0,42	0,41	0,40	0,39	0,8
1,270	0,67	0,66	0,65	0,63	0,61	0,9
1,415	0,99	0,98	0,97	0,94	0,91	1,0
1,555	1,41	1,40	1,37	1,33	1,29	1,1
1,700	1,91	1,90	1,86	1,81	1,74	1,2
1,840	2,50	2,49	2,44	2,36	2,28	1,3
1,980	3,17	3,15	3,08	2,99	2,88	1,4
2,120	3,89	3,87	3,79	3,67	3,53	1,5
2,260	4,67	4,64	4,54	4,39	4,22	1,6

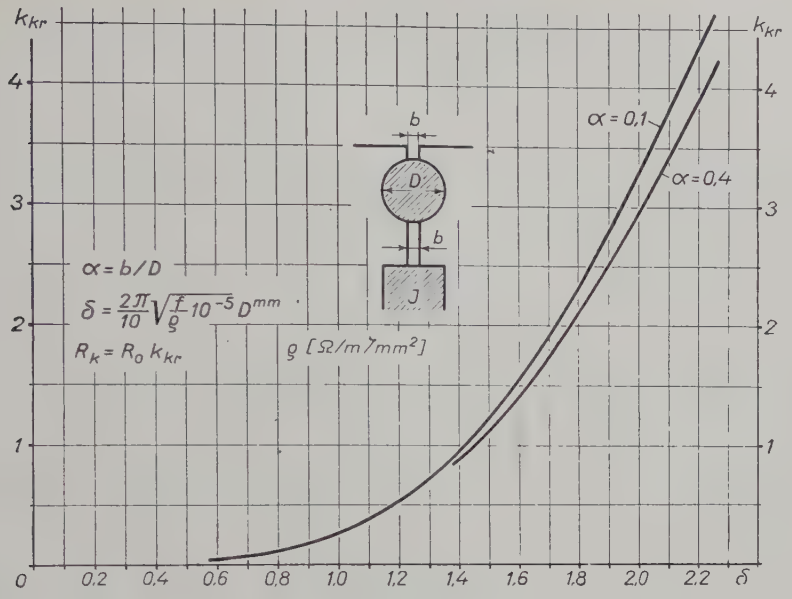

Abb. 9

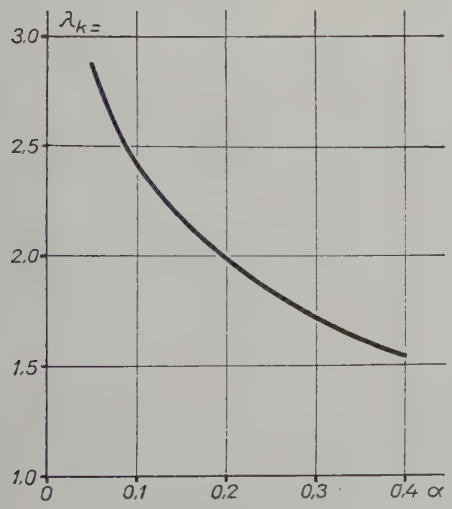

Abb. 10

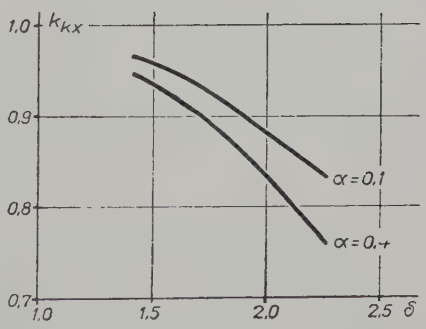

Abb. 11

Die Werte von $\lambda_{k=}$ sind in Reihe $\delta = 0$ der Tab. IV und in Abb. 10 in Funktion von α zu finden.

$\lambda_{k\sim}$ kann auf Grund der Gleichung (23*b*) berechnet werden. Die Ergebnisse sind in Tab. IV*a* (auf zwei Zehntel aufgerundet) angeführt. Der Reaktanz-

abnahmefaktor k_{kx} ist in Tab. IV*b* und in Abb. 11 zu finden:

$$k_{kx} = \frac{\lambda_k \sim}{\lambda_k =} \,. \tag{26}$$

In dem allgemeinen Fall, wo in beiden Stäben Strom fließt ($\mathbf{i}_1 \neq 0$; $\mathbf{i}_2 \neq 0$) können für die beiden Stäbe folgende Spannungsgleichungen aufgeschrieben werden:

$$\mathbf{U}_1 = \mathbf{Z}_{11}\mathbf{I}_1 + \mathbf{Z}_{12}\mathbf{I}_2 \,. \tag{27a}$$

$$\mathbf{U}_2 = \mathbf{Z}_{12}\mathbf{I}_1 + \mathbf{Z}_{22}\mathbf{I}_2 \tag{27b}$$

$\mathbf{Z}_{11}$ ist die Eigenimpedanz des oberen, $\mathbf{Z}_{22}$ die des unteren Stabes, $\mathbf{Z}_{12}$ die gegenseitige Impedanz zwischen den beiden Stäben, $\mathbf{U}_1$ und $\mathbf{U}_2$ bedeuten die an den unteren bzw. oberen Stab gelegten Spannungen, die im gegebenen Fall — z. B. in kurzgeschlossenem Käfig — auch die vom Primärfeld induzierten Spannungen sein können.

$\mathbf{Z}_{11}$ und $\mathbf{Z}_{12}$ enthalten die Impedanz des Hauptfeldes, die Streureaktanzen und den Widerstand der Stäbe. Ihre Berechnung erfolgt in der üblichen Weise.

Tabelle IVa

Werte der Streuleitfähigkeiten $\lambda_k =$ und $\lambda_k \sim$

δ	$\alpha = 0{,}05$	$\alpha = 0{,}1$	$\alpha = 0{,}2$	$\alpha = 0{,}3$	$\alpha = 0{,}4$	w_0
0	2,86	2,42	1,98	1,72	1,54	0
1,415	2,78	2,33	1,90	1,64	1,46	1,0
1,700	2,70	2,26	1,83	1,56	1,38	1,2
1,980	2,59	2,14	1,73	1,46	1,28	1,4
2,260	2,47	2,02	1,60	1,34	1,17	1,6

Tabelle IVb

Werte des Faktors $k_{kx} = \frac{\lambda_k \sim}{\lambda_k =}$

δ	$\alpha = 0{,}05$	$\alpha = 0{,}1$	$\alpha = 0{,}2$	$\alpha = 0{,}3$	$\alpha = 0{,}4$	w_0
1,415	0,970	0,965	0,957	0,952	0,947	1,0
1,700	0,942	0,936	0,925	0,907	0,900	1,2
1,980	0,904	0,885	0,872	0,846	0,835	1,4
2,260	0,860	0,835	0,805	0,780	0,760	1,6

Bei der Berechnung der den Streukraftlinien entsprechenden Reaktanzen und der Stabwiderstände ist auf Grund des vorhergehenden die Wirkung der im Rundstab induzierten Wirbelströme im Falle $\mathbf{Z}_{11}$ nach Gleichung (13) und im Falle $\mathbf{Z}_{22}$ nach Gleichung (23) in Betracht zu ziehen.

Die gegenseitige Impedanz $\mathbf{Z}_{12}$ besteht aus zwei Teilen. Ein Teil entspricht denjenigen Kraftlinien, die mit beiden Stäben verkettet sind, jedoch über den oberen Stab nicht durchgehen (über die obere Nutenöffnung sich schließende Kraftlinien, Zahnkopfstreuung, Luftspaltfeld usw.); der andere Teil ist die Impedanz von Kraftlinien, die über den oberen Stab durchgehen. Die Form des oberen Stabes beeinflußt nur den letzten Teil. Wie im Anhang 6 gezeigt wird, gleicht dieser Teil $(\mathbf{Z}'_{12})$ der Impedanz $\mathbf{Z}_{12}$ der Hälfte der vorher bereits bestimmten Impedanz $\mathbf{Z}_k$ (23*a*, 23*b*):

$$\mathbf{Z}'_{12} = \frac{\mathbf{Z}_k}{2} \,. \tag{28}$$

Hiermit wurden sämtliche Kennwerte (Eigen- und gegenseitige Impedanz) der kreisförmigen Nut bestimmt, und so können die Wirbelstromwirkungen in beliebiger Schaltung berücksichtigt werden.

Beispiel

Die Nutenanordnung eines Doppelkäfigläufers ist in Abb. 12 dargestellt. Die oberen Stäbe sind aus Aluminiumbronze ($\varrho_1 = 0{,}115$ Ohm m/mm²), die unteren aus Bronze mit spezifischem Widerstand $\varrho_2 = 0{,}05$ Ohm m mm². Es soll das Ersatzschaltbild der Käfige — lediglich unter Berücksichtigung der in der Nut befindlichen Teile — für die Frequenz von $f = 50$ Hz bestimmt werden. Das Ersatzschaltbild des Motors ist in Abb. 13 gezeigt. X_S ist die Streureaktanz des Ständers, R_S der Ständerwiderstand, X_0 die Reaktanz des Hauptfeldes, X jener Teil der Läuferreaktanz, der von den oberhalb des oberen Stabes sich schließenden Streukraftlinien herrührt (obere Nutenschlitzstreuung, Luftspaltstreuung usw.). Die Berechnung dieser Teile ist für uns von keiner Bedeutung, weshalb wir uns im folgenden nur mit den von den Klemmen *a*—*b* rechts befindlichen Elementen des Schaltbildes befassen werden. Der Einfachheit halber sind sämtliche Widerstände und Reaktanzen auf die Axiallänge $l = 1$ cm und auf einen Stab bezogen.

Die zur Berechnung der Impedanz nötigen Kennwerte bezüglich der oberen Nut sind

$$a_1 = \frac{2{,}5}{25} = 0{,}1$$

$$\delta_1 = \frac{2\pi}{10}\sqrt{\frac{50\cdot 10^{-5}}{0{,}115}}\cdot 25 = 1{,}035$$

$$R_{01} = 0{,}115\,\frac{0{,}01}{12{,}5^2\,\pi} = 2{,}34\cdot 10^{-6}\,\Omega\,.$$

Auf Grund der Abb. 4 und 5 ist

$$k_{r1} = 0{,}1 \qquad k_\chi \cong 1 \qquad \lambda_= = 1{,}028.$$

Mit diesen Werten erhalten wir für die Eigenimpedanz des oberen Leiters:

$$Z'_{11} = R'_{11} + j\,X'_{11} = (1 + k_{r1})\,R_{01} + j\omega\,\mu_0\,l\,\lambda = (2{,}58 + j\,4.05)\,10^{-6}\,\Omega\,.$$

Die Kennwerte für den unteren Käfig sind:

$$\alpha_2 = \frac{2{,}5}{20} = 0{,}125$$

$$\delta_2 = \frac{2\pi}{10}\sqrt{\frac{50\,10^{-5}}{0{,}05}}\,20 = 1{,}256$$

$$k_{r_2} = 0{,}2 \qquad \lambda_{=} = 0{,}95 \qquad k_{x_2} \simeq 1 \qquad R_{02} = 1{,}59\,10^{-6}\,\Omega.$$

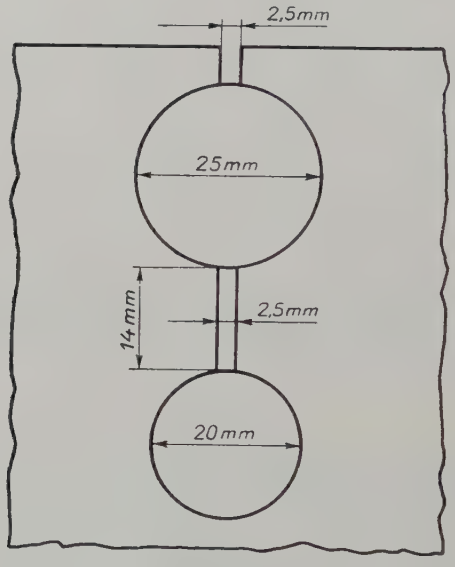

Abb. 12

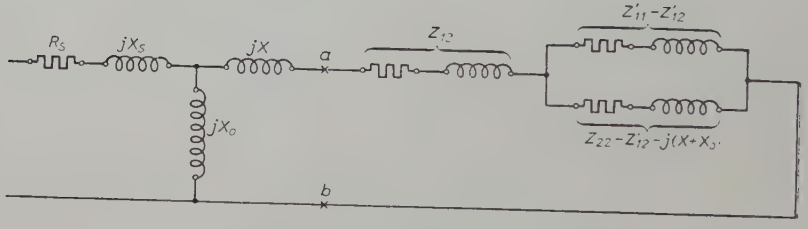

Abb. 13

Aus Abb. 9 und 10 erhalten wir mit den Werten des oberen Käfigs folgende Werte:

$$k_{kr} = 0{,}25 \qquad \lambda_{k=} = 2{,}42 \qquad k_{x_k} \sim 1\,.$$

Die magnetische Leitfähigkeit im Halsteil zwischen den beiden Käfigen ist:

$$\lambda_n = \frac{14}{2{,}5} = 5{,}6.$$

Mit diesen Werten ergibt sich für die Eigenimpedanz des unteren Stabes:

$$\mathbf{Z}'_{22} = R'_{22} + j X'_{22} = [R_{02}(1 + k_{r_2}) + R_{01} k_{kr}] + j \omega \mu_0 l [k_{xk} \lambda_{2=} + k_{kx} \lambda_{k=} + \lambda_n] =$$
$$= (2{,}49 + j\, 35{,}6)\, 10^{-6}\, \Omega.$$

Schließlich beträgt die gegenseitige Impedanz zwischen den beiden Käfigen auf Grund der Gleichung (28):

$$\mathbf{Z}'_{12} = R'_{12} + j X'_{12} = \frac{1}{2} (k_{kr} R_{01} + j \omega \mu_0 l \lambda'_k) = (0{,}293 + j\, 4{,}76)\, 10^{-6}\, \Omega.$$

Die Elemente des Ersatzschaltbildes sind:

$$\mathbf{Z}'_{11} - \mathbf{Z}'_{12} = (2{,}287 - j\, 0{,}71)\, 10^{-6}\, \Omega$$
$$\mathbf{Z}'_{22} - \mathbf{Z}'_{12} = (2{,}197 + j\, 30{,}84)\, 10^{-6}\, \Omega.$$

Die Vernachlässigung der Wirkung der Wirbelströme hätte in den Widerständen eine Abweichung verursacht. In diesem Falle hätte sich nämlich das Ergebnis folgendermaßen gestaltet:

$$R_{11} = R_{01} = 2{,}34 \cdot 10^{-6}\, \Omega$$
$$R_{22} = R_{02} = 1{,}59\, 10^{-6}\, \Omega$$
$$R_{12} = 0.$$

VI. Übersicht

Mit den im vorhergehenden beschriebenen Berechnungen ist es gelungen, den Widerstand und die Nutenstreureaktanz der in Kreisprofilnuten gebetteten massiven Leiter bei Berücksichtigung der Stromverdrängung zu bestimmen. Aus den angeführten Tabellen und Diagrammen geht hervor, daß bei den in der Praxis meist vorkommenden geometrischen Abmessungen und Frequenzen in erster Reihe der Widerstandserhöhungsfaktor eine Rolle spielt und der Reaktanzabnahmefaktor in der Nähe der Einheit liegt. Es kann auch festgestellt werden, daß die Erscheinung der Stromverdrängung besonders den Widerstand der aus Kupfer hergestellten Dämpferwicklungen von Einphasen-Synchronmaschinen bzw. der unter Umständen ebenfalls aus Kupfer erzeugten Anlaßkäfige von selbstanlaufenden mehrphasigen Synchronmaschinen wesentlich abändern kann, da infolge des geringen spezifischen Widerstandes des Kupfers bei einer Frequenz von 100 Hz bzw. 50 Hz die Eindringtiefe verhältnismäßig klein ist, so daß der Widerstandserhöhungsfaktor über einem Stabdurchmesser von 8—10 mm bedeutend ist.

Die Läuferimpedanz von Asynchronmotoren mit Doppelkäfigläufer kann — wenn einer oder beide Käfige aus Rundstäben hergestellt werden — mit Hilfe der mitgeteilten Diagramme und Tabellen ebenfalls bestimmt werden.

Die Wirkung der Wirbelströme ist in diesem Falle im allgemeinen nicht stark, weil die Käfige normalerweise aus Messing, Bronze, Aluminiumbronze usw. hergestellt werden, welche Materialien viel größeren spezifischen Widerstand besitzen als Kupfer. Wegen der verhältnismäßig beträchtlichen Eindringtiefe ist sogar bei größeren Durchmessern und 50 Hz Frequenz die durch Stromverdrängung verursachte Widerstandserhöhung nicht bedeutend. In diesem Falle ist der Mehrverlust der im oberen Käfig durch den Strom des unteren Käfigs induzierten Wirbelströme bzw. der dementsprechende zusätzliche Widerstand beachtenswert.

Bei der Ableitung der Ergebnisse wurde in solchen Rechnungen außer den allgemein benutzten vereinfachenden Annahmen nur eine einzige Annäherung angewendet, und zwar die längs der Nutenöffnung gleichmäßige tangentiale Feldstärkenverteilung. Die tatsächliche Feldstärkenverteilung ist, wie im Abschnitt II erwähnt, hiervon abweichend. Die Abweichung ist am größten, wenn Gleichstrom im Stab fließt. Bei höheren Frequenzen nähert sich die Feldstärkenverteilung dem angenommenen idealen Zustand und stimmt damit bei unendlicher Frequenz überein, da in diesem Falle der im Stab fließende Strom sich an der Oberfläche des Stabes in der Nähe der Nutenöffnung in unendlich dünner Schicht gleichmäßig verteilt. Weiterhin kann — auf Grund hier nicht auseinandergesetzter Betrachtungen — gezeigt werden, daß die Abweichung der Feldstärkenverteilung vom angenommenen idealen Fall im untersuchten Bereich nur einen unwesentlichen Fehler im Widerstandserhöhungsfaktor verursacht, im ungünstigsten Falle einige Prozente. Ihr Einfluß auf die Streureaktanz ist größer, aber die Abweichung von den im vorhergehenden bestimmten Werten ist auch in diesem Falle unbeträchtlich.

An dieser Stelle möchte ich Frl. Hedwig Sas, Mathematikerin in der Elektrotechnischen Fabrik Ganz meinen Dank aussprechen, die den größten Teil der numerischen Rechnung machte, sowie Herrn Stephan Rácz, Dozent des Lehrstuhls für Betriebswesen elektrischer Maschinen, der mit seinen nützlichen Ratschlägen meine Arbeit förderte.

Anhang 1

Die Lösung der Gleichung (6a) wird als die Summe der Glieder folgender Form gesucht

$$\mathbf{E}_z(r_1, \varphi) = \sum_{n=1}^{\infty} \mathbf{E}_{zn}(r) \cos n\varphi. \tag{A. 1.1}$$

Wird dies in Gleichung (6a) eingesetzt und nur das Glied mit Ordnungszahl n untersucht, erhalten wir:

$$\frac{\partial^2 \mathbf{E}_{zn}(r)}{\partial r^2} + \frac{1}{r} \frac{\partial \mathbf{E}_{zn}(r)}{\partial r} - \left(\frac{n^2}{r^2} + j\omega\mu_0\sigma \right) \mathbf{E}_{zn}(r) = 0. \tag{A. 1.2}$$

Durch Einführung der neuen Veränderlichen $w = \sqrt{-j\,\omega\,\mu_0\,\sigma}\,r$ kann obige Beziehung zu einer BESSELschen Differentialgleichung umgeändert werden, deren Lösung

$$\mathbf{E}_{zn}(r, \varphi) = C_{1n}\,\mathrm{J}_n(w) + C_{2n}\,\mathrm{N}_n(w) \qquad \text{(A. 1.3)}$$

ist. Nachdem $\mathbf{E}_{zn}\ (r\,;\ \varphi)$ an der Stelle von $r = 0$ endlichen Wert haben muß, wird $C_{2n} = 0$.
Wird Gleichung (A. 1.3) in Gleichung (6c) eingesetzt, erhalten wir:

$$\mathbf{H}_{\varphi n}(r, \varphi) = \frac{1}{j\,\omega\,\mu_0} \cdot \frac{\partial\,\mathbf{E}_{zn}}{\partial\,w}\,\frac{\partial\,w}{\partial\,r} = C_{1n}\,\frac{\sqrt{-j\,\omega\,\mu_0\,\sigma}}{j\,\omega\,\mu_0}\,\mathrm{J}'_n(w)\cos n\,\varphi\,. \qquad \text{(A. 1.4)}$$

Vergleichen wir obige Gleichung mit der auf Radius $r = r_0$ durch Gleichung (3) vorgeschriebenen Randbedingung, erhalten wir:

$$C_{1n} = \frac{\mathbf{I}}{r_0\,\pi} \cdot \frac{j\,\omega\,\mu_0}{\sqrt{-j\,\omega\,\mu_0\,\sigma}\,\mathrm{J}'_n(w_0)}\,\frac{\sin n\,\alpha}{n\,\alpha}\,. \qquad \text{(A. 1.5)}$$

Dies wieder in Gleichung (A. 1.3) eingesetzt und die Summierung auf jedes n von ganzer Zahl durchgeführt, ergibt das den Gleichungen (7) entsprechende Ergebnis.

Anhang 2

Es soll folgende Bezeichnung eingeführt werden:

$$A_n = \frac{j\,\mathrm{J}_n(w_0)}{w_0\,\mathrm{J}'_n(w_0)}\,; \qquad \text{(A. 2.1)}$$

hiermit wird Gleichung (9) auf der Strecke $-\alpha < \varphi < \alpha$:

$$\mathbf{E}_z(r_0, \varphi)\,\hat{\mathbf{H}}_\varphi(r_0, \varphi) = \frac{\mathbf{I}\,\omega\,\mu_0}{\pi}\left[\frac{A_0}{2} + \sum_{n=1}^{\infty} A_n\,\frac{\sin n\,\alpha}{n\,\alpha}\cos n\,\varphi\right]\frac{\hat{\mathbf{I}}}{2\,r_0\,\alpha}\,. \qquad \text{(A. 2.2)}$$

Die an der Oberfläche durchströmende komplexe Leistung wird:

$$\mathbf{S} = l\int_{-\alpha}^{\alpha}\mathbf{E}_z(r_0, \varphi)\,\hat{\mathbf{H}}_\varphi(r_0, \varphi)\,r_0\,d\,\varphi = \mathbf{I}\,\hat{\mathbf{I}}\,\frac{\omega\,\mu_0\,l}{r_0\,\pi}\left[\frac{A_0}{2} + \sum_{n=1}^{\infty} A_n\left(\frac{\sin n\,\alpha}{n\,\alpha}\right)^2\right] =$$
$$= \mathbf{I}\,\hat{\mathbf{I}}\,\frac{|w_0|^2\,l}{r_0^2\,\pi\,\sigma}\left[\frac{A_0}{2} + \sum_{n=1}^{\infty} A_n\left(\frac{\sin n\,\alpha}{n\,\alpha}\right)^2\right]. \qquad \text{(A. 2.3)}$$

Durch Vergleich der Gleichung (A. 2.3) mit der rechten Seite der Gleichung (10), ergeben sich für R_b und X_b die Gleichungen (13*a*—*b*).

Anhang 3

Es soll folgende Bezeichnung eingeführt werden:

$$\sqrt{-j}\,v = \frac{w_0}{2} = \frac{\sqrt{-j}\,|w_0|}{2}\,. \qquad \text{(A. 3.1)}$$

Hiermit erhalten wir auf Grund der Potenzreihe der Besselfunktionen:

$$J_n(w_0) = \frac{(\sqrt{-j}\,v)^n}{n!}\left[1+\frac{j\,v^2}{n+1}-\frac{v^4}{2(n+1)(n+2)}-\frac{j\,v^6}{2\cdot 3\cdot(n+1)(n+2)(n+3)}+\cdots\right]=$$

$$=\frac{(\sqrt{-j}\,v)^n}{n!}\cdot(a_1+j\,a_2) \qquad \text{(A. 3.2)}$$

$$w_0\,J_n'(w_0)=\frac{(\sqrt{-j}\,v)^n}{n!}\left[n+\frac{j\,v^2(n+2)}{n+1}-\frac{v^4(n+4)}{2(n+1)(n+2)}-\right.$$

$$\left.-\frac{j\,v^6(n+6)}{2\cdot 3(n+1)(n+2)(n+3)}+\cdots\right]=\frac{(\sqrt{-j}\,v)^n}{n!}(b_1+j\,b_2). \qquad \text{(A. 3.3)}$$

Diese Werte in Gleichung (A. 2.1) eingesetzt, ergibt sich:

$$A_n=\frac{j(a_1+j\,a_2)}{b_1+j\,b_2}=\frac{(a_1\,b_2-a_2\,b_1)+j(a_1\,b_1+a_2\,b_2)}{b_1^2+b_2^2}; \qquad \text{(A. 3.4)}$$

somit

$$\mathrm{Re}\left[\frac{j\,J_n(w_0)}{w_0\,J_n'(w_0)}\right]=\mathrm{Re}\,[A_n]=\frac{a_1\,b_2-a_2\,b_1}{b_1^2+b_2^2}. \qquad \text{(A. 3.5)}$$

Aus den Gleichungen (A. 3.2) und (A. 3.3) erhalten wir durch Absonderung die Werte a_1, a_2, b_1 und b_2:

$$a_1=1-\frac{v^4}{2(n+1)(n+2)}+\frac{v^8}{2\cdot 3\cdot 4(n+1)\cdots(n+4)}-\cdots \qquad \text{(A. 3.6)}$$

$$a_2=\frac{v^2}{n+1}-\frac{v^6}{2\cdot 3\cdot(n+1)(n+2)(n+3)}+\frac{v^{10}}{2\cdots 5(n+1)\cdots(n+5)}-\cdots \qquad \text{(A. 3.7)}$$

$$b_1=n-\frac{v^4(n+4)}{2(n+1)(n+2)}+\frac{v^8(n+8)}{2\cdot 3\cdot 4(n+1)\cdots(n+4)} \qquad \text{(A. 3.8)}$$

$$b_2=v^2\,\frac{n+2}{n+1}-\frac{v^6(n+6)}{2\cdot 3(n+1)(n+2)(n+3)}+\frac{v^{10}(n+10)}{2\cdots 5(n+1)\cdots(n+5)} \qquad \text{(A. 3.9)}$$

Werden diese Werte in Gleichung (A. 3.5) eingesetzt und aus der Potenzreihe des Zählers und des Nenners nur die ersten drei Glieder berücksichtigt, erhalten wir:

$$a_1\,b_2-a_2\,b_1=\frac{2}{n+1}\left[v^2+\frac{v^6}{(n+1)(n+2)(n+3)}+\right.$$

$$\left.+\frac{v^{10}}{2(n+1)(n+2)^2(n+3)(n+4)(n+5)}+\cdots\right] \qquad \text{(A. 3.10)}$$

$$b_1^2+b_2^2=n^2+v^4\,\frac{n^2+8(n+1)}{(n+1)^2(n-2)}+v^8\,\frac{n^2+16(n+2)}{2(n+1)^2(n+2)^2(n+3)(n+4)}+\cdots \qquad \text{(A. 3.11)}$$

Bei einem gegebenen Wert v kann die Beziehung (A. 3.5) mit Hilfe obiger Ausdrücke für verschiedene Werte von n berechnet werden woraus die Rechnungen in Gleichung (13a) durchgeführt werden können. Bei der Bestimmung der in der Tabelle angeführten Werte wurden zu jedem Wert v acht Glieder der Summierung nach n in Betracht gezogen, was im Falle $v \leqq 1$ genügende Genauigkeit sichert.

Anhang 4

Der imaginäre Teil der Gleichung (A. 3.4) ist:

$$\mathrm{Im}\,[A_n] = \frac{a_1 b_1 + a_2 b_2}{b_1^2 + b_2^2} \,. \tag{A. 4.1}$$

Der Nenner wurde bereits vorher berechnet (A. 3.11). Der Zähler ergibt sich, durch Anwendung der Beziehungen (A. 3.6) ... (A. 3.9) und mit Berücksichtigung der ersten drei Glieder, zu:

$$a_1 b_1 + a_2 b_2 = n + \frac{v^4}{(n+1)^2} + \frac{v^8}{2\,(n+1)^2\,(n+2)^2\,(n+3)} + \cdots \tag{A. 4.2}$$

Durch Auswerten der Gleichung (A. 4.1) für verschiedene Werte n und durch Einsetzen der erhaltenen Ergebnisse in Gleichung (13*b*) kann die Streuleitfähigkeit bestimmt werden.

Die Gleichstrom-Streuleitfähigkeit erhalten wir mit dem Grenzübergang $v \to 0$. Wird in Gleichungen (A. 4.2) und (A. 3.10) die Substituierung $v = 0$ gemacht, erhalten wir für den Ausdruck (A. 4.1) den Wert:

$$\mathrm{Im}\,[A_n] = \frac{1}{n} \,. \tag{A. 4.3}$$

Ferner im Falle $n \to 0$ mit der Bedingung $v \to 0$ ebenfalls aus den Gleichungen (A. 4.2) und (A. 3.10):

$$\frac{1}{2}\,\mathrm{Im}\left[\frac{j\,\mathrm{J}_0(w_0)}{w_0\,\mathrm{J}_0'(w_0)}\right] = \frac{1}{8} \,. \tag{A. 4.4}$$

Werden die Gleichungen (A. 4.3) und (A. 4.4) in Gleichung (13*b*) eingesetzt, ergibt sich für die Gleichstrom-Streuleitfähigkeit die Gleichung (16).

Anhang 5

Auf Grund der Abb. 8 und der Gleichungen (21) und (22), unter Berücksichtigung der in Gleichungen (A. 2.1) angewendeten Bezeichnung, ist:

$$\mathbf{S}_1 = l \int_{-\alpha}^{\alpha} \mathbf{E}_z(r_0, \varphi)\,\hat{\mathbf{H}}_\varphi(r_0, \varphi)\,r_0\,d\varphi =$$

$$= \mathbf{I}_2\,\hat{\mathbf{I}}_2\,\frac{2\,\omega\,\mu_0\,l}{\pi\,r_0}\left[\sum_{\nu=1}^{\infty} A_{(2\nu-1)}\left(\frac{\sin(2\nu-1)\,\alpha}{(2\nu-1)\,\alpha}\right)^2\right] =$$

$$= \mathbf{I}_2\,\hat{\mathbf{I}}_2\,\frac{2\,l\,(w_0)^2}{\sigma\,r_0^{\,2}\,\pi}\left[\sum_{\nu=1}^{\infty} A_{(2\nu-1)}\left(\frac{\sin(2\nu-1)\,\alpha}{(2\nu-1)\,\alpha}\right)^2\right] . \tag{A. 5.1}$$

Desgleichen:

$$\mathbf{S}_2 = l \int_{\pi-\alpha}^{\pi+\alpha} \mathbf{E}_z(r_0, \varphi)\,\hat{\mathbf{H}}_\varphi(r_0, \varphi)\,r_0\,d\varphi =$$

$$= \mathbf{I}_2\,\hat{\mathbf{I}}_2\,\frac{2\,l\,|w_0|^2}{\sigma\,r_0^{\,2}\,\pi}\left[\sum_{\nu=1}^{\infty} A_{(2\nu-1)}\left(\frac{\sin(2\nu-1)\,\alpha}{(2\nu-1)\,\alpha}\right)^2\right] . \tag{A. 5.2}$$

Wird die Summe der Gleichungen (A. 5.1) und (A. 5.2) mit der Gleichung (20) verglichen) ergeben sich für Z_k die Gleichungen (23).

Anhang 6

Wird Gleichung (27*a*) mit $\hat{\mathbf{I}}_1$ und Gleichung (27*b*) mit $\hat{\mathbf{I}}_2$ multipliziert und die beiden Ausdrücke addiert, erhalten wir:

$$\mathbf{U}_1 \hat{\mathbf{I}}_1 + \mathbf{U}_2 \hat{\mathbf{I}}_2 = \mathbf{I}_1 \hat{\mathbf{I}}_1 \mathbf{Z}'_{11} + \mathbf{I}_2 \hat{\mathbf{I}}_1 \mathbf{Z}'_{12} + \mathbf{I}_1 \hat{\mathbf{I}}_2 \mathbf{Z}'_{12} + \mathbf{I}_2 \hat{\mathbf{I}}_2 \mathbf{Z}'_{22} \,. \tag{A. 6.1}$$

Die gestrichelten Werte bedeuten denjenigen Teil der betreffenden Impedanz, der von den mit dem oberen Leiter verketteten Kraftlinien herrührt; nach dem vorhergesagten ist nämlich nur dieser Teil der Untersuchung wert. Laut Bezeichnungen im Abschnitt V ist $\mathbf{Z}'_{22} = \mathbf{Z}_k$. Somit ist Gleichung (A. 6.1) die komplexe Form der Leistung des oberen Leiters. Dasselbe kann auch mit den elektrischen und magnetischen Feldstärken ausgedrückt werden.

Auf Grund des Prinzips der Superposition setzen sich die Feldstärken aus zwei Teilen zusammen:

$$\mathbf{E}_z(r_0, \varphi) = \mathbf{E}_{1z} + \mathbf{E}_{2z} \tag{A. 6.2}$$

$\mathbf{E}_{1z}$ ist die vom Strom $\mathbf{I}_1$ des oberen Leiters erzeugte Feldstärke, $\mathbf{E}_{2z}$ die vom Strom $\mathbf{I}_2$ des unteren Leiters erzeugte Feldstärke [siehe Gleichungen (7*a*) bzw. (22)].

Die magnetische Feldstärke ist ähnlicherweise:

$$\mathbf{H}_\varphi(r_0, \varphi) = \mathbf{H}_{1\varphi} + \mathbf{H}_{2\varphi}\,, \tag{A. 6.3}$$

wo auf der Strecke $-\alpha < \varphi < \alpha$

$$\mathbf{H}_{1\varphi} = \frac{\mathbf{I}_1}{2\, r_0\, \alpha} \qquad \mathbf{H}_{2\varphi} = \frac{\mathbf{I}_2}{2\, r_0\, \alpha} \tag{A. 6.4}$$

und auf der Strecke $(\pi - \alpha) < \varphi < (\pi + \alpha)$ (untere Nutenöffnung)

$$\mathbf{H}_{1\varphi} = 0 \qquad \mathbf{H}_{2\varphi} = -\frac{\mathbf{I}_2}{2\, r_0\, \alpha} \,. \tag{A. 6.5}$$

Das Integral des POYNTINGschen Vektors an der Oberfläche des oberen Leiters ist:

$$\mathbf{S} = \int_F \mathbf{E}_z \hat{\mathbf{H}}_\varphi \, d\, F = \int_F (\mathbf{E}_{1z} \hat{\mathbf{H}}_{1\varphi} + \mathbf{E}_{2z} \hat{\mathbf{H}}_{1\varphi} + \mathbf{E}_{1z} \hat{\mathbf{H}}_{2\varphi} + \mathbf{E}_{2z} \hat{\mathbf{H}}_{2\varphi})\, d\, F \tag{A. 6.6}$$

Beim Vergleich der Gleichungen (A. 6.6) und (A. 6.1) ergibt sich, daß die ersten Glieder der rechten Seite gleich sind, da die Impedanz $\mathbf{Z}'_{11}$ eben mit der Bedingung berechnet wurde, daß nur im oberen Rundleiter Strom fließt [Gleichung (A. 2.3)]. Ebenso sind die vierten Glieder der rechten Seite beider Gleichungen gleich, und zwar die Werte nach Gleichung (A. 5.2). Da sowohl die elektrischen als auch die magnetischen Feldstärken mit den entsprechenden Strömen proportional sind, ist ebenfalls ersichtlich, daß auch die übrigen Glieder der Gleichungen einander entsprechen: somit erhalten wir aus der Gleichheit der zweiten Glieder der rechten Seiten:

$$\mathbf{Z}'_{12} = \frac{\int_F \mathbf{E}_{2z} \hat{\mathbf{H}}_{1\varphi} \, d\, F}{\mathbf{I}_2 \hat{\mathbf{I}}_1} \,. \tag{A. 6.7}$$

Ist $\mathbf{H}_{1\varphi}$ in der unteren Nutenöffnung gleich Null, so genügt es, die Integration nur für den oberen Abschnitt zu machen. Nach Substituierung des Wertes $\mathbf{E}_{2z}$ aus Gleichung (22) und des Wertes $\mathbf{H}_{1\varphi}$ aus Gleichung (A. 6.4) sowie nach Durchführung der Integration erhalten wir aus Gleichung (A. 6.7) folgendes Ergebnis:

$$\mathbf{Z}'_{12} = \frac{2\,l\,|w_0|^2}{\sigma\, r_0^2\,\pi}\left[\sum_{\nu=1}^{\infty} A_{(2\nu-1)}\left(\frac{\sin(2\nu-1)\,\alpha}{(2\nu-1)\,\alpha}\right)^2\right] = \frac{\mathbf{Z}_k}{2}, \qquad \text{(A. 6.8)}$$

das der Gleichung (28) gleich ist.

Literatur

1. Stevenson, A. R.—Park, R. H.: Graphical Determination of Magnetic Fields. Theoretical Considerations. Transactions 1927.
2. Rothert, H.: Über die Nutstreuung elektrischer Maschinen Teil II—III. (Archiv für Elektrotechnik, Bd. XXXII, 1938.)
3. Retter Gy.: Mágneses terek és körök (Magnetische Felder und Kreise). Tankönyvkiadó, 1952.
4. Simonyi, K.: Theoretische Elektrotechnik. Deutscher Verlag der Wissenschaften, Berlin 1956.
5. Lengyel, Z.: Különleges kalickás forgórészek tervezése (Entwurf von Spezial-Käfigläufern). Mérnöki Továbbképző Intézet, 1955.
6. Hess, H.: Stromverdrängungsmotoren mit Ein- und Mehrnutläufern, Eindringtiefe. Archiv für Elektrotechnik, 1930.
7. Laible, Th.: Stromverdrängung in Nutleitern von trapezförmigem und dreieckigem Querschnitt. Archiv für Elektrotechnik, 1933.
8. Schuisky, W.: Die Stromverdrängungsmotoren. Archiv für Elektrotechnik, 1933.
9. Rogowsky: Über zusätzliche Kupferverluste. Archiv für Elektrotechnik, 1913.
10. Retter Gy.: Mélyhornyos jellegű különleges forgórészkalickák rúdjainak számításáról (Berechnung der Stäbe von Tiefnutläufern). Elektrotechnika, 1956.
11. Jahnke—Emdre: Tafeln höherer Funktionen. Teubner, Leipzig 1952.
12. Tölke: Besselsche und Hankelsche Zylinderfunktionen. Verl. Wittwer, Stuttgart 1936.
13. Freud G.: Über die Stromverdrängung in kreiszylindrischen Leitern. Acta Technica Hungarica, 1954.

Zusammenfassung

Die vorliegende Abhandlung befasst sich mit der analytischen Bestimmung des Widerstandes und der Streuungsreaktanz der in den kreisförmigen Nuten der elektrischen Maschinen liegenden massiven Leitern unter der Voraussetzung, daß die tangentiale Komponente der magnetischen Feldstärke in der Nutenöffnung gleichmäßig verteilt ist.

Für die auf Grund der abgeleiteten Zusammenhänge errechneten Werte der Gleichstrom-Streuleitfähigkeit, der Wechselstromwiderstand und Reaktanz werden Diagramme und Tabellen vorgelegt. Desgleichen veranschaulichen Tabellen und Diagramme die Werte, die sich auf die der Abb. 7 entsprechenden Anordnung beziehen.

Dipl. Ing. R. Tuschák, Budapest XIII., Szent István park 5.

ON THE POSSIBILITY OF CONTROLLED POWER PRODUCTION USING THERMONUCLEAR FUSION*

By

G. Kálmán, L. Pócs, G. Schmidt and K. Simonyi

Institute for Theoretical Electricity of the Polytechnical University, Budapest

(Received January 12, 1957)

The problems of thermonuclear power production are at present dealt with at three different levels.

1. In the National Laboratories of the Great Powers. There is no information available either for the scientific world or for the general public, about the theoretical and experimental work which is being carried on there, which involves large investments of material and mental energies. What we know is the fact only that research is going on and we may guess at its probable directions [1—3].

2. The papers published on the subject up to now are partly the work of scientists not belonging to the above spheres and are restricted to purely theoretical considerations or to the astronomical aspects of the problem [4—8] and partly they contain only to some partial results to the above mentioned laboratories [9—20]. Besides of these only very few articles are to be found which bear any relation to the above problem [21, 22].

3. Owing to the importance of the question the subject has been treated quite often in the daily press as well as in the popular scientific literature in a rather speculative way.

Scientific public opinion seems to be most impressed by the rather pessimistic paper by Thirring [6] in which he reaches the conclusion that owing to the unfavourable balance between fusion power output and radiation losses the realization of controlled thermonuclear reactions does not seem feasible. In the following we want to prove first of all that this balance is more favourable than presumed up to now as the radiation for the realizable plasma dimensions does not follow the assumed black body radiation law. Thus realization is not made impossible by the radiation laws.

Further, we shall make an estimation as to orders of magnitude in connection with some considerations partly suggested earlier by one of us [7, 8].

* The above article contains the lecture of the authors given at the Conference of Physicists at Veszprém (23. 8. 1956). After the manuscript had been finished the papers published in the August 1956 number of Nuclear Science and Engineering by E. Teller, and in the July 1956 number of the Reviews of Modern Physics by R. F. Post came to hand. Some of the statements contained in these papers are in accordance with the results given here.

Let us start from the energy balance of the plasma, i. e. of a gas of finite dimensions, fully ionized because of the high temperature. At a given temperature T the nuclei of deuterium or those of a gas mixture of deuterium and tritium collide. Some of these collisions initiate a nuclear reaction and thus a

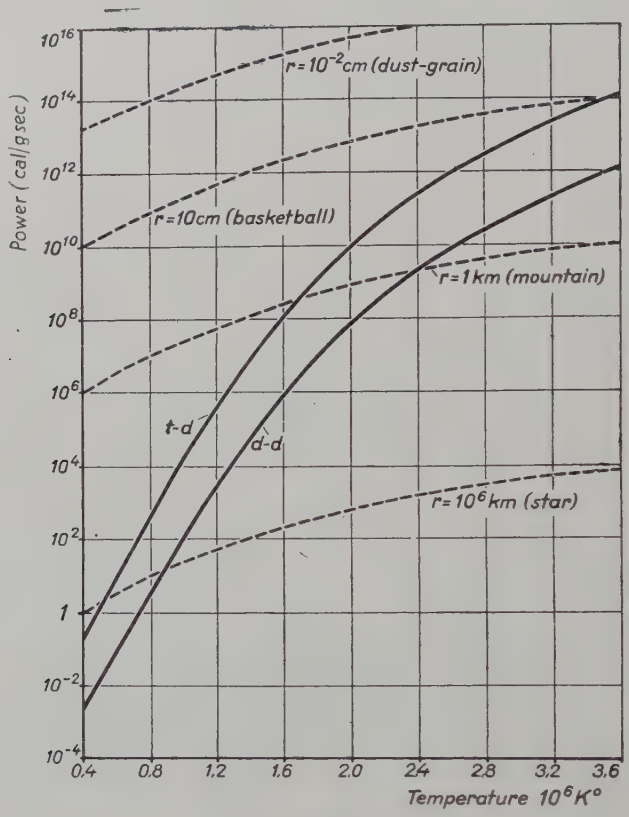

Fig. 1

release of energy. Assuming a gas where the energy distribution follows a Maxwell law, the energy dependence on the temperature is given according to [23] by the following relation :

$$W = a\varrho c_1 c_2 T^{-2/3} \; e^{-b/T^{1/3}}, \tag{1}$$

where a, b are constants, ϱ is the gas density, c_1, c_2 are the relative concentrations of the two gases, and T is the absolute temperature.

The variation in the specific power output with temperature i. e. the power output per unit mass according to the above equation is shown in Fig. 1 by the solid line with respect to the reactions D—D and T—D. The broken

lines in the same figure show for different values of F according to the formula

$$W_{\text{rad}} = \sigma T^4 F \tag{2}$$

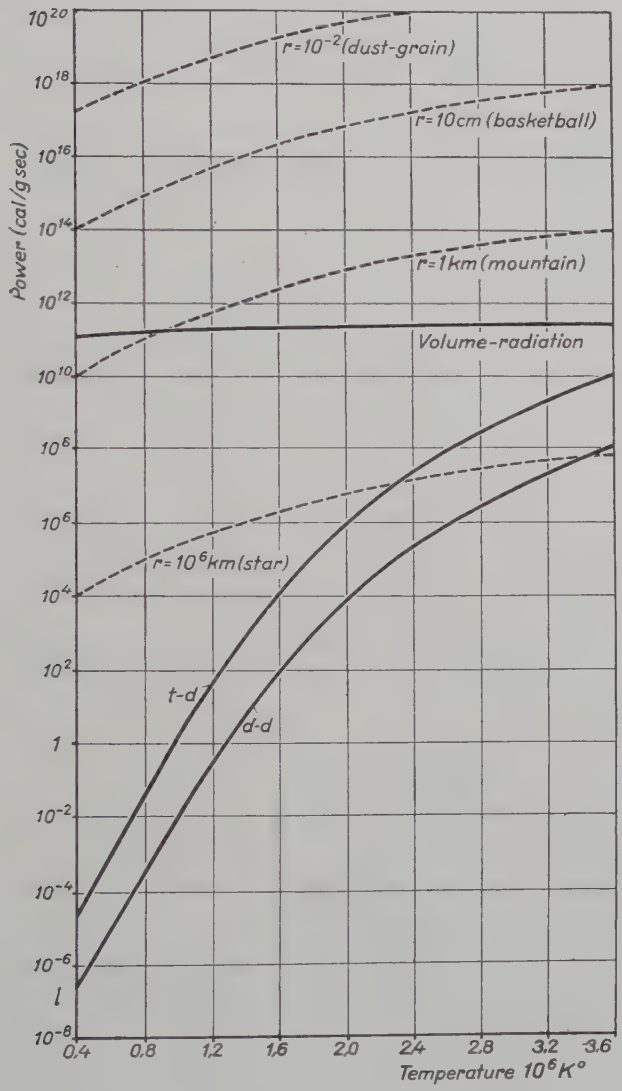

Fig. 2

the radiation output per g for a gas of 1 g/cm³ density. In the formula $\sigma = 5{,}7 \cdot 10^{-5}$ erg/cm² grad sec is the Stefan—Boltzmann constant; F is the surface.

In the following we shall refer to these lines as Thirring curves. A body of small dimensions emits relatively to its mass more radiation than a bigger

one having the same density and being at the same temperature, for the Stefan—Boltzmann law implies a radiation proportional to the surface and the quotient surface/volume increases with decreasing dimensions.

The intersecting point of the curves corresponds to the stationary state.

We note [28] in connection with these curves first of all that a material density of 1 g/cm^3 is not feasible as it would require a pressure of 10^8—10^9 *at* at the temperatures occurring at nuclear reactions. Thus we have to consider a lower density. For a lower density the curves of the specific energy production will be displaced downwards and the curves of the specific radiation output will be shifted upwards (Fig. 2). The rate of reactions namely and hence the energy output, too, is proportional to the second power of density. The *specific* power production is therefore proportional to the density. On the other hand the quantity of matter in the given volume is proportional to the density and thus the radiation energy per g of matter in the given volume is inversely proportional to the density.

The density has to be reduced not only because of the high pressure. The fusion of 1 g deuterium-tritium mixture releases an energy of 10^{11} cal. It can be seen from the figure that in case of the given density the power output becomes enormous. With such a high power output the energy of 1 g of gas mixture would not be sufficient even for 1 microsecond and consequently the reactor could not be operated steadily because the material consumed cannot be replaced. Besides, this fast release of energy is comparable to an explosion, the energy of which cannot be put to practical use.

Our second remark is the following [28].

The radiation of a body of a temperature of several million degrees consists mainly of soft X-ray quanta. X-rays penetrate even solid bodies and thus they go much more easily through the much thinner plasma. Therefore the radiation produced in the plasma — if the total volume is not of an extraordinary magnitude — leaves the plasma without having been absorbed and re-emitted, etc. anywhere by it. Thus the plasma, below a given volume, represents *not a surface* but a *volume* radiator. Therefore the Stefan—Boltzmann law cannot be applied and the broken lines in the figures do not represent the real case.

Let us calculate the radiated energy provided the plasma is wholly transparent i. e. all photons produced leave the plasma immediately. Our calculations will not be exact as we are interested in the orders of magnitude only.

The radiation emitted by electrons consists of bremsstrahlung and of radiation occurring at the recombinations.

Energy loss of electrons due to bremsstrahlung. The energy loss of an electron along a path of 1 cm is

$$\frac{dE}{dx} = -NE\Phi\,, \tag{3}$$

if there are N atoms in 1 cm^3 [24], where E is the energy of an electron (kinetic energy + rest energy) and for non-relativistic energies

$$\Phi = \frac{16}{3} \frac{r_0^2 Z^2}{137} \approx 3 \cdot 10^{-27} \text{ cm}^{-1}, \tag{4}$$

r_0 is here the classical electron radius, i. e. $r_0 = 2{,}8 \cdot 10^{-13}$ cm, and Z the atomic number which has been taken to be 1 as here hydrogen isotopes are being considered.

If the electron travels with a velocity v, it emits a radiation, the energy of which per sec is given by

$$NE\Phi v = 3 \cdot 10^{-27} NEv. \tag{5}$$

The number of electrons moving in 1 cm^3 of the plasma be n and the velocity distribution be given by $f(v)$, then the energy leaving the space element of 1 cm^3 per sec is

$$w = \int_0^\infty 3 \cdot 10^{-27} nNEvf(v)\, dv. \tag{6}$$

As we deal here with energies of some thousand eV, the kinetic energy of the electrons is negligible compared to their rest energies (0,5 MeV), and thus $E \approx mc^2$ and it follows that

$$w \approx 3 \cdot 10^{-27} nNmc^2 \int_0^\infty vf(v)\, dv. \tag{7}$$

Let us assume the electrons to have a Maxwell velocity distribution, then, as is well-known

$$\int_0^\infty vf(v) = \frac{2}{\pi} \sqrt{\frac{2KT}{m}}. \tag{8}$$

Substituting (8) into (7) we obtain that

$$w \approx 3 \cdot 10^{-27} nNmc^2 \frac{2}{\pi} \sqrt{\frac{2KT}{m}}. \tag{9}$$

If we consider deuterium or deuterium-tritium gas in a fully ionized state we have $n \approx N$. At a density of 1 g/cm^3 — the density the calculations of Thirring are referring to — (9) gives directly the radiation output per 1 g.

At this density the value of N is for deuterium $3 \cdot 10^{23}$, and for a mixture of deuterium-tritium in equal proportion $2{,}4 \cdot 10^{23}$. Introducing these values in (9), we obtain

$$w_{DD} \approx 1{,}4 \cdot 10^{20} \sqrt{T} \text{ erg/g sec} = 3{,}3 \cdot 10^{12} \sqrt{T} \text{ cal/g sec}, \tag{10a}$$

$$w_{DT} \approx 0{,}9 \cdot 10^{20} \sqrt{T} \text{ erg/g sec} = 2{,}1 \cdot 10^{12} \sqrt{T} \text{ cal/g sec}. \tag{10b}$$

If the density of the gas is lower by four orders of magnitude (i. e. if the pressure of the gas is about 1 *at* at normal temperatures) then

$$w_{DD} \approx 3{,}3 \cdot 10^{8} \sqrt{T} \text{ cal/g sec}, \tag{11a}$$

$$w_{DT} \approx 2{,}1 \cdot 10^{8} \sqrt{T} \text{ cal/g sec}. \tag{11b}$$

More generally we can write :

$$w_{DD} \approx 3{,}3 \cdot 10^{12} \varrho \sqrt{T} \text{ cal/g sec}, \tag{12a}$$

$$w_{DT} \approx 2{,}1 \cdot 10^{12} \varrho \sqrt{T} \text{ cal/g sec}. \tag{12b}$$

Energy loss of electrons due to recombination. It is to be expected that this part of the radiation will turn out to be smaller than the former, as owing to the high temperature the probability of recombination is very small.

Let the number of ions (per cm^3) be N, and that of electrons n, and let the velocity distribution function of the electrons be $f(v)$. The energy loss of electrons per sec due to recombination is then [24]

$$\int_0^\infty h\nu n N \Phi' v f(v)\, dv, \tag{13}$$

where, at rather high energies

$$\Phi' = \frac{2\,(h\nu)^2}{m^2 v^2 c^2} \Phi_0 \frac{64 \cdot 137^3}{Z^2} \left(\frac{I}{h\nu}\right)^{7/2}, \tag{14}$$

and

$$h\nu = I + \frac{1}{2} m v^2. \tag{15}$$

I, the ionization energy of the gas, is in case of hydrogen 13,5 eV ; $\Phi_0 = 6{,}57 \cdot 10^{-28}$ cm^2. At lower energies, the value of Φ' is less, but as we anyhow want to prove that this term of the radiation is negligible, we may safely

calculate with a value higher than the true Φ'. Substituting (14) and (15) into (13) and assuming that the electrons follow the Maxwell velocity distribution, we obtain, by evaluating the integral, for the radiation energy originating from unit volume per sec

$$w_{\text{rec}} \approx 2nN \frac{1}{m^2 c^2} \frac{64 \cdot 137^3}{Z^2} I^3 \left(\frac{m}{KT}\right)^{1/2} \left(\frac{1}{2\pi}\right)^{3/2}. \tag{16}$$

In the integration $\left(I + \frac{1}{2} mv^2\right)^{-1/2}$ was substituted by the bigger $I^{-1/2}$. At 1 g/cm³ density w_{rcc} represents the specific energy loss. Substituting the values of the constants and taking into account that here too $n \approx N$,

$$w_{\text{rec DT}} \approx 2{,}7 \cdot 10^{22} \frac{1}{\sqrt{T}} \text{ erg/g sec} = 6{,}5 \cdot 10^{14} \frac{1}{\sqrt{T}} \text{ cal/g sec}. \tag{17}$$

Comparing this with (10*b*) we may see that at about 1 million degrees (17) is smaller by 4 orders of magnitude and so may be easily neglected.

Thus the radiation of the hot, fully ionized plasma, as far as it can be considered transparent, is given by formula (10) and (11) resp. Its essence is that the radiation is independent of the size of the surface and, therefore, in contrast to the Thirring curves, here only one radiation curve appears. This curve calculated according to equation (11) is plotted in Fig. 2.

Obviously, the plasma can be considered as transparent as long as the surface radiation curve, belonging to its volume, runs above the space radiation curve. At low temperatures — where the emitted radiation is of longer wavelengths — and in case of larger volume, however, it is opaque. Then the Stefan — Boltzmann law and the considerations of Thirring are becoming valid.

We may state therefore that the construction of a fusion reactor is indeed possible with a plasma of small dimensions, as the energy loss — and at the same time the energy production — is proportional to the volume and not to the surface. *This applies only so long as we consider the energy balance between fusion power production and radiation loss only.* Because of the proportionality of energy production and radiation the point of intersection between the energy production curve and the radiation curve is independent of density and dimension.

This point of intersection defines the minimum temperature necessary to maintain a stationary fusion-power production. From Fig. 2 we can guess by extrapolation its value for the DT reaction to be about 10^7 °K. The power released is about 10^{12} cal/g sec in the case of a density $3 \cdot 10^{19}$/cm³. We will use in the following in our numerical calculations these values as basic data.

Thus output may be decreased at will by reducing the density without increasing in the temperature. The solid curves of Fig. 2 will be displaced upwards and downwards resp. by varying the density. In this way it seems to be possible to reach very high temperatures on the one hand, and to avoid explosion-like energy release, on the other.

The values quoted below may give an illustration of the fact mentioned here :

n/cm^3	$5 \cdot 10^{19}$	$5 \cdot 10^{15}$	$5 \cdot 10^{13}$
p mm Hg (T = 273 °K)	710	0,07	0,0007
p at (T = 10^6 °K)	35 000	3,5	0,035
ϱ g/cm^3	$2 \cdot 10^{-4}$	$2 \cdot 10^{-8}$	$2 \cdot 10^{-10}$
V cm^3/g	$5 \cdot 10^3$	$5 \cdot 10^7$	$5 \cdot 10^9$
P_{DT} MW/g	$6 \cdot 10^6$	600	6
t sec (time of 1 g fuel-consumption)	0,1	10^3	10^5

Up till now, the fact has not been mentioned, that the quantity of reaction products leaving the space of the plasma depends on size and density. The loss of particles may influence disadvantageously the energy balance inside the plasma, but may be useful in view of controlling.

As can be seen from the Fig. 2, the curves of energy output and of radiation are intersecting in such a way that if production increases radiation increases to a smaller degree, i. e. the stationary state is unstable. This difficulty may possibly be overcome with help of the following consideration.

The fusion products arising near the surface may leave the plasma before transferring their energy. Care must be taken that in the stationary case this energy loss should not be significant. If. however, care is taken that, when the reaction intensity increases and the plasma becomes hot, the heat expansion is anisotropic, an increase of the specific surface can be attained with increasing temperature. Larger surface results in greater energy loss and consequently in a cooling-down. The problem can thus be solved in principle and becomes now a technical task.

*

The most difficult problem of steady operation is the holding together of the gas at several million degrees. In the natural thermonuclear reactions occurring in the stars a strong gravitational field due to the large dimensions assures the holding together of the plasma and the "wall". By "wall" is here meant the surface layer of a thickness of several thousand kms in which the temperature falls from its internal value of some million degrees to some thousand degrees. A wall of such character although not impossible in principle for terrestrial dimensions is hardly feasible. As the plasma is at this temperature in a fully ionized state, we may hope that it can be hold together in a given part of space by means of an electromagnetic field. In the literature the role

the electromagnetic wall plays for the first time mentioned in connection with the name of Richter [6]. We cannot but indicate its possibilities and difficulties.

The notion of an electrostatic potential wall is well-known : it prevents for instance the electrons from leaving the inside of metals. Unfortunately these electrostatic forces have such an effect only upon charges of the one sign and facilitate the departure of the charges of the other sign.

If we produce a static field along an axis according to Fig. 3, the particles of, let us say, positive charge cannot leave in the direction of the axis. Their

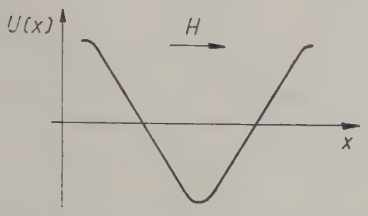

Fig. 3

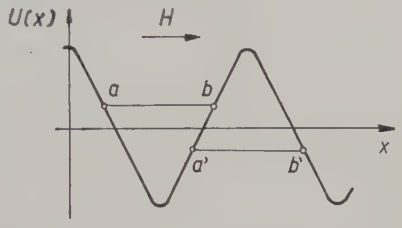

Fig. 4

departure in a radial direction can be reduced by means of a magnetic field in the direction of the axis. In this way the number of escaping charges will be reduced by $1/H^2$ [15]. As the original field deteriorates already through very few enclosed charged particles only very few charged particles can be accumulated. The number of enclosed particles may be increased by the potential shown in Fig. 4 : We place charges of alternate signs in the successive potential wells.

With this arrangement the effect of space charge on the outer field will be reduced. Owing to the magnetic field the particles in the potential wall travel, as a matter of fact, mainly in the direction of the axis between the points a and b (Fig. 3), their velocities being smallest in the points of reversal, i. e. in a and b resp. and, therefore, it is here that the density of particles and, consequently, the charge density is the highest. The particles of opposite charge travel between a' and b', their density being also the highest at these points. The regions of the highest charge density overlap and compensate each other so that the outer field will be deteriorated to a smaller degree. This picture is, of course, only approximately true as the charge distribution inside the well changes in case there are particles of opposite charges near to the potential well.

Unfortunately, even so we are able to enclose very few particles only. According to our rough estimation [29] the number of deuterons of an energy of 100 eV which may be enclosed is sufficient only for the production of an energy of $2 \cdot 10^{-2}$ cal/sec.

This example shows that sufficient amounts of charges of one sign can not be accumulated. Therefore — as mentioned before — we have to try to hold together the plasma. As in the plasma, however, there are charged particles of both signs wich are affected by the electrostatic field in opposite ways, we have to look for another "wall".

Let a particle travel in an inhomogeneous field on a spiral path the axis of which is parallel to the field intensity and which points towards increasing

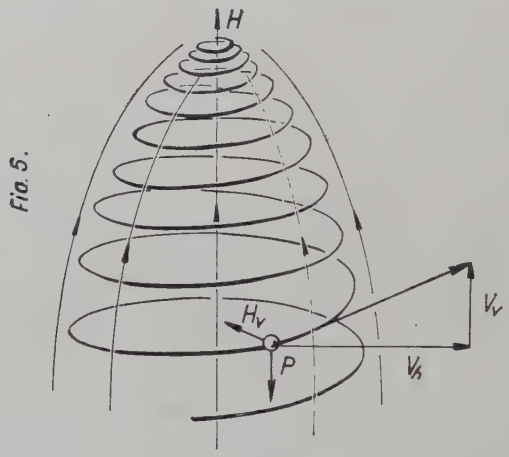

Fig. 5.

Fig. 5

intensities (Fig. 5). The horizontal component of the field intensity H_v together with the horizontal component of the particle velocity gives a force oriented vertically downwards which reduces the vertical component of the particle velocity more and more, so that the slope of the spiral path becomes increasingly smaller and the path flattens and turns back and the particle returns on increasingly wide paths [25, 26].

If the inhomogeneous magnetic field is generated between two poles, no particle, of either sign, can leave the field because they always turn round before the poles. Actually, the matter is not so simple. Namely, if a particle starts from the middle in about the direction of the field it is turned back only by a field of very high intensity. If from the middle the same number of particles depart in all directions with the same velocity, half per mille of the particles will pass a surface where the field intensity is $H = 1000\ H_0$ [29]. Furthermore, the particles stray from their original trajectories due to collisions with one another which results in diffusion.

By means of a homogeneous magnetic field, it is possible to build a wall for charges of both signs. According to Fig. 6 the charges may be kept in the inside of a double solenoid and the departure of charges may occur at the two limiting surfaces only. The area of these surfaces can be made negligibly small

compared to the total surface by increasing the length of the solenoid. Finally, a completely enclosed field may be produced by a double torus. This field keeps back the constituents of either sign of the plasma, when the plasma is assumed to be very thin. The thinness of the plasma has to be emphasized : it is only in this case that the electrons and the nuclei move like independent particles. Otherwise, we should have to consider the more complicated phenomenon of plasma diffusion. From this point of view plasma may be considered thin

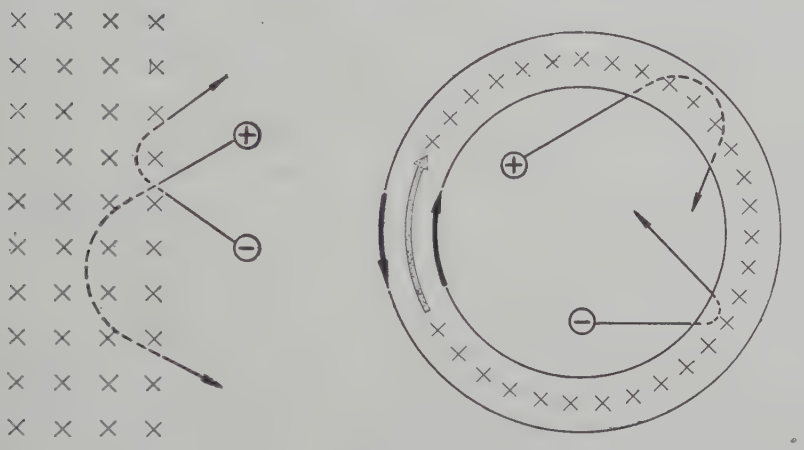

Fig. 6

when the free path of the ions is much longer then the ion orbit in the magnetic wall.

Here only the generally known fact [27] is mentioned that in a plasma carrying big currents, the force produced by the magnetic field of the current itself constitutes a natural coercive force ("pinch effect").

*

In order or attain the necessary high temperatures a very high concentration of energy is required. Here a focused explosion wave, or ultrasonic wave [22] may be considered. The sudden discharge of accumulated electrostatic or magnetic energies seems to be most promising [2, 7—20]. Considering that 1 kWs $= 0{,}6 \cdot 10^{22}$ eV, it can be seen that with the still realizable energy of $10^2 - 10^3$ kWs each atom of a gas of $10^{-1} - 10^{-2}$ moles could be provided with the required energy of some 100 eV. Of course, the efficiency of the energy transfer constitutes a difficult technical problem.

In principle there is a possibility which is essentially different from the above. Would it not be possible to apply to terrestrial dimensions the analogy of the mechanism of the origin of high-energy cosmic radiation as assumed by Fermi [25]? Let us assume that balls of small but macroscopic dimensions

are kept in unceasing motion in a gas mixture. Even their relatively slow motion is connected with a very high temperature according to the relation $1/2\, mv^2 = 3/2\, kT$. If we can assume that a ball behaves like *one* particle, the ball will by colliding with the moleculas transfer their energy to them according to the law of equipartion. Let us assume our gas to be in a fully ionized state. The injected metallic balls collide with and are heated up by the high-energy electrons and ions and possibly evaporate. The actual collision between the positively charged particles and the wall of the balls may be prevented by a positive charge given to the balls. The balls will interact with the particles of positive charge following the law of elastic collisions and until equilibrium

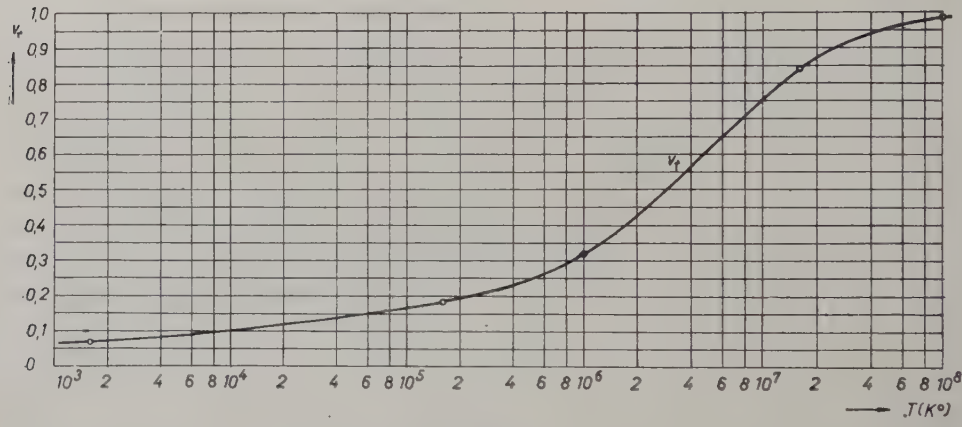

Fig. 7

state is reached the balls will impart — on the avarage — excess energy to the ions.

It would be possible to bring about a similar interaction between balls and the electrons, too, by magnetizing the metallic balls into dipoles. The magnetic field in this way will, namely, prevent the electrons from reaching the balls, in the same way as the magnetic field of the earth prevents the low-energy cosmic particles from reaching the Earth. The result of our detailed calculations [30] basing ourselves on this analogy is shown in Fig. 7. Here the fraction of electrons reaching a ball is shown for a ball of realizable magnetic momentum and of such dimensions that even if a potential is required to repulse the positive ions, a field intensity which is not too high will be produced. It can be seen that even at relatively low temperatures our ball cannot be effectively protected from the impacts of electrons.

There is a further difficulty: neither the electric nor the magnetic field prevents radiation from reaching the balls. Thus the balls will be heated not only by the electrons colliding with them, but also by the photons impinging

on them. The latter difficulty may be overcome if the balls can be regarded as transparent.

In practice the energy transfer described here is hardly feasible. However, the balls provided with charges and dipoles may perhaps play the part of a moving electromagnetic wall and thus decrease diffusion of the plasma. The balls heated to a very high temperature are removed from the plasma.

Collisions with a "dematerialized" magnetic fields may lead out of these difficulties. Similar collisions increasing the energy may be realized by the motion of the magnetic walls as shown in Fig. 6. An energy transfer of this character is mentioned by Soviet research workers, too [15, 16]. A more effective energy transfer may be effected by keeping the magnetic walls vibrating for longer periods by means of an external force.

*

Accelerators may also have a part to play in power production. According to [7, 8] the condition of excess energy production is

$$v = \frac{E_r}{E_0} > \frac{1}{\eta_n \eta_t} - 1 , \tag{18}$$

where v is the probability that a reaction will occur ; E_r is the energy of the reaction ; E_0 the energy of the injected particle ; η_n accelerator efficiency and η_t is the thermal efficiency of the re-transformation of heat into energy. The probability v that a reaction will occur, has been calculated [8] from the curves of the effective cross section $\sigma(E)$ and of the range $R(E)$ for a tritium target bombarded by deuterium, based on the relation

$$v = N_T \int_0^{\infty} \sigma(E) \frac{dR}{dE} dE , \tag{19}$$

and with this the excess energy produced by the reaction D-T is obtained as

$$\eta = v \frac{17{,}6}{E_0} . \tag{20}$$

This excess energy is too small to be of practical use, it is, however, measureable by macroscopic means. From Fig. 8 the importance of an increase of range is to be seen. At a given density of the gas this increase is only possible by reducing the energy transferred to the electrons. In the following we shall investigate whether there is any possibility of doing this effectively.

We proceed first to determine the upper limit of the energy gain [28].

Let us assume first that the electrons for some reason do not participate in the energy transfer. In this case the deuterium or tritium gas loses its energy

exclusively by the elastic collisions with the nuclei. Now, the question arises as to the probability of a reaction occurring during the slowing-down of the deuteron to thermal energies. The problem is similar to that of the slowing-down of neutrons and, accordingly, the integral equation applied in our considerations will be similar to that known from reactor physics.

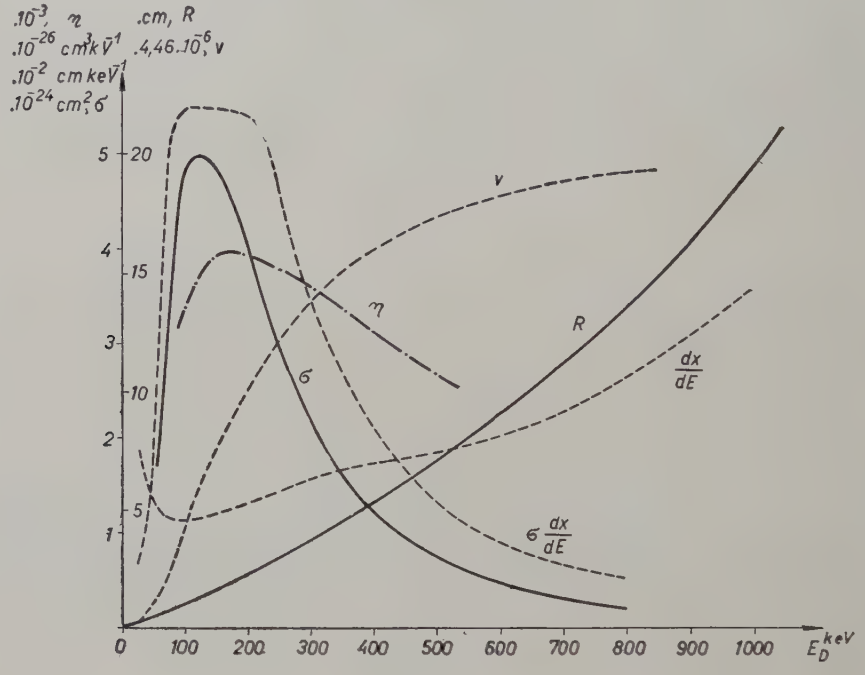

Fig. 8

Let us assume a deuteron gas of infinite dimensions, in the unit volume of which a given number of fusions is initiated continuously by means of some external effect — for instance by tinjections from an accelerator. The energy of the reaction products is transferred to the nuclei. In this way a certain energy distribution $n(E)$ is obtained, which satisfies the following integral equation

$$\int_{E-E_{\min}}^{E_{\max}} \sigma(E', E-E')\, n(E')\, v'\, dE' + \int_{E}^{E_{\max}} \sigma(E'', E)\, n(E'')\, v''\, dE'' = \\ = \{\Sigma(E) + \varphi(E)\}\, n(E)\, v\,, \tag{21}$$

where $\sigma(E_1, E_2)$ is the effective cross section of that process in which a particle of energy E_1 loses an energy E_2 and where

$$\Sigma(E) = \int_{E_{\min}}^{E} \sigma(E, E')\, dE' \tag{22}$$

represents the total effective cross section of the particles of energies E scattered anywhere. E_{max} is the energy of primary deuterons to which the energy of the reaction products is transferred directly ; E_{min} is the assumed minimum of energy transferred in elastic collision ; $\varphi(E)$ is the effective cross section of fusion. By means of a rough estimation this integral equation may be simplified and thus the function $n(E)$ determined. With this the number of further fusions per one initial fusion can be obtained. This number is found to be 3—4. This means that leaving the electron gas out of consideration with respect to the energy balance, a divergent energy-producing process would be obtained. It seems thus to be worth while to investigate the possibility of such neglect.

It is obvious that in case of normal ionization, that is when the temperature of the plasma is some thousand degrees the electrons may still be considered cold as compared to the injected deuterons which have a temperature of 10^7—10^8 °K. Thus the energy transfer will occur in the known manner.

It might be suggested that an *ordered* motion of the electrons knocked on away from the deuteron beam may reduce the energy transfer in case of a target current of high intensity.

Elementary calculations [29] show that if heavy particles arrive successively, the energy of each being transferred to the electrons knocked on by the preceding one, the energy transferred by the n-th heavy particle will be

$$\Delta E_n \approx \Delta E_1 (1 - 2\varkappa)^{n-1}, \tag{23}$$

where ΔE_1 is the energy transferred to the electron at rest by the first heavy particle and

$$\varkappa = \frac{\ln\left\{1 + (b_{max}/\Lambda)^2\right\}}{(b_{max}/\Lambda)^2}. \tag{24}$$

b_{max} is the maximal impact parameter and

$$\Lambda = \frac{e^2}{m_r c^2},$$

where c is the velocity of the heavy particle, the reduced mass m_r being about the same as that of the electron. As the value of $\varkappa$ is very small, there is no considerable decrease in the energy transfer.

Thus we see that although the increase of range is possible in principle, cannot expect a rate of increase which would change the energy balance corresponding to (18). The combination, however, of a plasma, having an energy comparable to that of the accelerated particle and an accelerator may be of importance.

From the above it seems possible to design, at least in principle, a reactor and all equipment — if only in rudimentary form — required to start it up and control it and to ensure its stability (Fig. 9).

This model serves two purposes: first to show the interdependence of the problems envolved and to formulate them clearly, and further it shows the order of magnitude of the physical quantities playing a role in fusion power production. It does not aim at being the prototype of a real reactor. We are of course aware of the fact that it might hardly possible to build a

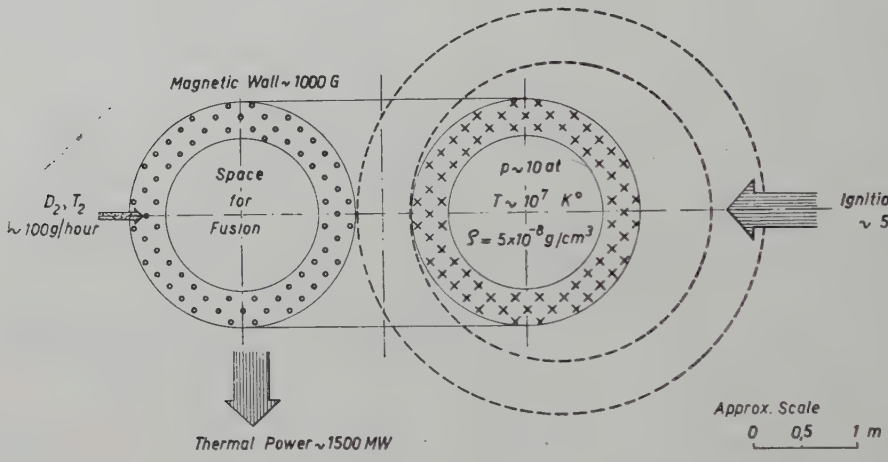

Fig. 9

reactor using the ideas developed here and that a completely different way might have to be followed.

Consider 1 g of D-T mixture. We may consider a simple deuterium gas, too, the conditions will not differ essentially, only the equilibrium temperature will be higher. Enclosing this quantity of gas in a volume of 20 m³, the value of the density will be $5 \cdot 10^{-8}$ g/cm³ ($n = 1{,}2 \cdot 10^{16}$ particles/cm³), and that of the pressure 0,2 mm Hg at room temperature. The power output by fusion of a gas of this density which is equal to the radiation output at equilibrium temperature is $4 \cdot 10^8$ cal/s $\approx$ 1500 MW according to equations (12). It is a rather high value but it can be conducted from the boundary area of the given volume. 1 g fuel supplies this energy for a period of 10^2 sec, thus the fuel consumed may be replaced.

If we decrease the density by one order of magnitude, we get the power of a usual electrical power station i. e. about 150 MW. But in this case other difficulties mentioned below will be increased.

This gas which for a D-T mixture has a temperature of about 10 million degrees may be enclosed in the torus coil mentioned above. For a magnetic

field intensity of $H \approx 1000$ G a homogeneous field, of an 50—100 cm width, constitutes practically an impenetrable wall for all particles of thermal energies. The rate of particle leakage and consequently the inner temperature may be controlled by varying the thickness of the magnetic wall. At a given thickness the rate of departure of high-energy particles will increase with increasing temperature. This phenomenon may insure in principle the realization of stable operation.

The electrons and deuterons, assumed to be of the same energy, penetrate to different depths into the magnetic wall. Thus, in contrast to the internally neutral plasma, negative charges are found on the inner edge of the wall and positive charges on its outside. Placing two electrodes in a suitable position we may obtain useful electric power immediately on account of the fusion energy. The energy leaving in form of radiation may be re-transformed into heat and used, for instance, to produce electric power in the usual way.

The radiation energy appears in the form of soft X-rays. Thus, it is possible to convert it directly into electrical energy using appropriate semi-conductors.

The pressure of the gas at the equilibrium temperature is approximately $p \approx 10$ at. This means a force of some tens of tons for the solenoid if there are ten windings on 1 m length of the torus. Fig. 6 shows, how a ring current is formed by the electrons and ions scattered back by the magnetic wall, the current attracting the inner solenoid and repulsing the outer one.

It is a rather surprising fact that all the quantities we have been dealing with up to now are of an order of magnitude which is common in engineering praxis. But there are grave counter arguments against its feasibility, too, which may compel us to abandon this way of approach. Some are listed below.

What will be the behaviour of the electromagnetic wall when interacting with the plasma instead of with individual particles. The physical picture given here may be considered as an asymptotic approximation only. The above-mentioned ring current carries millions of Ampers. The distortion of the magnetic field cannot be neglected so that the equations of magnetohydrodynamics must be solved.

In order to prevent the charged reaction products from escaping we have to increase the strength of the wall by at least one order of magnitude.

The free path of elastic collisions of the nuclei and even more so the free path of the reaction products, especially that of the neutrons, is too long. They collide frequently with the walls, than with one another. Therefore, the probability of colliding with the windings of the solenoid is great. Thus, the area of these windings must be as small as possible. On the other hand these have to carry ten thousands of Amperes and to withstand tens of tons. They must be cooled, too, although the power per unit area is not too high and the field distortion in the direct neighbourhood of the windings may decrease the number of particles colliding directly with the windings. This is the greatest

difficulty which can hardly be eliminated in this construction. All these considerations show the importance of a magnetic wall without windings. Such a wall is e. g. realized in the pinch effect.

The energy carried by the neutrons is entirely lost. The equilibrium temperature will thus be higher and the pressure increases, too.

The possibility of control can be determined only by a quantitative analysis of the dissipation of power through radiation taking into consideration the effect of diffusion, too.

To initiate the process of fusion, i. e. to impart to each particle an energy of a few keV, an energy of the order of magnitude of 50 MWs is required. In the Soviet experiments energies of 0,5 MWs were involved. The energy transfer is feasible in principle by discharging the condenser batteries charged up to the given energy through a ring coupled to the torus, or discharging the magnetic energy stored up. But it is very difficult to realize it.

We conclude that there are quantities, like balance between power production and radiation, pressure and size fitting well ordinary engineering praxis ; but there are discouraging aspects like the problem of confinement, ingnition, regulation which are yet to be solved and possibly in another direction than that discussed here.

*

The consideration of the possibility of fusion power production is of importance at present, also in view of the solution of several interesting problems in physics, which are connected with this subject. It is important even if in time a law similar in character to the second law of thermodynamics would be proved : The fusion reactor is not feasible in terrestrial dimensions. Let us remember the proof of the second law of thermodynamics : certainty of this fundamental law is given just by the many unsuccessful experiments to realize the perpetuum mobile. Everybody who deals with the problem of the realization of fusion-reactors nowadays does it in the belief that his experiments either help its realization or at worst are required to support a law of the above-mentioned character.

Summary

In this paper a formula is derived which differs from the Stefan—Boltzmann law in respect of the plasma radiation. According to this the specific radiation output is independent of geometrial dimensions. Fusion power production and radiation reach equilibrium at a well-defined temperature independent of geometry and even of density.

The possibilities of power production by accelerators are also discussed with an essentially negative result.

The sketch of a scale-drawn reactor is reproduced here which helped to formulate the problems to be solved.

References

1. Fusion reactors — when? Nucleonics, **13,** 9 (Oct. 1955).
2. From Perhapsatron to Columbus. Nucleonics, **13,** 23 (Dec, 1955).
3. Thermonuclear power — the search for ideas. Nucleonics, **14,** 42 (Feb. 1955).
4. O'Meara, P. E.: An enhanced reactor. Phys. Rev. **89,** 982 (1952).
5. Salpeter, E. E.: Nuclear reactions in the stars. Phys. Rev. **88,** 547 (1952).
6. Thirring, H.: Thermonuclear power reactor — are they feasible? Nucleonics, **13,** 62 (Nov. 1955).
7. Simonyi, K.: Über die Möglichkeit der Nutzbarmachung der Atomenergie ohne Kettenreaktion. Acta Phys. Hung. VI. 157 (1956).
8. Simonyi, K.: Az atomenergia hasznosításának lehetősége. KFKI Közlemények, **4,** No. 1, 83 (1956).
9. Ware, A. A.: A study of a high-current toroidal ring discharge. Phil. Trans. Roy. Soc, A **243,** 197 (1951).
10. Cousins, A. W., Ware, A. A.: Pinch effect in a high-current toroidal gas discharge. Proc. Phys. Soc. (London) B **64,** 159 (1951).
11. Bostick, W. H., Levine, M. A., Combes, L. S.: Spectrographic evidence for the existence of the pinch effect. Sci. Rep. No. 2, Res. Lab., Tufts College (1952).
12. Fischer, H.: Short electrical breakdowns 1. AFCRC—TR—54—100 (1954) U. S. Dep. of Commerce, Office of Techn. Services, Washington.
13. Bostick, W. H., Levine, M. A.: Experiment on the behaviour of an ionized gas in a magnetic field. Phys. Rev. **97,** 13 (1955).
14. Vollrath, R. E., Samson, J. A. R.: Obtaining high temperatures for nuclear fusion. Bull. Am. Phys. Soc. **30,** No. 8 9A (1955).
15. Kurchatov, I. V.: Thermonuclear fusion. Engineering, No. 4705, 322 (May 11. 1955).
16. Арцимович Л. А., Андрианов А. М., Базилевская О. А., Прохоров Ю. Г., Филиппов Н. В.: Исследование импульсных разрядов. Атомная Энергия, **1,** No. 3, 76 (1956).
17. Леонтович М. А., Осовец С. М.: О механизме сжатия тока. Атомная Энергия, **1,** No. 3, 81 (1956).
18. Арцимович Л. А., Андрианов А. М., Доброхотов Е. И., Лукьянов С. Ю., Подгорный И. М., Синицын В. И., Филиппов Н. В.: Жесткое излучение импульсных разрядов. Атомная Энергия, **1,** No. 3, 84 (1956).
19. Лукьянов С. Ю., Синицин В. И: Спектроскопические исследования импульсного разряда. Атомная Энергия, **1.** No. 3, 88 (1956)
20. Лукьянов С. Ю., Подгорный И. М.: Жесткое рентгеновское излучение сопровождающее разряд в газе. Атомная Энергия, **1,** No. 3, 97 (1956)
21. Fowler, W. A.: Cross sections of thermonuclear reactions. Phys. Rev. **81,** 655 (1951).
22. Thibaud, J., Perrier, D.: Luminosité à la rencontre d'ondes de choc. Il Nuovo Cimento, VIII, 705 (1951).
23. Gamov, G., Critchfield, C. L.: Theory of atomic nucleus and nuclear energy-sources. Oxford, 1949.
24. Heitler, W.: The quantum theory of radiation. Oxford, 1954.
25. Fermi, E.: On the origin of the cosmic radiation. Phys. Rev. **75,** 1169 (1949).
26. Alfvén, H.: Cosmical electrodynamics. Oxford, 1950.
27. Tonks, L.: Theory of magnetic effect in the plasma of an arc. Phys. Rev. **56,** 360 (1939).
28. Schmidt, Gy.: Nagyhőmérsékletű plazma sugárzása. KFKI Közlemények, **5,** 56 (1957).
29. Pócs, L., Schmidt, Gy.: Az elektromágneses fal problémájáról. KFKI Közlemények, **5,** 63 (1957).
30. Klopfer, E.: Az ekvipartició-elv egy szélső esete. KFKI Közlemények, **5,** 83 (1957).
31. Kálmán, G.: A sokszorozási tényező deuteron-gázban. KFKI Közlemények, **5,** 72 (1957).
32. Temes, G.: Korreláció egymást követő részecskék energiaveszteségei között. KFKI Közlemények, **5,** 77. (1957).
33. Simonyi, K.: Egy fúziós reaktor vázlata. KFKI Közlemények, **5,** 98. (1957).
34. Ridenour, L.: Scientific American **182,** No. 3, 11 (1950).

G. Kálmán
L. Pócs
G. Schmidt
Prof. K. Simonyi

Budapest, XI., Budafoki út 4—6, Hungary

SOME PROBLEMS OF APPLICATION AND PRACTICAL DESIGN OF NEUTRON AMPLIFIERS I.

By

A. Neszmélyi and K. Simonyi

Institute for Theoretical Electricity of the Polytechnical University, Budapest

(Received January 12, 1957)

In the last few years several methods have been developed for the calculation of subcritical neutron-multiplying systems [1—6], but the results published could not be used directly for the design of a system with a given multiplication.

In the early summer of 1955, we began to carry out calculations concerning the mass multiplication relations of subcritical systems [7], for which there were no data in the literature. The fact, that certain subcritical systems are succesfully employed indeed in university teaching [8], raised the question of practical dimensioning of such systems.

The main problems arising are the following : what is the extent of multiplication to be obtained by using different quantities of variously enriched fuel and different moderators and reflectors, further, how easily can the multiplication be adjusted through the feeding-in of fissionable material ; what is the stability of the systems, what are the economic aspects?

In the following neutron amplifier means any subcritical system, which contains fissionable material and moderator and is built for the purpose of continuously increasing the neutron flux produced by the extraneous source by means of fissionable material.

The first part of this article contains our calculations relating to the static neutron amplifier — i. e. the case, when the position and intensity of the extraneous neutron source is independent of time. Our considerations concerning sources varying with time will be described in the second part.

1. The amplification factor

According to the general reactor theory [9], the neutron density in a finite, bare, homogeneous medium containing a neutron source, independent of time, can be expressed as follows :

$$\varrho(\bar{r}) = l_0 \sum_{n=1}^{\infty} \frac{S_n Z_n(\bar{r}) \bar{P}_\infty(B_n^2)}{1 + L^2 B_n^2 - \frac{k_\infty}{p} \bar{P}_\infty(B_n^2)}, \tag{1}$$

where the $Z_n(\bar{r})$ autofunctions satisfy the equation :

$$\Delta Z + B^2 Z = 0 \tag{2}$$

and the requirement

$$Z(\bar{r}_{\text{extr}}) = 0 \tag{3}$$

r_{extr} referring to the extrapolated boundary of the system with eigenvalues B_n^2. The extraneous source is represented by

$$S(\bar{r}) = \sum_{n=1}^{\infty} S_n Z_n(\bar{r}) .$$

$\bar{P}_\infty (B_n^2)$ is the Fourier transform of the infinite slowing-down kernel at thermal energies. Calculating it for a neutron point source located in the origin of the coordinate system, the results, according to the Fermi age theory and the m — group slowing-down theory, respectively, are the following :

$$\bar{P}_\infty = p \exp[-B_n^2 \tau], \tag{5}$$

$$P_\infty = p \left[\prod_{i=0}^{m=1} (1 + L_i^2 B_n^2) \right]^{-1} \tag{6}$$

Here p is the resonance escape probability, l_0 the average lifetime of thermal neutrons in an infinite medium, τ the Fermi age of thermal neutrons and L_i the diffusion length in the i-th energy interval.

Now, starting from [1], we can define the multiplication at any point of the system as the ratio of neutron densities with and without fissionable material :

$$A(\bar{r}, k_\infty) = \frac{\varrho(\bar{r}, k_\infty)}{\varrho(\bar{r}, 0)} = \frac{\displaystyle\sum_{n=1}^{\infty} \frac{S_n Z_n(\bar{r}) \bar{P}_\infty (B_n^2)}{1 + L_0^2 B_n^2 - \frac{k_\infty}{p} \bar{P}_\infty (B_n^2)}}{\displaystyle\sum_{n=1}^{\infty} \frac{S_n Z_n(\bar{r}) \bar{P}_\infty (B_n^2)}{1 + L_0^2 B_n^2}} . \tag{7}$$

The ratio of thermal neutrons contained in the system is in the two cases

$$\bar{A}(k_\infty) = \frac{\int_V \varrho(\bar{r}, k_\infty)\, d\bar{r}}{\int_V \varrho(\bar{r}, 0)\, d\bar{r}} = \frac{\displaystyle\sum_{n=1}^{\infty} \frac{S_n \bar{P}_\infty (B_n^2)}{1 + L_0^2 B_n^2 - \frac{k_\infty}{p} \bar{P}_\infty (B_n^2)} \int_V Z_n(\bar{r})\, d\bar{r}}{\displaystyle\sum_{n=1}^{\infty} \frac{S_n \bar{P}_\infty (B_n^2)}{1 + L_0^2 B_n^2} \int_V Z_n(\bar{r}) d\bar{r}} . \tag{8}$$

Expressions (7) and (8) may serve as definitions of neutron amplification for a bare medium with time independent flux.

These expressions are suitable for the calculation of any bare, homogeneous and with appropriate averageing, of any heterogeneous, fuel-moderator arrangement. In the latter case, naturally, the microscopic behaviour of neutron density does not alter the multiplication value. The multiplication property of the fuel here is characterized by k_∞ alone, the diffusion and slowing-down by L_0 and τ and L_i, respectively.

2. The "minimal" amplification factor

For the study of a chain reaction, it is necessary that the flux distribution in the neutron amplifier differ significantly from the case without multiplication. Depending on the size of the system, this condition is fulfilled for various k_∞, in these cases, however, the corresponding values of $\bar{A}$ are nearly identical.

To investigate the dependence of the relative neutron density $\varrho(k_\infty, z)/\varrho(k_\infty, 0)$ on $\bar{A}$, let us employ spherical geometry and suppose, we can apply the age theory. The application of spherical geometry does not mean a restriction, it we think of the "equivalent transformation" of other geometries [10], which is usually performable with satisfactory accuracy.

Then (4), (7) and (8) can be written as:

$$S = S_0 \frac{n}{2R^2} \tag{9}$$

$$A(r, k_\infty) = \frac{\sum_{n=1}^{\infty} \frac{n \exp[-n^2\pi^2\tau R^{-2}]}{1 + n^2\pi^2 L_0^2 R^{-2} - k_\infty \exp[-n^2\pi^2\tau R^{-2}]} \sin n\pi \frac{r}{R}}{\sum_{n=1}^{\infty} \frac{n \exp[-n^2\pi^2\tau R^{-2}]}{1 + n^2\pi^2 L_0^2 R^{-2}} \sin n\pi \frac{r}{R}}. \tag{10}$$

$$\bar{A}(k_\infty) = \frac{\sum_{n=1}^{\infty} (-1)^{n+1} \frac{\exp[-n^2\pi^2\tau R^{-2}]}{1 + L_0^2 n^2\pi^2 R^{-2} - k_\infty \exp[-n^2\pi^2\tau R^{-2}]}}{\sum_{n=1}^{\infty} (-1)^{n+1} \frac{\exp[-n^2\pi^2\tau R^{-2}]}{1 + L_0^2 n^2\pi^2 R^{-2}}} \tag{11}$$

In place of the natural parameters of these expressions:

$$k_\infty, \frac{r}{R}, \frac{\sqrt{\tau}}{R}, \frac{L}{R}$$

it is often advantageous to introduce the parameter group :

$$k_\infty,\ z = \frac{r}{R},\ \frac{\sqrt{\tau}}{L},\ \frac{R}{\sqrt{\tau}} \tag{12}$$

In Fig. 1 the values of $\varrho\ (k_\infty,\ z)/\varrho\ (k_\infty,\ 0)$ are represented, which were calculated from (10) and (11), in the case of a large, natural uranium—water sytem, using the constants of Table I, further the values of L_i mentioned in Chap. 4.

The parameters are k_∞ and $\bar{A}$. It may be clearly seen the growing-up of the neutron density, especially at medium z values.

A $(k_\infty,\ z)$ increase very fastly with z and after a maximum — as it can be easily shown — its value is at the boundary :

$$\lim_{z \to 1} A\ (k_\infty, z) = A\ (0, k_\infty)\ .$$

In the origin it can be written : $A_c = A\ (0,\ k_\infty) \leq A\ (z,\ k_\infty)$.

Naturally, the shape of the curves in Fig. 1 depends on the size of the system. The $\varrho/\varrho_{\max}$ values of a smaller-sized amplifier are higher. But from such a representation it is always possible to find for each purpose a suitable $A_{\min}$, [a minimal amplification factor], below which, the multiplication can be considered to be only a large perturbation on the original flux.

3. The correlation of the parameters

The practical description of a neutron amplifier may consist in giving the enrichment of the fuel, the mixing ratio of fuel and moderator (in the case of a heterogeneous system the suitable lattice parameters), further the dimensions and the moderator.

Tha parameter group (12) cannot be considered suitable for such a description, these parameters, however, may be preferred to the parameters of [1] and (11), because they can be transformed in the simplest way into a set of "practical" parameters. Namely, τ (respectively the analogous L_i) in case of a homogeneous system and $\gamma \gg 1$, [9] depends only on the moderator, while k_∞ and L_0 are the functions of enrichment and dilution. We cannot, however, choose these parameters (at least three) independently, because of the properties of the known moderators. We do not deal here with the general case and in the following we shall consider systems containing U^{235} and U^{238} fuel only.

For a homogeneous system it is advantageous to introduce the following notations :

$$\gamma = \frac{N_{\text{mod}}}{N_{U^{235}}}\ , \tag{13}$$

where we shall call γ the "dilution". N is the number of nuclei in the volume element. Further

$$d = \left(1 + \frac{N_{U^{238}}}{N_{U^{235}}}\right)^{-1} \tag{14}$$

may characterize the degree of enrichment. Then it is possible to perform for all moderators the following transformation :

$$\begin{aligned} k_\infty &= k_\infty(\gamma, d) \\ L_0 &= L_0(\gamma, d) \end{aligned} \tag{15}$$

Here d and γ are now "practical" parameters.

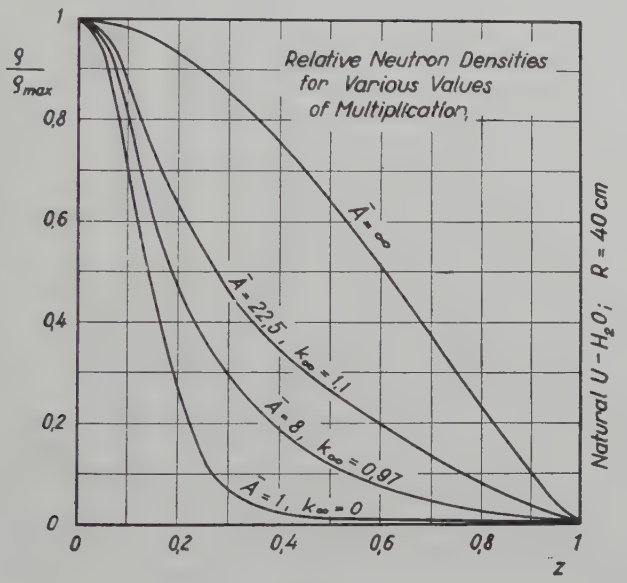

Fig. 1

Fig. 2 represents such a transformation in case of water, calculated [7] from the original definitions, on the basis of the published cross sections. It is noticeable, that L_0 varies weakly with enrichment and that above 10% k_∞ does not grow appreciably.

The maxima of k_∞ for various moderators can be read off from Fig. 3 [11], which represents the critical radii of unreflected spherical reactors with high enrichment.

In heterogenous systems, besides d and the volume ratio V_{mod}/V_{fuel} which is equivalent to γ, additional parameters are playing a role. These are the data characterizing the size of the lattice cell, the clad of uranium and the occasional air gap. References [12—15] contain their published optimal values in case of natural and slightly enriched uranium.

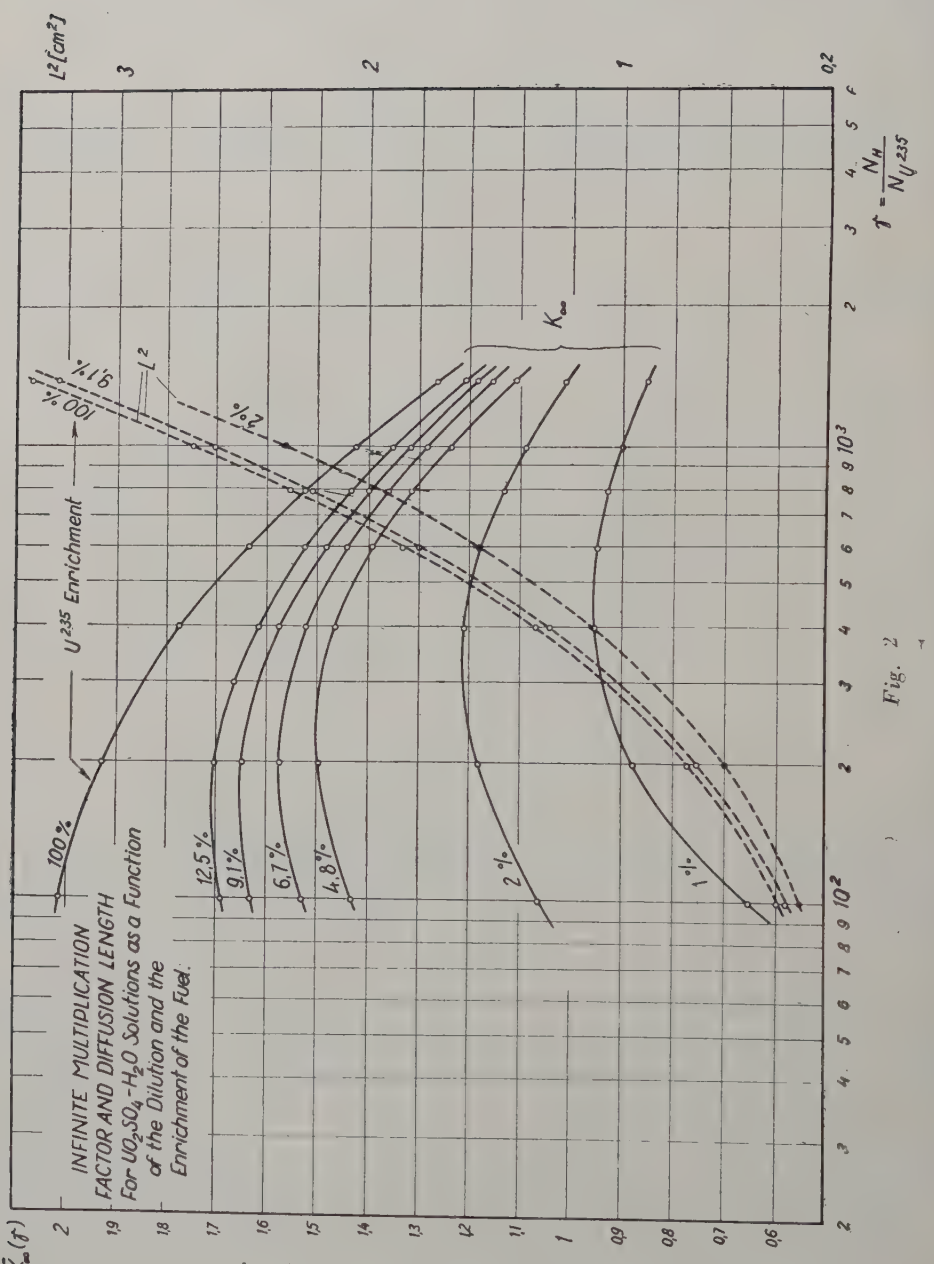
INFINITE MULTIPLICATION FACTOR AND DIFFUSION LENGTH For UO_2SO_4-H_2O Solutions as a Function of the Dilution and the Enrichment of the Fuel.
U^{235} Enrichment
100 %
12.5 %
9.1 %
6.7 %
4.8 %
2 %
1 %
K_∞
L^2
L^2 [cm^2]
$\tau = \frac{N_H}{N_{U^{235}}}$
$\bar{K}_\infty(\tau)$

Fig. 2

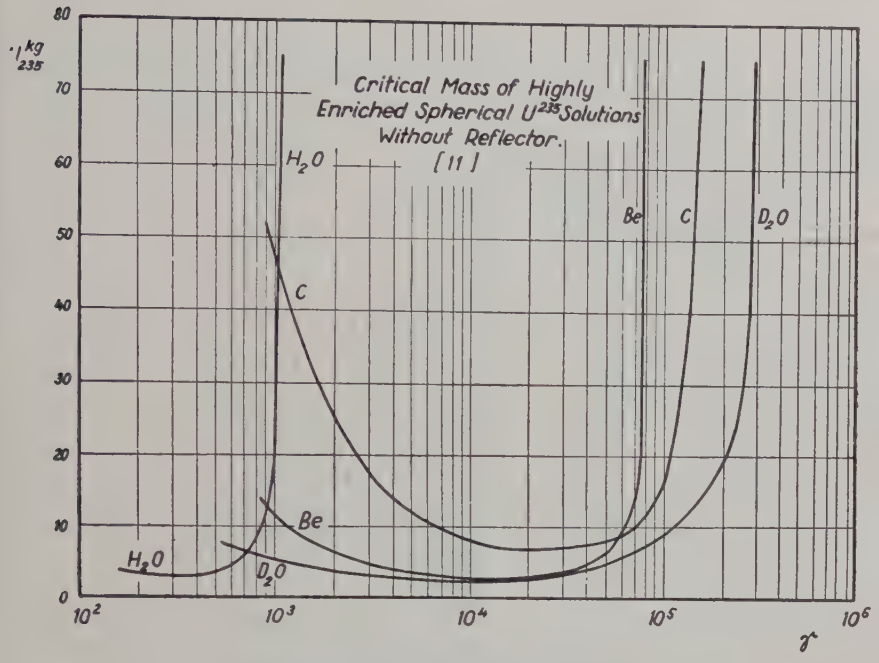

Fig. 3

4. Characteristics of unreflected, static amplifiers

With the aid of (11) and taking into account the appropriate relations between the parameters, the curves for multiplication in optimal cases may be drawn. We here discuss only a few typical examples of them.

Fig. 4 represents the characteristics of a homogeneous spherical amplifier with 9,1% enrichment, which were calculated on the basis of the four-group theory. The k_∞ and L_0 values are to be seen in Fig. 2, while the L_i were chosen according to [9] as follows : $L_1 = 4{,}49$ cm, $L_2 = 2{,}05$ cm, $L_3 = 1{,}00$ cm.

It may readily be seen that in the interval of γ which was investigated, there are critical values of mass, radius and γ^{-1}, below them the amplifier cannot become critical. The structure of the curves suggests the existence of an interesting part of the characteristics at small γ-s.

In the case of $1 < k << 2$, for heterogeneous systems, we can deduce from

$$k_{\mathrm{eff}} = \frac{\bar{A}_1 - 1}{\bar{A}_1} = \frac{k_\infty}{1 + M^2 B_g^2} \tag{16}$$

(taking into account the first harmonic only), the following expression :

$$\frac{V}{V_{cr}} = \left[1 + \frac{1}{\bar{A}_1 (k_\infty - 1)}\right]^{-\frac{3}{2}} \tag{17}$$

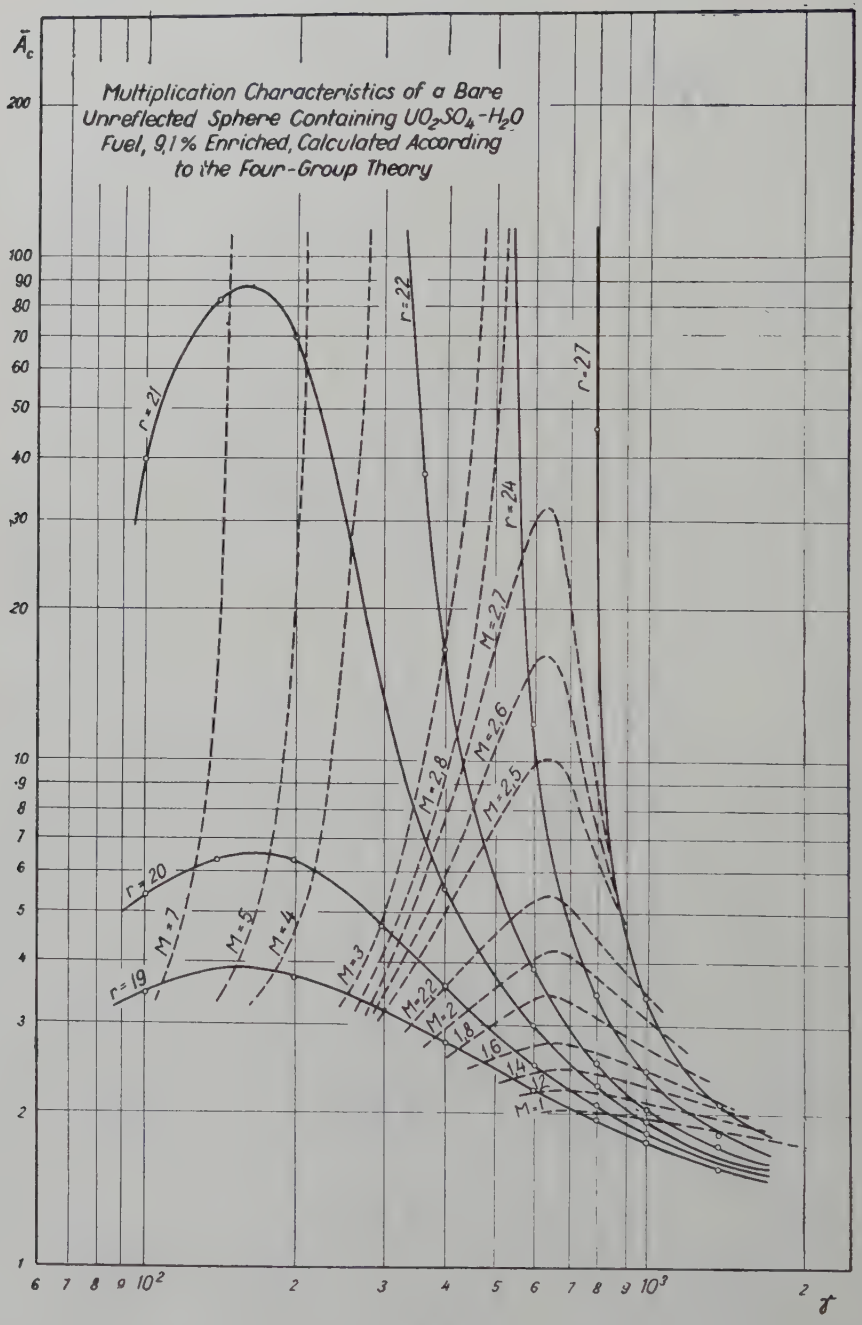
$\bar{A}_c$
Multiplication Characteristics of a Bare Unreflected Sphere Containing UO_2SO_4-H_2O Fuel, 9,1% Enriched, Calculated According to the Four-Group Theory
200
100
90
80
70
60
50
40
30
20
10
9
8
7
6
5
4
3
2
1
r=21
r=22
r=27
r=24
r=20
r=19
M=2,7
M=2,6
M=2,5
M=2,8
M=3
M=4
M=5
M=7
M=2,2
M=2
1,8
1,6
1,4
1,2
M=1
6 7 8 9 10^2 2 3 4 5 6 7 8 9 10^3 2
γ

Fig. 4

which is represented by Fig. 5, where the curve relating to the case $k_\infty = 1{,}45$ and $\gamma = 640$ of Fig. 4 is also drawn in.

We can read off that for identical $\bar{A}$, V/V_{cr} decreases surprisingly quickly with k_∞, while V_{cr} naturally increases.

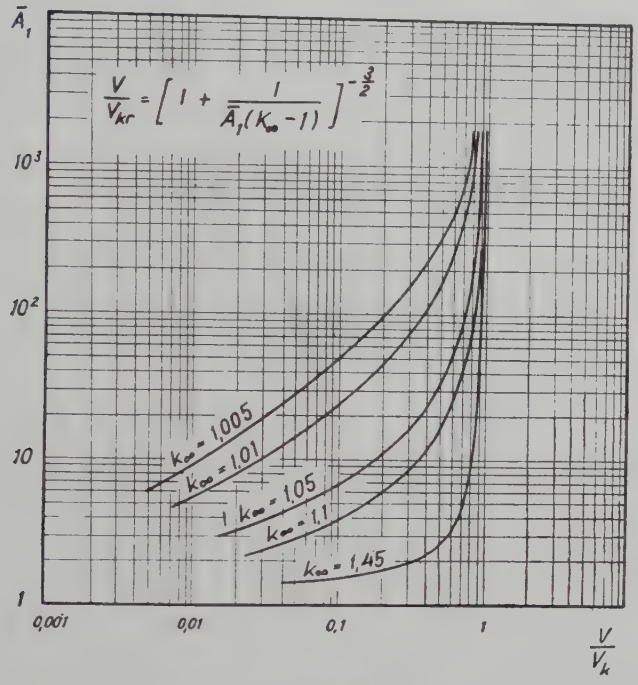

Fig. 5

Fig. 6 represents the attainable gain of natural uranium — ordinary water systems as function of volume for the lattice arrangement of Table I. The calculation was carried out according to (11), taking into account the ten first harmonics only, using the four-group model.

Table I

Moderator	V_{mod}/V_U	r_0, cm	k_∞	L_0^2, cm^2	M^2, cm^2	Ref.
H_2O	1,5	1,5	0,97	2,7	31	[8] [14] [15]
D_2O	29,6	2,54		125	232	[13]
C		2	1,055	402	696	[12]

Representing the multiplication calculated from the approximate expression (17) for variously moderated heterogeneous arrangements as the function of volume, with the parameters obtainable from Table I, we obtain the curves of Fig. 7. The negative values of B^2 are indicated for the sake of completeness only. It is a useful diagram for the estimation of the gain in subcritical systems, even for $k_\infty \leq 1$.

We may conclude on the basis of Figs. 5 and 7 that far from critical radii, with identical volume and moderator, the decrease of k_∞, up to the natural degree of enrichment does not mean significant decrease in the amplification.

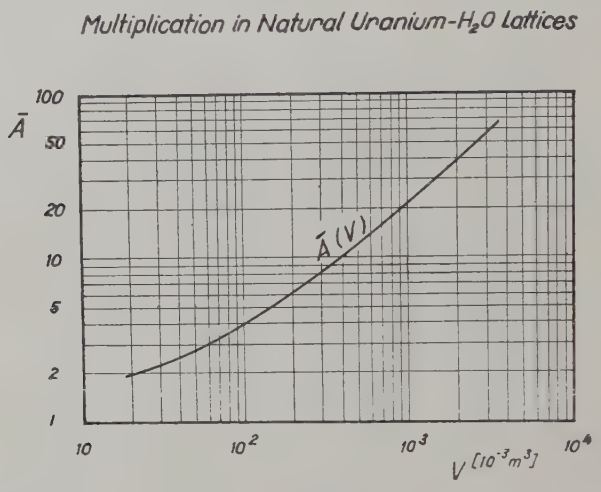

Fig. 6

5. Reflected amplifiers

The reflector savings concerning critical reactors may serve as a first approximation for estimate of the decrease in size of reflected amplifiers. The precize calculation of reflector savings becomes very circumstantial as the number of groups increases considerably. To estimate the attainable accuracy we represented in Fig. 8 two experimental curves and the critical radii and mass calculated according to the methods described in [9], for a homogeneous sphere reflected by an infinite H_2O reflector, and containing highly enriched UO_2SO_4-H_2O solution.

It may be clearly seen that the curves representing the one-group theory and the two-group method go near each other and the latter approximates fairly well the experimental curves. Applying the one-group theory we used the values for B_c obtained in the unreflected case with the aid of the four-group theory. This method is very advantageous by estimating the size.

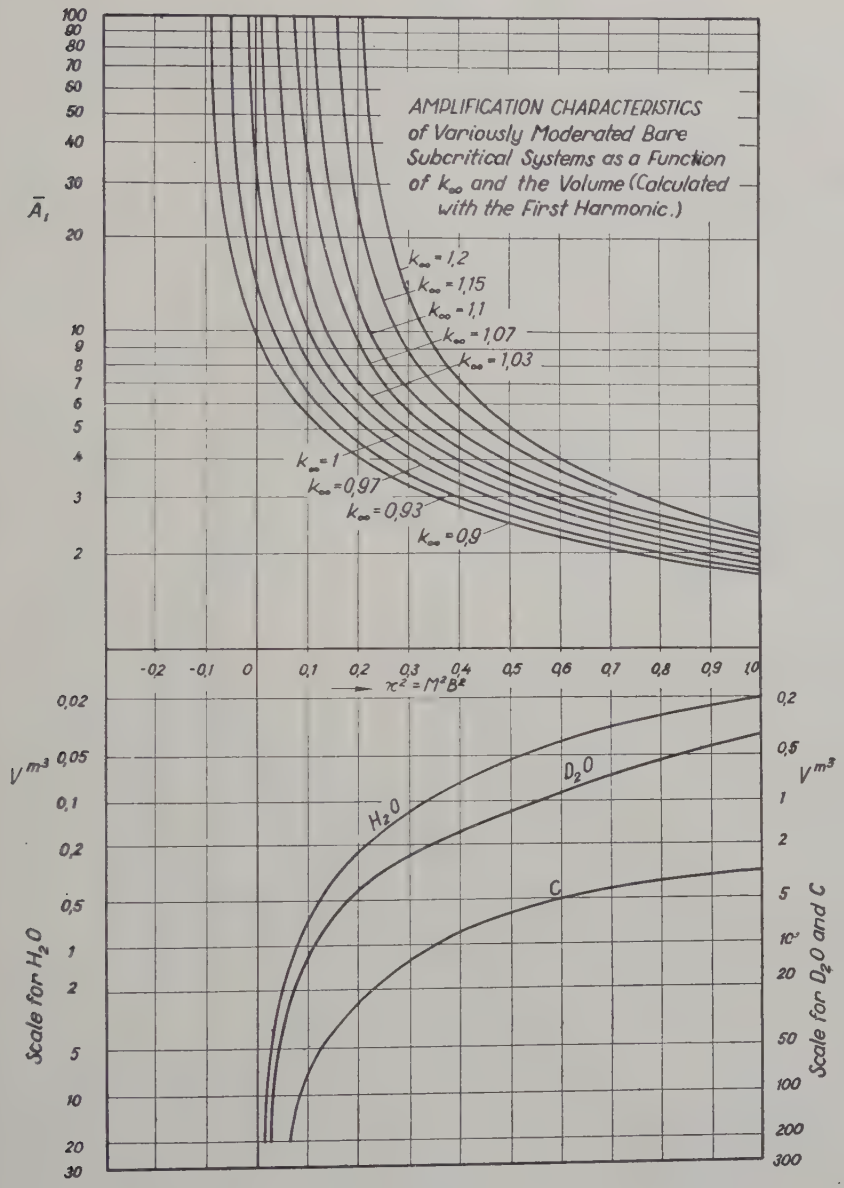

Fig. 7

We may judge the effect of usual reflectors in reducing the critical size from the data of Table II [6c], which relate to water solutions, in case of various "infinite" reflectors. We can conclude that the water reflector in spite of its large capture cross section is a relatively efficient reflector.

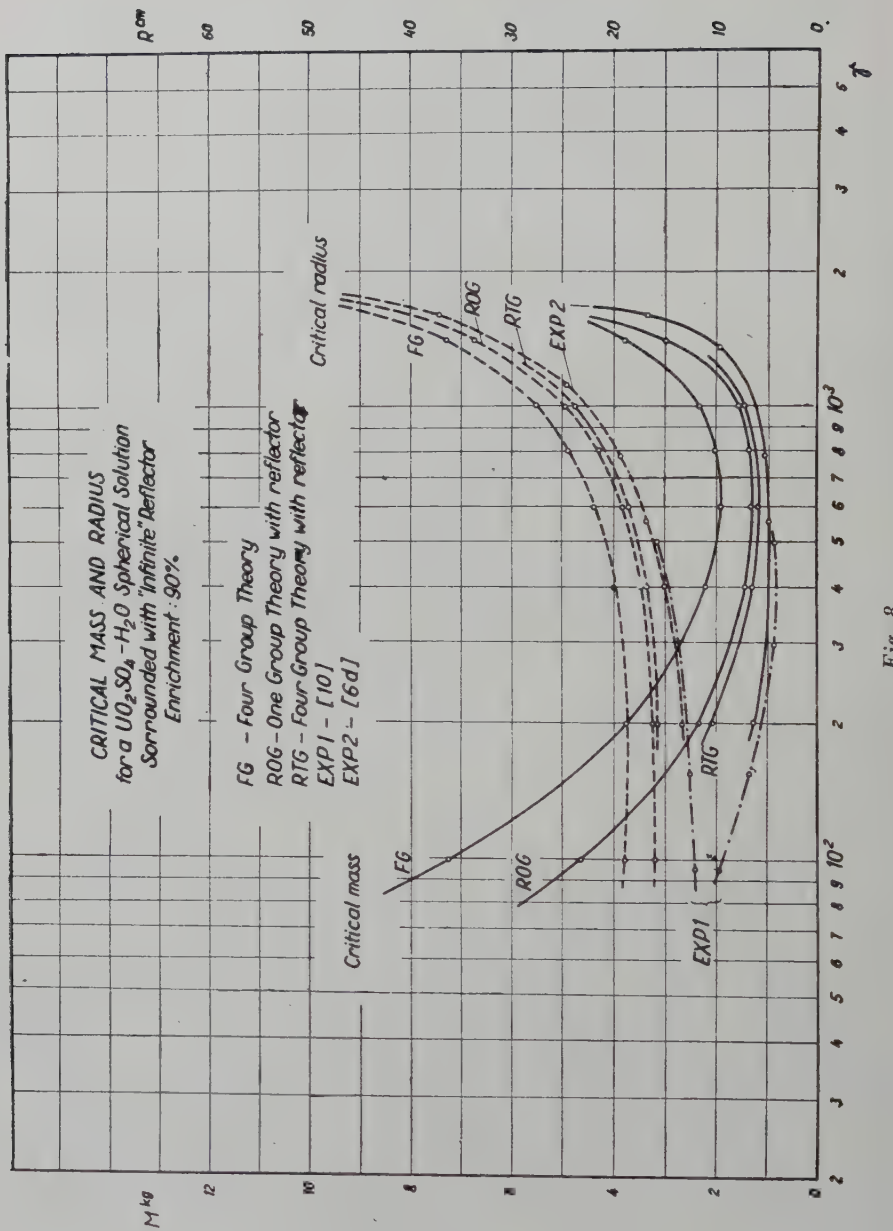
CRITICAL MASS AND RADIUS
for a UO_2SO_4-H_2O Spherical Solution
Surrounded with "Infinite" Reflector
Enrichment: 90%
FG - Four Group Theory
ROG - One Group Theory with reflector
RTG - Four Group Theory with reflector
EXP1 - [10]
EXP2 - [6d]
Critical mass
Critical radius
M kg
R cm
FG
ROG
RTG
EXP2
EXP1

Fig. 8

Table II

Reflector	One-group theory		Experimental [6c]	
	r_{cr} cm	M_{cr} g	r_{cr} cm	M_{cr} g
U 235 %	9,1		12,5	
γ	600		720	
BeO 2,8 g/cm³	16,2	778	15,0	489
Graphite 1,6 g/cm³	16,85	876	16,1	600
D_2O	16,8	870	16,3	622
H_2O	22,03	1970	20,7	1273
Unreflected	24,83	2820	27,3	2920

The dimensioning of reflected neutron amplifiers may be carried out by using equation (11), equating the value of the neutron flux and current density at the core-reflector interface and satisfying the requirement that the flux should be zero at the extrapolated boundary of the whole system. Then, instead of the known one-group reflector equation :

$$\operatorname{ctg} B_c R = \frac{1}{B_c R}\left(1 - \frac{D_c}{D_r}\right) - \frac{D_r}{D_c B_c L_r} \operatorname{cth} \frac{T}{L_r} \tag{18}$$

we obtain :

$$\sum_{n=1}^{\infty} a_n \left\{ n B_c R \cos n B_c R + \sin n B_c R \left[\frac{D_r}{D_c}\left(\frac{R}{L_r} \operatorname{cth} \frac{T}{L_r} + 1\right) - 1 \right] \right\} = 0 , \tag{19}$$

where T is the reflector thickness and

$$a_n = \frac{n \exp\left[-\tau B_n^2\right]}{1 + L^2 B_n^2 - k_\infty \exp\left[-\tau B_n^2\right]} = a_n(B_c, n) . \tag{20}$$

We can improve our results by substituting the unreflected four-group values B_c, as we mentioned above.

The values of reflector saving will become dependent on the gain because of (19). In case of systems of smaller size, when k_∞ is greater, this dependence

can be neglected, for in cases in medium gains, which are interesting of practical purposes, the mass of reactor and multiplier scarcely differ. In case of small k_∞, the difference will be greater.

6. Stability

In water-uranium systems a negative temperature coefficient may be obtained [6b, 15] by choosing suitable lattice parameters in heterogeneous ceses, too. For the sake of simplicity we took the T. C. to be $3 \cdot 10^{-4}$/grad [11] and from this it is immediately apparent that in laboratory conditions a gain of about 20 cannot be described as satisfactorily stable (allowing for a variation in temperature of $\pm$ 15 C°).

In heterogeneous systems stability of temperature it is recommended, in homogeneous systems, with a greater gain, it must definitely be assured.

So as to investigate the feeding-in of fuel in homogeneous systems, we may introduce the sensitivity curve. (Under sensitivity the derivative of the gain with respect to the mass at a given radius is to be understood here). In the case of $R = 24$ cm in Fig. 4, such a relation is represented by Fig. 9.

With respect to safety, the curves $R(\gamma, M) < R_{kr}$ of Fig. 4 deserve attention, however, their realization is made impossible because of their being uneconomic, as they require great amount of fuel. In the case of homogeneous systems when greater gains are obtained it is therefore more advantageous to feed-in at optimal dilution. If, however, this operation is being carried out at above indoor temperature, with some simple safety equipment, then control of the amplifier may be reduced to temperature regulation in the appropriate k_∞ interval. As to the design of safety circuits information may be obtained e. g. from [16—17]. In case of $\delta k_\infty = 1\%$, $T - T_{\text{lab}} = 20°$ C, $dT/dt \leq 0{,}4$ grad/s : $\delta k/dt = 1{,}2 \cdot 10^{-4}$/sec and $P_{\min} \gtrapprox 50$ sec. Thus we can determine upper and lower limit of multiplication for the case considered.

7. Conclusions

From our results we may conclude, that when realizing amplification factors, which are not too great, the price of a neutron-amplifier equals only the price of the fissionable material and the neutron source by both the homogeneous and the heterogeneous case. The necessary quantity of fissionable material is nearly the same for an amplifier or a critical reactor is case of medium enrichment, whereas in case small k_∞, the difference is essential.

Medium enriched homogeneous or a natural-uranium heterogeneous system, with a suitable water reflector both offer certain advantages. As to the costs of

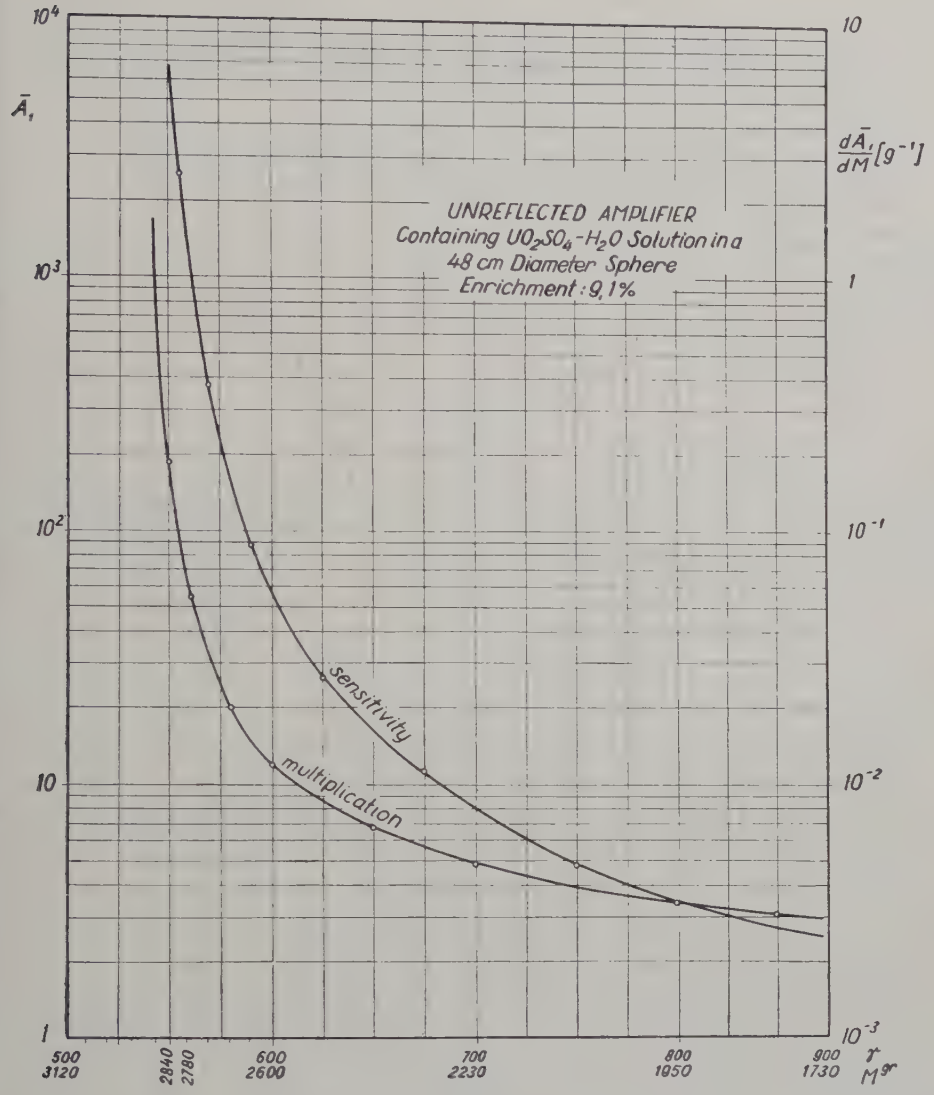

Fig. 9

fissionable material, they are roughly the same [8, 18]. However, an arrangement of greater geometrical dimensions appears in regard to its use to be more versatile.

The small-sized homogeneous system is with adequate precautions suitable for the increase of the intensity of a smaller neutron source. The bigger-sized not enriched heterogeneous system may be absolutely safe ($k_\infty < 1$), suitable for most of the usual measurements carried out in a reactor-school, and just

on account of its greater size it may be operated by many persons. From these points of view it has many advantages over the water-boiler type reactor, employed in university teaching [19].

A reactor, especially for the university of a small country, is rather a valued research tool, than a versatile means of education of reactor engineers.

As the neutron amplifier does not consume the fuel, it is probable that in case of borrowing from a central pool, the use of the neutron amplifier may become an appreciated and more wide-spread means of the university education.

Finally we wish to express our thanks to all who helped us in carrying out the calculations.

Summary

Our calculations concern the value of multiplication to be obtained in static neutron-multiplying systems using different quantities of variously enriched fissionable material and several types of geometrical layouts and reflectors. The economic and safety aspects of these systems are also considered. In the second part the problems relating to the application of neutron sources varying with time will be dealt with.

References

1. WALLACE: Neutron Distributions in Elementary Diffusion Theory, Nucleonics 1949 Febr p. 30 and March p. 48.
2. GALLONE, SALVETTI: Metodi simbolici di calcolo relativi alla moltiplicazione dei neutroni, Nuovo Cimento, 7, p. 482 (1950).
3. GALLONE, SALVETTI: Influenza della funzione di sorgente sulla distribuzione dei neutroni termici in un mezzo moltiplicante, Nuovo Cimento 7, p. 626 (1950).
4. GALLONE, ORSONI, SALVETTI: Sorgenti di neutroni variabili nel tempo in mezzi moltiplicanti (I), Nuovo Cimento 8, p. 960 (1951).
5. IYENGAR, MANI: Thermal Neutron Distribution Due to Time-Dependent Fast Neutron Sources in Non-Multiplying Media, Proc. Ind. Ac. Sci. 1955, 175 p.
6. Sel. Ref. Mat. Genf 1955, Reactor Handbook, Physics *a)* pp. 56—57, *b)* p. 501, *c)* pp. 490—494, *d)* p. 510.
7. NESZMÉLYI: Neutron-erősítők, MTA. Közp. Fizikai Kutató Int. Közleményei, 3. évf. 616. o. (1955). (Proceedings of the Hungarian Central Research Institute for Physics.)
8. BORST: Subcritical Reactor in a Pickle Barrel — NYU's Training Tool, Nucleonics 14, p. 66, 1956. Aug.
9. GLASSTONE—EDLUND: The Elements of Nuclear Reactor Theory, Van Nostrand, 1954.
10. CALLIHAN—MORFITT—THOMAS: Small Thermal Homogen Critical Assemblies Proc. Int. Conf. Genf 1955, Vol. 5, p. 145.
11. GLASSTONE: Principles of Nuclear Reactor Engineering, Van Nostrand, 1955, p. 188.
12. GUGGENHEIM—PRICE: Uranium-Graphite Lattices, Nucleonics Febr. 1953, p. 50.
13. COHEN et al.: Exponential Experiments on D_2O Uranium Lattices, Proc. Int. Conf. Genf 1955, Vol. 5. p. 268.
14. PERSSON: Criticality of Normal Water Natural Uranium Lattices, Nucleonics 12, 1954. Okt. p. 26.
15. KOUTS et al.: Exponential Experiments with Slightly Enriched Uranium Rods in Ordinary Water, Proc. Int. Conf. Genf 1955, Vol. 5. p. 183.
16. SCHULTZ: Control of Nuclear Reactors and Power Plants, Mc Graw Hill, 1955, p. 231.
17. Sel. Ref. Mat. Genf 1955, Research Reactors, p. 62.
18. Research Reactors, Nucleonics 12, Apr. 1954. pp. 7—15.

A. NESZMÉLYI
Prof. K. SIMONYI Budapest, XI., Budafoki út 4—6, Hungary

SIMPLE DESIGN OF FERROMAGNETIC SERIES RESONANCE CIRCUITS

By
J. Antal and A. Kőnig
Physical Institute of the Polytechnical University, Budapest

(Received January 14, 1957)

1. Introduction

The ever increasing interest for circuits containing ferromagnetic inductors calls more and more new applications for, in which the nonlinear characteristics of the ferromagnetic inductor is of prime importance e. g. magnetic flip-flop circuits, stabilizators, etc. In an earlier publication [1] authors reported on a simple *ac* stabilizator as a possible application of the series resonance circuit containing ferromagnetic core. There some qualitative aspects were given about the behaviour of such a circuit and by the aid of a simple graphical construction quantitative estimations were also suggested. In the present paper by further development of the above method the ferromagnetic series resonance circuit is more generally treated and calculating methods based chiefly on graphical construction are briefly outlined for such circuits.

2. Induction coils with ferromagnetic core

The followings are restricted to series resonance circuits with inductors having ferromagnetic core. Such a circuit (Fig. 1) is composed of a condenser C and an inductivity L. It is supposed that both are ideal circuit elements but the ohmic resistance R of the inductivity is taken into account and in the Figure it is drown as a separate element.

The ferromagnetic core implies — as it is well-known — that the flux in the core will not be a linear function of the current flowing through the coil. In case of *dc* magnetization (coil with a given number of turns) the shape of that function is the same as the magnetization curve of the iron core shown in Fig. 2 (hysteresis is omitted).

With *ac* magnetizing current the situation practically will be the same because the relation between mean values of magnetic induction and magnetizing current is similar to that of the curve shown on Fig. 2. That is the permeability of the iron core and the inductivity of the inductor, too, is a function of the

magnetizing current

$$\mu = \mu(i)$$

and

$$L = L(i).$$

For a given iron core this relation can be determined in good approximation

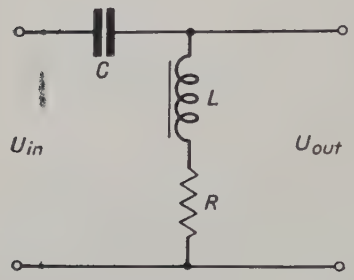

Fig. 1

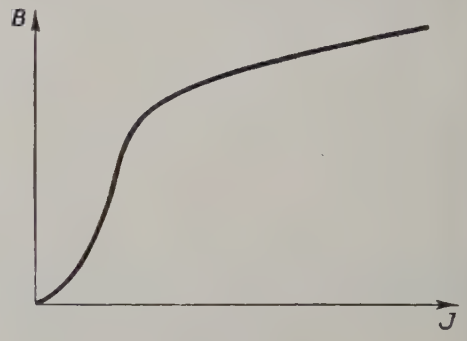

Fig. 2

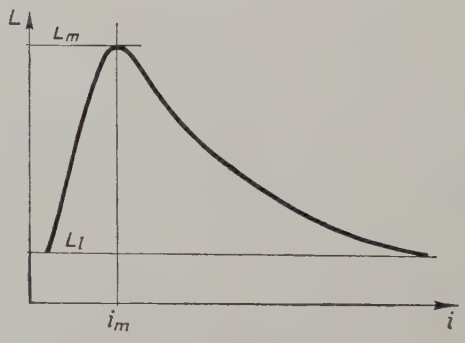

Fig. 3

by measuring the *ac* impedance of the coil as a function of current flowing through it. A typical $L(i)$ relation is shown in Fig. 3.

3. The unloaded series resonance circuit

The resonance circuit of Fig. 1 is connected to an *ac* voltage source with angular frequency ω. Let the input voltage be U_{in} and let us find the output voltage U_{out} that is the voltage on the inductivity

$$U_{\text{in}} = -j\frac{i}{C\omega} + U_{\text{out}}$$

where

$$U_{out} = i\,(R + j\omega L)$$

When the

$$L = L\,(i)$$

relation is given, then with the aid of

$$i = \frac{U_{in}}{R + j\left(\omega L - \frac{1}{C\omega}\right)},$$

U_{out} may be calculated and

$$U_{out} = U_{in}\,\frac{R + j\omega L}{R + j\left(\omega L - \frac{1}{C\omega}\right)}.$$

It is very difficult, however, to use the $L(i)$ relation chiefly because it is not easy to find a suitable analytical approximation for it. To remove the difficulties the authors in their reported paper proposed a graphical method. Let be

$$Z = R + j\left(\omega L - \frac{1}{C\omega}\right),$$

so the absolute value of the impedance of a series resonance circuit will be

$$|Z| = \sqrt{R^2 + \left(\omega L - \frac{1}{C\omega}\right)^2}.$$

Taking into account that the inductivity is a function of the current the impedance will be also a function of the current flowing through. This $|Z| = f(i)$ relation is derived by graphical construction. In Fig. 4 the absolute value of the impedance is plotted as function of inductivity (in arbitrary units). In this construction ω, R and C are constants.

If $L_0 = \frac{1}{\omega^2 C}$ then resonance will occur where $L = L_0$ and the resistance of the circuit

$$Z_{L = L_0} = R.$$

Because usually $R \ll \frac{1}{C\omega}$ the impedance diagram is composed approximately of two straight lines. If we draw besides this diagram the $L(i)$ relation, then

we can evaluate $|Z|$ as a function of i. (Fig. 5) As a result of this graphical construction we have the relation

$$|Z| = Z(i)$$

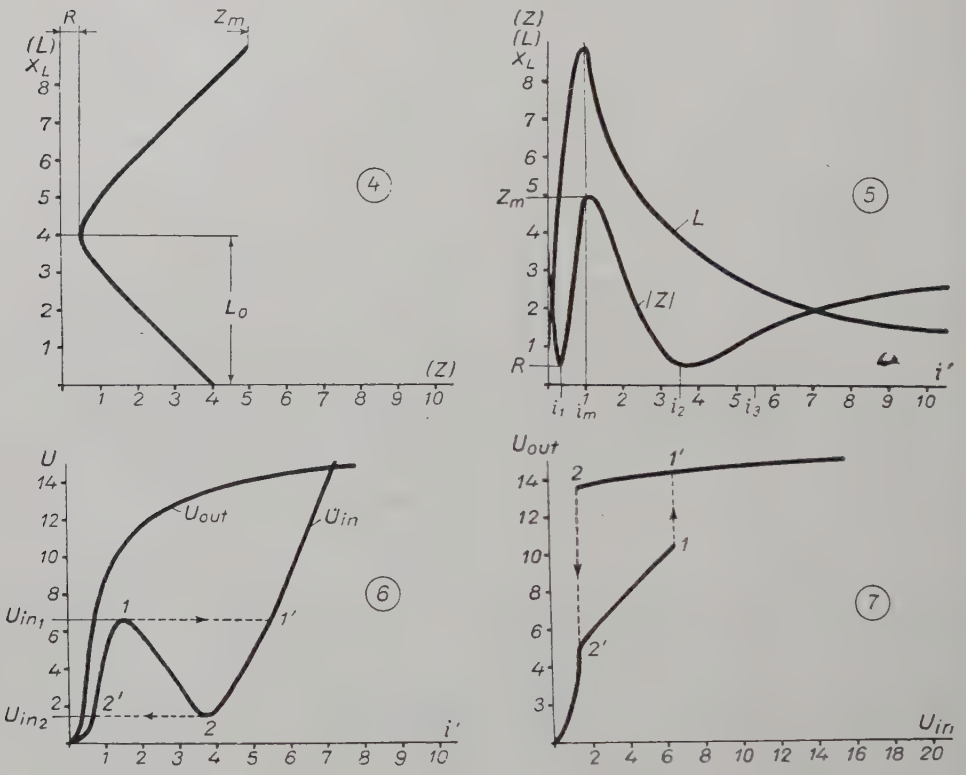

Fig. 4–7

As it can be seen there are two currents i_1 and i_2 where the inductance $L = L_0$ that is resonance occurs. Here the absolute value of impedance attains a minimum and is equal to R.

At $i = i_m$ the inductivity L has a maximum value L_m and the impedance is also a maximum Z_m.

Finally, to obtain the relation $U_{\text{out}}(U_{\text{in}})$ following products are formed

$$U_{\text{in}} = i\,|Z|$$

and

$$U_{\text{out}} = \omega L i$$

where in the second product R is neglected. These can be seen in Fig. 6 where two curves are plotted

$$U_{\text{in}} = U_{\text{in}}(i) \qquad \text{and} \qquad U_{\text{out}} = U_{\text{out}}(i).$$

The points (1) and (2) on the U_{in} curve will in good approximation belong to i_m and i_2 respectively. Furthermore

$$\begin{aligned}
\text{if} \quad & i = 0, \quad \text{then} \quad U_{\text{iu}} = 0, \\
& = i_1, \qquad\qquad = i_1 R_1 \\
& = i_m, \qquad\qquad = i_m Z_m \approx U_{\text{in1}}, \\
& = i_2, \qquad\qquad = i_2 R \approx U_{\text{in2}}, \\
& = i_3, \qquad\qquad = U_{\text{in1}},
\end{aligned}$$

from which even i_3 can be obtained.

While in contrast

$$\begin{aligned}
\text{if} \quad & i = 0, \quad \text{then} \quad U_{\text{out}} = 0, \\
& = i_1, \qquad\qquad = \omega L_0 i_1 = \frac{i_1}{C\omega}, \\
& = i_m, \qquad\qquad = i_m \omega L_m = U_m, \\
& = i_2, \qquad\qquad = \omega L_0 i_2 = U_{\text{out2}} \\
& = i_3, \qquad\qquad = U_{\text{out1}}.
\end{aligned}$$

From this data the relation $U_{\text{out}}(U_{\text{in}})$ can be constructed (Fig. 7).

This Figure enables us to evaluate the qualitative behaviour of the circuit. Increasing the input voltage from zero to U_{in1} (point 1) the current, which meanwhile attained the value i_m, suddenly jumps to another much higher value i_3 (point 1'). When we decrease the input voltage untill U_{in2} (point 2) the current which has here an approximate value i_2 suddenly jumps to a much lower value (point 2').

It can be seen that in the interval $U_{\text{in2}} < U_{\text{in}} < U_{\text{in1}}$ there are two possible current values belonging to every U_{in} value. That range of the curve lying between the points (1—2) has no real meaning because in this interval the impedance is negative and the circuit is unstable. In this interval the two stable current value can be obtained with trigger like rising or decreasing input voltage.

There is also a similar jump in output voltage U_{out} in the (1—1') and (2—2') regions, respectively. When the input voltage approaches the value U_{out} the voltage across the inductivity jumps to U_{out1} and because an augmented current

flows we are in the saturation region where the output voltage U_{out} will change only slowly when input voltage U_{in} is changed. If U_{in} decreases until reaches U_{in2}, U_{out} will also decrease until reaches U_{out2} where sudden jump occurs to a much lower value.

Owing to saturation the quotient

$$\delta = \frac{U_{out1} - U_{out2}}{U_{in1} - U_{in2}}$$

can have very low value and so the circuit will operate not only as a bistable nonlinear circuit but also as a simple voltage stabilizator.

The above figures give no direct information about the application of this circuit as a stabilizator in respect of power which it can deliver, therefore the loaded condition will also be considered.

4. The loaded series resonance circuit

Fig. 8 represents the loaded condition. In this figure a resisto $1r$ is connected across the inductivity as a shunting element. As compared to the real load this represents a simplification yet we will confine ourselves to pure ohmic load.

In order to use the graphical construction the load which is connected in parallel will be transformed in a series impedance (Fig. 9).

In this conversion let be

$$Z_1 = Z_1', \; Z_2 = Z_2' \text{ and } i_1 = i'$$

so the voltage across the inductivity U_{out} will be the same in both cases.

It is very easy to show, that

$$Z_3' = \frac{Z_1 Z_2}{Z_s} .$$

Since

$$|Z_1| = \frac{1}{C\omega}, \; Z_2 = r$$

and

$$|Z_2| = L\omega ,$$

supposing

$$R \ll L\omega ,$$

the substitution series resistance Z_3' which will be denoted by R_s

$$R_s = \frac{L}{C \cdot r} .$$

Naturally, since

$$L = L(i),$$

the substitution resistance

$$R_s = R_s'(i)$$

will also be a function of current.

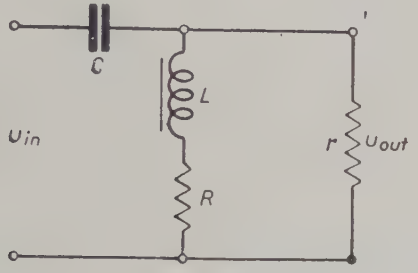

Fig. 8

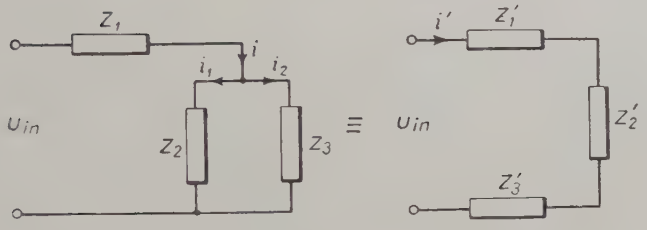

Fig. 9

As we shall see the value of the substitution resistance is important chiefly at the current i_2 where jumping occurs so as a first approximation L can be regarded to be constant and equal to L_0.

So at least approximately :

$$R_s \approx \frac{L_0}{C \cdot r}.$$

Figs. 10—13 show the influence of loading. It can be seen that with rising R_s the curve $U_{in}(i)$ straightens and finally the two stable state, and the negative impedance disappear.

Naturally, this impairs the stabilization and the load will throw out the circuit from its state of higher output voltage.

The former graphical construction can be used in this case, too, if the loss resistance R would be increased by the substitution resistance R_s of the load.

So we can say quantitatively that the load can be only so large that the range of the curve $U_{in}(i)$ between (1—2) would be just horizontal.

This is accomplished when

$$(R_s + R)\, i_2 = U_{\text{in}_1}.$$

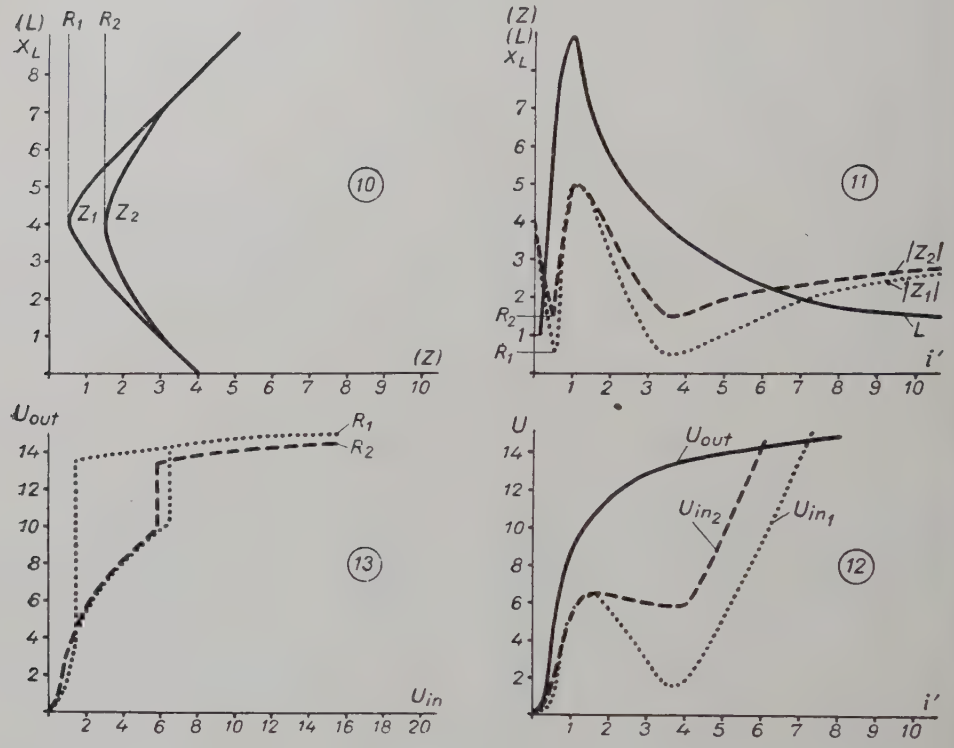

Fig. 10—13

Taking into account that

$$U_{\text{in}_1} \approx i_m Z_m,$$

so

$$R_0 = R + R_s = Z_m \frac{i_m}{i_2}.$$

If $R_s \gg R$, then $R_0 = R_s$ and the value of the loading resistance

$$r = \frac{L_0}{CR_s} \approx \frac{L_0 i_2}{CZ_m i_m} \approx \frac{1}{C\omega} \frac{i_2}{i_m} \frac{L_0}{L_m}.$$

So the load carrying capacity at a given inductivity can be increased by the increase of the capacitor C. This expression will throw some light upon the desirable ferromagnetic characteristics. It is advantageous to use such iron cores which give a steeper slope and a greater drop on the curve $L(i)$ between the maximum and L_0.

5. Design of loaded series resonance circuits

At the design following data are generally given :

a) U_{in} the input voltage,

b) $\pm \Delta U_{in}$ permissible variation of input voltage,

c) W the desired power (ohmic load),

d) $L = L(i)$ function (e. g. so that the data of measurements performed on a coil with given cross section and number of turns is given at a particular angular frequency),

e) ω the angular frequency.

The data to be computed are :

a) q the final cross section,

b) N the final number of turns,

c) C the necessary capacitor,

d) R the permissible loss-resistance (this is composed of the copper losses of the coil and of iron losses),

e) δ stabilization factor.

As we have seen before :

$$r \approx \frac{1}{C\omega} \frac{i_2}{i_m} \frac{L_0}{L_m} = \frac{1}{C\omega} \frac{i_2 L_0 \omega}{i_m L_m \omega}$$

$$\approx \frac{1}{\omega C} \frac{U_{\text{out}}}{U_m},$$

where

$$U_{\text{out}} \approx U_{\text{out}_1} \approx U_{\text{out}_2}$$

and

$$U_m = i_m L_m \omega,$$

so

$$W = \frac{U_{\text{out}}^2}{r} = C\omega U_m \cdot U_{\text{out}}$$

$$= C\omega L_0 \omega i_2 U_m,$$

therefore

$$i_2 = \frac{W}{U_m}.$$

Since the curve $L = L(i)$ is given, U_m accross the given inductivity can be computed.

Using L_0, which belongs to the computed current i_2 we have the capacity

$$C = \frac{1}{\omega^2 L_0}.$$

and the output voltage

$$U_{\text{out}} \approx U_{\text{out}_2} = i_2 \omega L_0.$$

If this capacity cannot be easily realized we can choose an other more realizable one. Let us denote the value of this new capacity C' then the new value of inductivity is given by

$$L_0' = \frac{1}{\omega^2 C'} .$$

If the number of turns belonging to L_0 is N then the required number of turns for L_0' is

$$N' = N \sqrt{\frac{L_0'}{L_0}}$$

since at constant cross section the inductivity varies with the square of the number of turns.

Naturally, now the value of i_m and i_2 will also change. The currents belonging to the new inductivity are

$$i_m' = i_m \frac{N}{N'} \quad \text{and} \quad i_2' = i_2 \frac{N}{N'} ,$$

respectively.

The voltages will change, too, namely

$$U_m' = U_m \frac{N'}{N}$$

and

$$U_{\text{out}}' = U_{\text{out}} \frac{N'}{N} .$$

Since

$$W = i_2 U_m = i_2' U_m' ,$$

the output power is constant.

At a given loss-resistance i_2 can not have any value because when

$$i_2 R = U_m ,$$

the circuit can not be loaded further. Therefore in practice it is advisable to limit the loss-resistance as follows

$$R \leq \frac{U_m}{10 i_2} .$$

Moreover, it is important that the minimum value of the input voltage should be greater than the turnover voltage

$$| U_{\text{in}} - \Delta U_{\text{it.}} | \geq U_{\text{in}_1} \approx U_m .$$

Finally, let us suppose that we have computed an inductivity L_0 and a capacity C for a given load W (the function $L = L(i)$ was measured with a given coil of cross section q and number of turns N). In this case the design procedure is as follows.

a) The cross section is given by the fact that the losses of the induction coil must not be greater than 0,1 W which fact sets a limit to the weight of iron in consequence of iron losses. With the so computed cross section we procede in a tentative calculation.

b) If we know the total and iron losses the copper losses can be calculated which in turn determins the number of turns which can be wound on the iron core and the diameter of the wire, too.

Let be the so computed cross section q',

the number of turns N',

and introduceing the following quotients

$$\nu = \frac{N'}{N},$$

$$\varkappa = \frac{q'}{q},$$

the obtainable inductance in the resonance point

$$L_0' = L_0 \varkappa \nu^2 .$$

c) The required capacity

$$C' = \frac{1}{\varkappa \nu^2} C .$$

The currents are

$$i_2' = \frac{i_2'}{\nu}, \quad i_m' = \frac{i_m}{\nu} .$$

The voltages

$$U_m' = U_m \varkappa \nu, \quad U_{\text{out}}' = U_{\text{out}} \varkappa \nu .$$

If the so computed values are not suitable we must choose another type of iron core which has smaller losses, or has different dimensions.

d) The stabilization factor δ is determined graphically.

6. Remarks

Finally, we have to examine the approximations used. The calculations were made with mean values. The most important approximations were the followings :

a) It is supposed that the points of overthrow (1) and (2) are at i_m and i_2, respectively. This approximation for i_2 is quite good, for i_m it is not so. In reality

the point (1) appears at a greater current and so the overthrow voltage which can be calculated by the equation as

$$U_{\text{in1}} = i_m Z_m$$

is lesser than in reality.

b) When calculating the substitution resistance of the lood the inductivity was taken as constant, L_0. At the same time when we computed r instead of Z_m we took a greater value $L_m \omega$ which means a greater lood.

However, by the introduction of the voltage U_m the approximation in point (a) is partly compensated because

$$U_m = i_m \omega L_m > U_{\text{in1}}$$

As the current of the induction coil flows through the capacitor, the capacitor must withstand this current and also the voltage drop required accross.

If the output voltage U_{out} is not a suitable one a transformer between the load and the output terminals will serve. Practically, the inductivity may be the primary of this transformer. In this case, the iron cross-section is given merely by the winding space requirements and one has to choose an iron core in wich the losses are low enough.

A few such circuits have been accomplished and there are good agreement between the data received by graphical construction, computation and measurements respectively ($\sim$5%). With a 25 watt load in a comparatively small volume the stabilization factor attained was $\delta \sim 0{,}2$.

7. Acknowledgements

We are indebted to Professor Dr. P. Gombás for kind permission to perform this work in the Institute. We owe our thanks to Mr. I. Katula and Mr. J. Peer for the successful cooperation in the measurements.

References

ANTAL, J.—KŐNIG, A.: Acta Phys. 7, 117 (1957).

Summary

The series resonance circuit with ferromagnetic core is treated. It is shown that such a circuit can be used not only as a nonlinear network with two stable states, but also as a simple *ac* stabilizator. Design procedures are given by the aid of a graphical construction for the unloaded as well as for the loaded cases.

J. ANTAL
A. KÖNIG Budapest, XI., Budafoki út 4—6, Hungary

BOOK REVIEW — BUCHBESPRECHUNG

Electric Power Transmission by L. Verebély, Vols. I-IV

Forty years of creative effort and university teaching have been concentrated in this comprehensive work edited by Prof. Dr. László Verebély in the years 1946—1950. In addition to the material delivered by the author during the past 25 years before students of electrical engineering at the Technical University, Budapest, the four volumes include detailed information on problems electrical engineers may come across in design work or industrial practice. In order to attain this aim a theoretical basis has been adopted. The methods of discussion have been chosen with a view to presenting the material in logical order so as to provide a valuable aid for electrical engineers engaged in both research and scientific work.

Volume I has been sub-titled Practical Electrostatics (University Press, Budapest, First edition 1946, 472 p., 367 figs., 26 tabs.). The introduction is devoted to the development of various theories on electricity from ancient times up to the present, surveyed in the light of the general evolution of natural sciences. The theoretical discussion of fundamental concepts of electrostatics meets the requirements of the practical engineer as well. This is followed by a detailed treatise on the dielectric strength of materials constituting the basic knowledge for up-to-date insulating techniques. Notes on the production of insulating materials comprise both theoretical and practical data relating to gaseous, liquid and solid insulating materials. A special section is devoted to insulators (pin insulators, bushings and line insulators) with the description of a wide range of both commonly used and special shapes. The Chapter entitled Insulator Testing deals with routine and special laboratory tests of insulators made of porcelain, glass, steatite and up-to-date synthetic resins. Equipment and measuring methods used in high-tension laboratories are discussed in the last part. Detailed information on insulators and insulating materials has been compiled in tables annexed to the volume.

Volume II sub-titled High- and Low-Tension Power Transmission Lines (University Press, Budapest, First edition 1947, 452 p., 304 figs., 15 tabs.) is devoted to the theory of electrical characteristics and performance calculations of high- and low-tension power transmission lines. An interesting survey of the history of electrical power transmission and of Hungarian contributions thereto is given in the Introduction. The general aspects of electrical power transmission are outlined and presented in a coherent system in Part I. The detailed discussion of low-tension D. C. and A. C. lines is followed by a chapter on the electrical characteristics of high-tension overhead lines as well as on vector diagrams and performance conditions of power transmission lines. Disturbing effects of high-tension lines upon neighbouring conductors are dealt with in conclusion in a manner to furnish practical advice on the basis of theoretical relationships. Analytical and graphical methods used for the study of A. C. circuits as well as a coherent summary of the symbolic method are given in the annex. The use of both methods is enlightened by practical examples. Fifteen tables containing data on overhead lines and cables are to be found at the end of the volume.

Volume III has been sub-titled Cables and Overhead Lines (University Press, Budapest, First edition 1948, 520 p., 438 figs., 29 tabs.). While the general theory of low- and high-tension power transmission lines is dealt with in Vol. II., special, mainly practical problems of cables and overhead lines are summed up in this volume. The material has been grouped under the following headings: High-Tension Cables, Overhead Lines, Transmission Towers, Construction and Mounting of Overhead Lines, Heat Effects in Transmission Lines. The treatment exceeds by far the scope of a university textbook, yet renders the book suitable to satisfy the needs of the engineer engaged in practical work. An entire section has been devoted to economic aspects and to D. C.

power transmission. The copious material compiled in 29 tables is a valuable aid for students and engineers designing overhead lines and cable network.

Volume IV carried the sub-title Switchgears and Protective Equipment, Overcurrents, Voltage Surges (Scientific Publishing House, Budapest 1950, 590 p., 634 figs., 33 tabs.). As conceded in the preface by the author, the selection of the material for this volume was not without difficulties due to the scope, divergence and constant evoluting of this subject. The limits to be observed in a similar comprehensive work have been successfully determined without however obscuring the picture of the present state of development or of the trend of future evolution. Main headings of individual parts again give an indication of the material: Bus Bars, Disconnecting Switches, Fuses, Circuit Breakers, Drives for Circuit Breakers, Tripping Elements and Relays. A clear summary of theoretical knowledge on the electric arc and its extinction has been inserted before the discussion of circuit breakers. Protective systems are dealt with under the following headings: Selective Protection of Equipment and Line Protection. The description of short circuits, their analysis and methods of limiting their effects constitute a seperate chapter. Preceding the section on protection against voltage surges author expounds the characteristics of line instability phenomena and travelling waves as well as the sources of voltage surges. The discussion of problems concerning the earthing of the neutral point, the advantages and drawbacks of several commonly applied systems constitute the last part of the volume. The 22 tables contain data mainly on bus bars made of various materials and mounted in various arrangements.

Extensive references on the subject under consideration are given at the end of each volume.

Volumes I. and II. have arrived to third edition, in 1956, enlarged to 586 and 584 pages. Second edition of volumes III. and IV. is prepaired for 1957.

The four volumes running into well over 2400 pages have greatly contributed to the successful education of Hungarian electrical engineers. The coherent manner of treatment and the systematic summary of the vast subject on electric power transmission have aroused the interest of foreign experts as well. Vol. II. has already been published in Czechoslovakia as a university textbook in 3200 copies sold out within a few months. Translation of Vol. I. under way.

F. Taky

Dr. Prof. Emil Mosonyi: Wasserkraftwerke Vol. I.

(Publishing House of the Hungarian Academy of Sciences, Budapest, 1956.

872 p. (B/5) + 598 Figs. + 6 Annexes)

The first volume of this exhaustive, abundantly illustrated comprehensive work on the general, engineering, mechanical, electric as well as economic aspects of water power utilization has recently been published by the Publishing House of the Hungarian Academy of Sciences. The work is planned to appear in two volumes by the author Dr. Emil Mosonyi B. C. E., D. Sc., Corresponding Fellow of the Hungarian Academy of Sciences, Professor of Hydraulics at the University of Technical Sciences, Budapest, Director of the Institute for Hydraulic Planning. The second volume is to be published this year.

The German edition in based on the first edition of the book "Water Power Utilization" published in Hungarian, in 1952., and received most favourably by the international technical literature. Here are some extracts from scientific journals: Water Power, January, 1954: „... it appears to be as fully exhaustive of the subject as the acknowledged standard works previously published in Europe and America..." or the Österreichische Wasserwirtschaft 1954: „The work is destined in the first place for students of civil engineering at the universities, nevertheless it can serve as an excellent book of reference for practicing civil engineers." The Bulletin Technique de la Suisse Romande writes: „The author makes his readers acquainted with the latest achievements of technical literature on the one hand and with the results of his own studies and investigations on the other. The entire work is of very high standing."

The German edition is not a mere translation of the Hungarian original. Maintaining the structure of the book unaltered,

the author, by including the latest scientific issues and practical examples, has considerably enlarged the extensive and divergent material of Vol. I., dealing with low-head developments. The illustrative material has been enriched by numerous photographs of water power stations built in recent times all over the world. The latest trends of water power development are being dealt with in detail. Thanks to this thorough revision the text as well as the number of figures have been increased by about 50 per cent as compared to the first Hungarian edition. The Gospodarka Wodna 1956/12. writes of this thoroughly revised edition: „In comparing Prof. E. Mosonyi's book with works of similar character it must be stated that this work is very exhaustive, problems are dealt with on a wider basis and definitions given are more correct... The subject is being presented in the most lucid way..."

In comparing the German with the first Hungarian edition the chapters dealing with tidal energy, water power resources, various types of run-of-river hydroelectric plants (block type station arrangement, twin power plant, pierhead plant, submersible plant) have almost completely been revised, while chapters on the history of water power utilization, the general layout of diversion canal type of developments and run-of-river power plants, economic aspects, intake works, water losses from the power canal, vertical shaft setting of wheels, rack heating, head gates, wheel efficiency, flow condition in the draft tube, determination of main dimensions for preliminary design purposes, propeller wheels, governors, generators and other electric equipment and machine halls have been enlarged considerably.

The importance of scale-model tests is repeatedly pointed out. The author devotes considerable space to the subject of the development of the new-type wheels, the tubular turbines and also indicates the trends of progress in other fields. The first Hungarian edition of the work was noted for its excellence in giving clear concepts and accurate definitions in every respect. The revised German edition also gives the precise determinations important concepts such as e. g. the effective head, slot loss and energy losses in flow entering the wheel, etc.

While the first Hungarian edition had been prepared primarily for educational purposes for university students and only in the second place for researchers and experts engaged in solving theoretical and practical problems of water power utilization, the revised German edition — following unaltered educational principles — is meant in the first place for specialists but is at the same time also a suitable text-book for universities, owing to its lucid and unequivocal arrangement. It is a very valuable guide for specialists besides civil engineers, for whom it is primarily meant, mechanical engineers engaged in the field of water power utilization, furthermore for economic experts. Besides civil engineering problems in the strict sense of the word also problems of mechanical and electric as well as of economic character are being dealt with in detail.

As already mentioned, the original arrangement of the Hungarian edition has been left untouched in the German edition. Besides general problems of water power utilization low-head power plants are extensively discussed. The principal chapters are the following: I. Utilization of water power — *A)* Resources of mechanical energy in water — *B)* History of water power utilization. II. Low-head power plants: *A)* The power curve — *B)* Types of development — *C)* The power canal and appurtenant structures — *D)* Types and parts of run-of-river power stations — *E)* The powerhouse. The chapter mentioned last deals besides the substructure of the powerhouse with the question of turbines, alternators, gates and closures and architectural construction as well as with the structural dimensioning of the power station. At the end of the individual chapters well chosen examples are given in order to facilitate the application of the material discussed for engineers of less experience. The large number of illustrations and figures is supplemented by 6 large explanatory drawings of details of Kaplan wheels, regulation, static dimensioning of power stations and reinforcement of structures. The practicability of the book is greatly enhanced by ample bibliography, list of symbols, conversion tables of units and author and subject index.

Volume II now in press leaves the original arrangement of chapters of the Hungarian edition untouched. It extends to high-head plants, midget plants, pumped storage systems and economic aspects of water power utilization covering the latest achievements and data, dealing with the material as fully exhaustively and accurately as Vol. I.

It should also be mentioned, that Vol. I of the English edition including data and material up to the beginning of 1957, is also in press.

The vast scientific material published, the flowing style and impeccable translation, the excellence of illustrative figures and constructional designs as well as the attractive appearance of the book meeting every possible demand ensures also internationally the first line for this book of great conception.

I. Pap

Instruments for laboratories and research institutes
Measuring instruments for the textile industry
Instruments for power-plant control
Medical and surgical instruments
Medical and surgical apparatus
Electric measuring instruments
Medical and dental furniture
Electro-medical apparatus
Veterinary instruments
Electronic instruments
Geodetic instruments
Dental supplies
Ampoules

Exporters :

METRIMPEX

Hungarian Trading Company
for Instruments
Letters : Budapest 62.
P. O. B. 202
Telegrams : Instrument
Budapest

Metrimpex

Automatic Telephone Exchanges
Cordless Toll Exchanges
Rural Telephone Exchanges
Private Automatic Branch Exchanges
CB and LB Switchboards
CB and LB Telephone Apparatus
Series Connected Apparatus
Coin Collector Apparatus
Repeater Station Equipment
Loading Coil Cases
Multichannel Carrier Equipment for Cables and Open Wire Lines
Microwave Multiplex Equipment
Radio Links
Short Wave and Medium Wave Broadcasting Transmitters
Mobile and Portable Transceivers
Transmission Measuring Instruments
Remote Control Equipment
High Frequency Generators

BUDAVOX

BUDAPEST TELECOMMUNICATION COMPANY

Letters: Budapest 62. P. O. B. 267. Cables: Budavox Budapest

Three-phase A. C. motors
For low voltages
with squirrel-cage rotors: 50 kW—500 kW
with slip-ring rotors: 1,5 kW—500 kW
For high voltages: up to 6000 V and for outputs up to 3500 kW
Explosion-proof design: outputs 0,66—30 kW with suitable explosion-proof switches
Crane motors: outputs ranging between 2,5 and 145 kW
Synchronous generators and motors, D. C. motors and dynamos according to buyer's specifications

Low-voltage switchgear
Manually operated switches, motor-protecting, reversing and star-delta circuit breakers, dry and oil types
High-capacity circuit breakers up to 2500 A

High-voltage switchgear
Oil circuit breakers: 10—30 kW, up to 600 A, for breaking capacities up to 400 MVA
Small-oil-volume circuit breakers: 10—120 kW, up to 600 A, for breaking capacities up to 2500 MVA
Expansion-type circuit breakers: for breaking capacities up to 600 MVA, rated current 600—2000 A (up to 30 kW)
Air-blast type circuit breakers: 10—30 kW, rated current 600—2000 A, breaking capacity 600 MVA

Isolating switches
High-voltage fuses
Transformers: output 1—60.000 kVA, up to 120 kV
Electric welding generator
Welding transformers
Low and high-voltage porcelain insulators
Plastic and other insulating materials
Electric conductors, resistance materials
Aluminium and other cables, cable armatures
Electric installation materials
Lighting fittings
Electric household appliances
Overload circuit breakers, electric hand tools
Accumulators dry batteries

TRANSELEKTRO

HUNGARIAN TRADING COMPANY FOR ELECTRICAL EQUIPMENT AND SUPPLIES

LETTERS: Budapest 62. P. O. B. 377.
TELEGRAMS: TRANSELECTRO Budapest Hungary

A kiadásért felel az Akadémiai Kiadó igazgatója
Műszaki felelős: Farkas Sándor
A kézirat nyomdába érkezett: 1957. III. 15. — Terjedelem: 9,75 (A 5) ív, 59 ábra

Akadémiai Nyomda, V., Gerlóczy u. 2. — 41946/57 — Felelős vezető: Puskás Ferenc

A Budapesti Műszaki Egyetem Periodica Polytechnica címen idegen nyelvű tudományos folyóiratot indít. A folyóirat három sorozatban — vegyészeti, villamossági, valamint gépész- és általános mérnöki sorozatban — jelenik meg, évente négyszer, sorozatonként egy-egy kötetben. Az egyes kötetek terjedelme 14—18 iv.

A Periodica Polytechnicában megjelenő tanulmányok szerzői az Egyetem tanári karából és tudományos dolgozóiból kerülnek ki. Főszerkesztő Dr. Csűrös Zoltán egyetemi tanár, akadémikus.

A folyóirat előfizetési ára sorozatonként és kötetenként 50,— Ft. Megrendelhető az Akadémiai Kiadónál (Budapest 62, Postafiók 440. NB. egyszámlaszám: 05-915-111-44), a külföld számára pedig a Kultúra Könyv és Hírlap Külkereskedelmi Vállalatnál (Bp. 62, Postafiók 149. NB. egyszámlaszám: 43-790-057-181), illetve a vállalat külföldi képviseleteinél és bizományosainál.

INDEX